PARTICLE COLLECTION FROM AQUEOUS SUSPENSIONS BY SOLID AND HOLLOW SINGLE FIBERS

Thesis by

Daniel Pan Yih Chang

In Partial Fulfillment of the Requirements

for the Degree of

Doctor of Philosophy

California Institute of Technology

Pasadena, California

1973

(Submitted May 11, 1973)

ACKNOWLEDGEMENTS

The inspiration, guidance and counseling of my advisor, Professor Sheldon K. Friedlander, will be deeply appreciated throughout my professional career and personal life. Without his timely criticisms and encouragement this research would not have been completed. Heartfelt thanks are offered to Professor James J. Morgan for direction and consultation, but even more so, for his lively interest and activities with students which brought a semblance of balance to the graduate student life.

I wish also to express my appreciation to Professors Lloyd Spielman and Joseph Fitzpatrick for making the results of their research available to me and for several helpful discussions.

The financial assistance received from the United States Public Health Service and National Institute of Environmental Health Sciences is gratefully acknowledged. Additional funds for research were received from the Ametek Corporation; the interest demonstrated by its officers was a stimulant to this research. Their philanthropy and interest is deeply appreciated.

Technical assistance was received from Messrs. Elton Daly and Robert Greenway in the construction of the test apparatus, Paul Knust-Graichen in methods of preparing blood, Dwight Landis and Robert Jung in gathering data during certain of the experiments. They are all thanked for their fine work.

Many other faculty, students and associates contributed to this research. In particular I wish to thank Drs. Rudolf Husar, Dennis

Kasper, James Maloney, and François Morel, Professors Jack McKee, William Wood, and Jerome Vinograd, Messrs. Karl Bell, Steve Heisler, George Jackson, and Paul Roberts, Miss Jasenka Vuceta, and Mmes. Marge Connely, Carla Willard and Janet Yeager for their discussions, moral support and help.

The excellent typing and illustrations are the handiwork of Mrs. Sharon Higley and Miss Pat Lee respectively.

Finally, I dedicate this work to my wife whose love, encouragement and patience carried us through difficult times.

ABSTRACT

An investigation of particle capture by single solid and hollow fibers was conducted. The experimental system consisted of a small water tunnel with a test section in which single fibers were inserted. The deposition rate of particles under conditions of controlled flow and chemical composition was measured with an optical microscope. Particles studied included human erythrocytes and latex spheres ranging in size from 2.0 μm polyvinyltoluene latex to 25.7 μm styrene-divinylbenzene copolymer latex. The fibers were composed of glass, fluoroethylene-propylene (teflon - FEP), and cellulose acetate. Surface chemistry was found to play a major role in the attachment of micron-size particles to the collector. However, electrical double layer theory could not predict the onset of rapid particle attachment quantitatively. Significant viscous interaction of particles approaching the collector surface was inferred from the data, confirming recent theory.

A novel application of hollow fibers with permeable membrane walls was developed. The membrane permeability permits modification of the fiber suspension interface by means of chemical addition and flow alteration. The destabilizing chemicals form a thin concentration boundary layer around the fiber surface, reducing the total amount of chemical needed. Slight suction at the fiber surface reduces the hydrodynamic resistance acting on the particles as they approach the surface. An increase in the collection efficiency can occur when these methods are applied.

TABLE OF CONTENTS

LIST OF FIGURES

LIST OF TABLES

Chapter I

Introduction

A. Motivation

Man's efforts to separate dispersed phases from liquids date back to the limits of recorded history. Today's water supplies are filtered to remove suspended inorganic and organic particulates such as clays, iron and alum flocs, algae, bacteria and viruses. Other applications of filters include: processing food, paper, chemicals and beverages; coalescing emulsions; protecting machinery from abrasive particles; and cleaning perfused and transfused blood. In spite of the widespread use of filters, scientific investigation into their operation did not began until this century, and the greater part of the research has been conducted within the past forty years. Today there still is not a unified theory which can predict filter efficienies and operating characteristics for the variety of applications in which filters are used.

Evidence of the need for additional research with bioparticles can be inferred from a comment from Galletti and Brecher's book Heart-Lung Bypass (1962):

> In the pioneer years of extracorporeal circulation, the usefulness of blood filters was often debated.... Osborne (1955) actually observed that in a series of filters of equal mesh, more debris was recovered from the last filter in the blood circuit than from the first.

During the past few years, improved blood compatible materials have been developed. Although a limited transfer of technology from other

areas of filtration research has taken place as well, dispelling previous notions that filters act only as sieves, particle capture mechanisms remain poorly understood (Hill et al., 1970).

The filtration of aqueous suspensions has progressed farther, stimulated by the economics of treatment plant operation and increasingly stringent effluent requirements. However, the rational design of filters for other than head loss is not possible without extensive pilot plant studies or reliance upon previous experience.

B. Summary of Depth Filtration Research and Medical Applications

Reviews of deep bed filtration research have been written by Camp (1964); Ives and Sholji (1965); Sakthivadivel and Irmay (1966); Mintz (1966); O'Melia and Stumm (1967); and Herzig et al. (1970). Only recent work not covered by the reviews will be mentioned here along with a brief sketch of filtration research and the current state of filtration of body fluids.

B-1. Depth filtration

The ability of a depth filter to retain particles has been modelled in terms of a "filter coefficient" or "impediment modulus." Deposition of particles on a filter results in changes in the filter coefficient, flow and head loss. To describe the operation of the filter a set of coupled differential equations must be solved. This set of equations can be solved analytically or numerically depending upon the simplifications made in expressing the filter coefficient. A stumbling block to this approach has been the attempt to correlate experimental data with a single filter coefficient, without identifying

all of the capture mechanisms or the conditions under which they apply.

The capture mechanisms entail two conceptually distinct steps, transport of particles to the collector surface and attachment of particles to the surface. In early studies (pre-1960's) only physical properties of the collector, fluid, and suspended particles were taken into account, (particle and grain diameters, viscosity, densities, velocity, etc.). Transport mechanisms were not treated as distinct processes until aerosol filtration methodology was applied to liquid filtration (1960's). During the same period, consideration of colloid chemical studies led to physical-chemical theories of particle capture (e.g., Mackrle and Mackrle, 1961; Heertjes and Lerk, 1967). Transport and attachment were next distinguished as separate steps (O'Melia and Stumm, 1967) after surface forces proved to be important for particles less than about 30 μm. Earlier investigators tended to lump the different transport mechanisms and attachment step together. As a result, the correlations they hypothesized could not be generalized to other than their own data.

Although many transport mechanisms have been identified, there is no unanimous agreement as to which are important over a given range of variables. The physical-chemical models for attachment have not fared any better. A complicating factor has been the difference between hydrophobic (clays, latices, oils, etc.) and hydrophilic particles (generally of biologic origin such as erythrocytes, bacteria viruses, algae, etc.)[1]. Recent research (Cookson, 1967a, b, 1969,1970;

[1]The terms "hydrophobic" (lyophobic in general) and "hydrophilic" (lyophilic in general) are applied to indicate the affinity of the material for water (any given solvent in general). See van Olphen, (1963) for details.

Yao, 1968; Yao et al., 1971; Spielman, 1968; Spielman and Goren, 1970, 1972a, 1972b; Fitzpatrick and Spielman, 1973; Spielman and Fitzpatrick, 1973; Spielman and Cukor, 1973) has been directed toward evaluating each of the transport mechanisms, the physical chemistry of particle attachment, and numerical solution of the equations governing the clogging process.

B-2. Filtration of body fluids

The filtration of body fluids has primarily developed from the need to remove debris from transfused or perfused blood. In recent years filtration has also been utilized to remove schistosomes from the blood stream and cells from lymph fluid (Goldsmith and Kean, 1966, 1967, 1969; Foss et al., 1963; Fitts et al., 1971).

The major effort has been to find blood compatible materials for use in the filter. Filters have been of the screen variety, relying upon sieving action for efficient removal of particles. Recently dacron was found to be effective as an implant material and has been applied as a wool mat to form effective depth filter to prevent the circulation of microemboli and air bubbles (Hill et al., 1970; Egleblad et al., 1972; Ashmore et al., 1972). Evidence indicating that microemboli in transfused blood can lead to pulmonary insufficiency has stimulated re-evaluation of screen filters currently used in transfusion sets. A recent study by McNamara et al. (1972) indicates that depth filters can be more effective in removing aggregates than screen filters.

The National Institutes of Health's program to develop artificial implantable organs has yielded information about cell contacts and adhesion (Fed. Am. Soc. Exp. Biol., Proc., 1971). Other research groups have contributed as well (Pethica, 1961; Abramson, 1964; Ambrose, 1964; Sawyer et al., 1964; Sawyer, 1965; Sawyer and Srinivasan, 1970; Brooks et al., 1967; Edmark et al., 1970; Milligan et al., 1970; Gileadi, 1972; Djerassi et al., 1972; Majeski et al., 1972). The myriad of related studies illuminate some of the factors involved and have, moreover, delineated the complexity of the problem. Currently, bio-particle filter design is largely a trial and error procedure. However, the systematic application of the newly gained knowledge from many diverse fields (chemical engineering, sanitary engineering, surface chemistry, biomedical materials research, and immunology) points to many exciting possibilities for selective filtration of particles. An example would be to selectively filter hepatitis virus from banked blood, using differences in the transport properties and chemical attachment of viruses and formed elements of blood.

C. Scope of the Current Study

The research evolved around two original objectives. The applicability of the double layer model to the particle attachment step was to be determined by comparing a bioparticle (human red blood cell) with a model inert particle (latex sphere). The validity of a recently proposed theory (Spielman and Goren, 1970) for particle collection by the interception mechanism was to be tested. Such experiments might provide a basis for predicting the collection

efficiency of both inert and bioparticles in the interception size range ($\sim$ 1 to 30 μm diameter).

A plexiglass test section providing steady flow, approximating that of a uniform stream, past an isolated cylindrical fiber was designed for the studies. The transparent test section permitted microscopic observation of the particles depositing in situ. The single fiber results can be related to packed fibrous beds by mathematically accounting for changes in the flow geometry (Spielman and Goren, 1968a).

Based on the results of the study, a novel application of hollow fibers was envisioned which utilizes the permeability of the fiber wall to modify the chemistry of the region near the collector. Control of the surface chemistry presents a possibility to enhance or diminish the deposition rate of particles on the fiber. Experiments to confirm the conceptual model were performed with the same test apparatus.

Chapter II

Theoretical Background

A. Transport Mechanisms

A-1. Description of transport mechanisms

Transport mechanisms recognized to be operating in depth filters include:

a) interstitial straining[1] - particles moving with the fluid may attempt to pass constrictions smaller than their own dimensions and be removed from the flow;

b) bridging - two or more particles can form a "bridge" at the same passage causing further deposition upon themselves;

c) gravitational sedimentation - where density differences exist between particle and fluid, the action of gravity causes a relative motion between particle and fluid which can bring the particle to the collector surface;

d) inertial impingement or impaction - even in the absence of gravity, the inertia of a particle will prevent the particle from following curved fluid streamlines and the particle may impact upon a collecting surface as the flow curves around it;

---

[1] Interstitial straining can be considered a special case of interception. It is distinguished because the calculated dependences of the filter coefficient upon particle and media dimensions differ, as well as the causes for particle retention.

e) interception - particles following fluid streamlines can be brought within a distance where the finite size of the particle results in a collision with the collector;

f) diffusion - as particles are being convected by the flow, random thermal motions of the particles can bring them into contact with the collector;

g) electrostatic or thermoprecipitation - electrical or thermal gradients due to charges or temperature differences can cause particles to migrate toward collecting surfaces.

Two additional mechanisms have recently been proposed. Ison and Ives (1969) have concluded that "arbitrarily shaped particles," subjected to a three dimensional shear field, exhibit a "random drift" which results in significant lateral transport of the particles. Agrawal (1966) has suggested that electrokinetic effects generate electrical fields which can move charged particles toward or away from collecting surfaces.

Goldsmith and Mason (1961) have found that deformable particles, in a shear field generated by a wall, migrate laterally across fluid streamlines away from the wall, whereas rigid spheres and discs do not. Saffman (1965) found that lateral migration of rigid spheres in shear fields is caused by small inertial effects. He computed the force acting on a rigid sphere moving in the direction of flow, but with a relative velocity with respect to the undisturbed streamline which would have passed through the center of the particle. The disc-like RBC used in the current study should behave as rigid particles

under the small shear fields generated by the fiber. Estimates of the lift on the rigid latex spheres used in this study using Saffman's (1965) result indicate that the lift force is small compared to London-van der Waals or double layer forces for narrow separations ($h/a_p \ll 1$). Therefore lateral motions resulting from shearing forces were not a factor in the experiments.

Although the magnitude of electrokinetic effects has not been predicted, they are expected to be proportional to the streaming potential (Agrawal, 1966). For highly porous materials these forces should be negligible, and have been disregarded in the single fiber experiments.

The present investigation is limited to studying the initial filtration efficiency of dilute suspensions of micron size particles ($\sim$ 1 to 30 μm diameter) through highly porous fibrous media (porosity, $f > 0.7$) at low Reynolds numbers. Therefore inertial impaction, interstitial straining, bridging, and thermoprecipitation are negligible compared to other mechanisms. Furthermore, except in the immediate neighborhood of the surface, large potential gradients cannot be maintained on collectors of fixed charge suspended in natural waters. Hence, electrostatic precipitation is eliminated as a significant transport mechanism. This leaves sedimentation, interception, and diffusion as potentially significant transport mechanisms.

Bioparticles consist primarily of water and have densities close to unity. Unicellular particles (bacteria, formed blood elements) range from a few tenths of microns to about 10 microns in

diameter. For these reasons gravitational sedimentation is generally not a significant transport mechanism for them. However, sedimentation can be a significant factor for inorganic particles in the size range of interest (1 to 30 μm diameter), and are included in this discussion even though all experiments reported here were designed to avoid sedimentation effects.

A-2. Analysis of selected mechanisms

A-2-a. Definition of single collector efficiency and filter coefficient

The single fiber collector efficiency, η, is defined to be the ratio of the cross-sectional area, perpendicular to the flow, completely cleared of particles to the cross-sectional area of the collector. Assuming every collision of a particle with the fiber results in removal, a dimensionless transport efficiency, η_t, can be attributed to each transport mechanism. The transport efficiency displays the effect of each physical variable on the number of collisions. The product of the fraction of successful collisions leading to particle capture, α, and the transport efficiency yields the collector efficiency. The single collector efficiency can be related mathematically to the different flow geometries prevailing in a packed bed or fibrous mat by using various flow models (Spielman and Goren, 1968a), and thereby to the filter coefficient, λ.

Assuming steady conditions and homogeneous media throughout any cross section perpendicular to the flow, a filter coefficient, λ, is defined by the equation

$$\frac{dn}{dx} = -\lambda n \ , \qquad \text{(II-A-1)}$$

where n is the particle concentration at any depth x of the filter. The loss of particles through an infinitesimal thickness, dx, of the filter is given by the product of the single collector transport efficiency, collector area per unit width, number of collectors in thickness dx, local particle concentration, and the fraction of particle collector contacts which lead to capture. For cylindrical collectors the loss is given by

$$\frac{dn}{dx} = -\frac{2(1-f)}{\pi a_f} \alpha \eta_t n \ , \qquad \text{(II-A-2)}$$

where a_f is the cylinder radius, f is the porosity and α is termed the collision efficiency, the fraction of particle-surface contacts leading to capture. Therefore the filter coefficient is related to the collection efficiency by the equation

$$\lambda = \frac{2(1-f)}{\pi a_f} \eta \ . \qquad \text{(II-A-3)}$$

A-2-b. Expressions for cylinder transport efficiencies

As mentioned previously, density differences give rise to particle motion relative to the fluid. The collection efficiency due to sedimentation, when the flow is laminar and is in the direction of gravity, is given by

$$\eta_G = \frac{v_s \cdot \text{area cleared}}{U \cdot \text{fiber cross-sectional area}} \ , \qquad \text{(II-A-4)}$$

where v_s is the settling velocity of the particles and U is the mainstream velocity of the fluid. For spherical particles obeying Stokes' law the settling velocity is given by

$$v_s = \frac{2(\rho_p - \rho_f) g a_p^2}{9\mu} \quad . \qquad \text{(II-A-5)}$$

In the above equation, ρ_p and ρ_f are the particle and fluid densities respectively, g is the acceleration of gravity, and μ is the fluid viscosity. Since contact occurs when the particles come within one particle radius of the fiber, the area cleared is given by the product of the particle diameter and fiber length. Equation II-A-4 becomes

$$\eta_G = \frac{2(\rho_p - \rho_f) g a_p^2}{9\mu U} (1+R) \quad , \qquad \text{(II-A-6)}$$

where R is the ratio of particle to fiber radius, also termed the interception parameter.

Several conclusions can be drawn from the form of the single collector efficiency. First, the efficiency decreases rapidly as the particles become smaller or as the particle density approaches that of the fluid. Second, because the particles are normally much smaller than the fiber, the dependence upon fiber diameter is weak. Third, there is a moderate dependence upon the flow rate.

The efficiency computed from the geometric interception model (GIM) commonly used in gas filtration differs from the sedimentation result. The GIM efficiency can be calculated by integrating the contribution of the inward normal velocity at a distance of one particle radius over the collector surface.

When interception is significant in liquid filtration, it is often the case that the particles are small compared to the collector and the Reynolds number, N_{Re} -based upon the collector diameter , is

less than one. Under these conditions, Friedlander (1957) has calculated the efficiency for isolated cylindrical fibers as

$$\eta_{GIM} = \frac{2A_F a_p^2}{a_f^2} = 2A_F R^2 , \qquad \text{(II-A-7)}$$

where

$$A_F = \frac{1}{2[(2.0 - \ln N_{Re})]} \qquad \text{(II-A-8)}$$

is a characteristic of the flow model employed. The derivation of Equations II-A-7 and II-A-8 is based upon Lamb's (1932) solution of the Oseen equations and assumes that the velocity profile near the cylinder surface is accurately predicted by the leading term of the expansion of that solution. Spielman and Goren (1968a) present alternative expressions for A_F for different flow models.

The GIM assumes that the particles are capable of following the fluid streamlines. The assumption is justified for aerosols where the low viscosity and molecular density of the carrier gas do not result in appreciable fluid dynamic interaction as the gap between the particle and collector narrows. However, for viscous liquids, Spielman has presented theoretical and experimental evidence that hydrodynamic interaction with collectors causes particles to deviate from the undisturbed fluid streamlines as the separation between particle and collector becomes small. In fact, using continuum theory for the liquid, one finds that no particles will deposit on the collector in a finite amount of time unless acted upon by an external force! The attractive force needed to overcome the

increasing fluid resistance with narrowing gap width is believed to be the London-van der Waals dispersion force.

Spielman and Goren's (1970) analysis, hereafter termed the hydrodynamic retardation model (HRM) is based upon the following assumptions:

i) the collector is cylindrical and the particle spherical;

ii) the undisturbed flow field about the cylinder is given by the leading term of Lamb's solution for the stream function

$$\Psi = 2A_F U \frac{(r-a_f)^2}{a_f} \sin\theta \qquad \text{(II-A-9)}$$

with the appropriate A_F;

iii) the flow field in the neighborhood of a small moving particle is governed by the incompressible creeping flow equations

$$\nabla p = \mu \nabla^2 \vec{v} \qquad \text{(II-A-10)}$$

where p is the pressure and $\vec{v}$ the vector velocity, the velocity field far from the collector is given by the undisturbed flow;

iv) the particle is small compared to the collector so that the cylinder may be treated as a plane wall when the streamlines begin to deviate from the undisturbed pattern;

v) London-van der Waals and hydrodynamic forces are the only ones acting on the particle, i.e., gravitational, electrostatic and random thermal forces are negligible.

The linearity of the creeping flow equations and the additivity of the boundary conditions are used to resolve the particle motion into

radial and tangential components. Applying dimensional reasoning to the equations of motion and the boundary conditions, the ratio of the HRM to GIM transport efficiencies is found to be a function of two dimensionless groups,

$$\frac{\eta_{HRM}}{\eta_{GIM}} = f\left(\frac{Qa_f^2}{9\pi\mu A_F U a_p^4}, \frac{a_p}{\lambda_w}\right), \qquad \text{(II-A-11)}$$

where the Hamaker constant, Q, and the characteristic wavelength of the dispersion forces, λ_w are material properties of the particle and collector. The first dimensionless group on the right hand side has been termed the adhesion number,

$$N_{Ad,f} = \frac{Qa_f^2}{9\pi\mu A_F U a_p^4} \qquad \text{(II-A-12)}$$

and accounts for the correction to the GIM resulting from hydrodynamic and dispersion forces. The second dimensionless group is a correction to the calculated dispersion force taking into consideration the finite propagation velocity of electromagnetic waves. Fibrous mat data have been successfully correlated ignoring the electromagnetic correction (Spielman, 1968; Fitzpatrick and Spielman, 1973).

Spielman and Fitzpatrick (1973) carried out numerical integrations of the particle trajectories using uncorrected dispersion forces for spherical, cylindrical, and rotating disc collectors. They obtained the ratio of the interception efficiencies as a function of the adhesion parameter in quantitative form and satisfactorily correlated several sets of data for granular packed bed filters with it

(Fitzpatrick and Spielman, 1973). The computed curve for cylindrical collectors has been reproduced in Figure II-A-1. Spielman and Cukor (1973) have extended the numerical integrations to include diffuse double layer interactions near spherical and rotating disc collectors. They found the interesting result that there is no abrupt change in the rate of collection as one passes from secondary minimum to primary minimum capture. Furthermore, the dependence of the collection efficiency on the parameter characterizing repulsion is practically discontinuous for large adhesion numbers. The explanation for the discontinuous behavior is that at large adhesion numbers the hydrodynamic forces are very small compared to double layer and dispersion forces. Then the criterion used for collection, zero net force acting on the particle at the point where the potential energy barrier becomes zero, does not depend strongly on the flow field. This corresponds to the Verwey-Overbeek (1948) method for determining the critical coagulation concentration of lyophobic sols.

Under conditions of negligible repulsion, the ratio of the model efficiencies, η_{HRM}/η_{GIM}, has roughly a one-quarter power dependence upon the adhesion number, $N_{Ad,f}$, over a wide range of values. Natanson (1957a) integrated the particle trajectory assuming only Stokes drag and dispersion forces and obtained an analytic solution. The asymptote shown for large $N_{Ad,f}$ is his result and has a one-third power dependence.

For instructive purposes, assume that the one-quarter power dependence represents the true functional dependence. Then the approximate dependence of the HRM efficiency upon the different

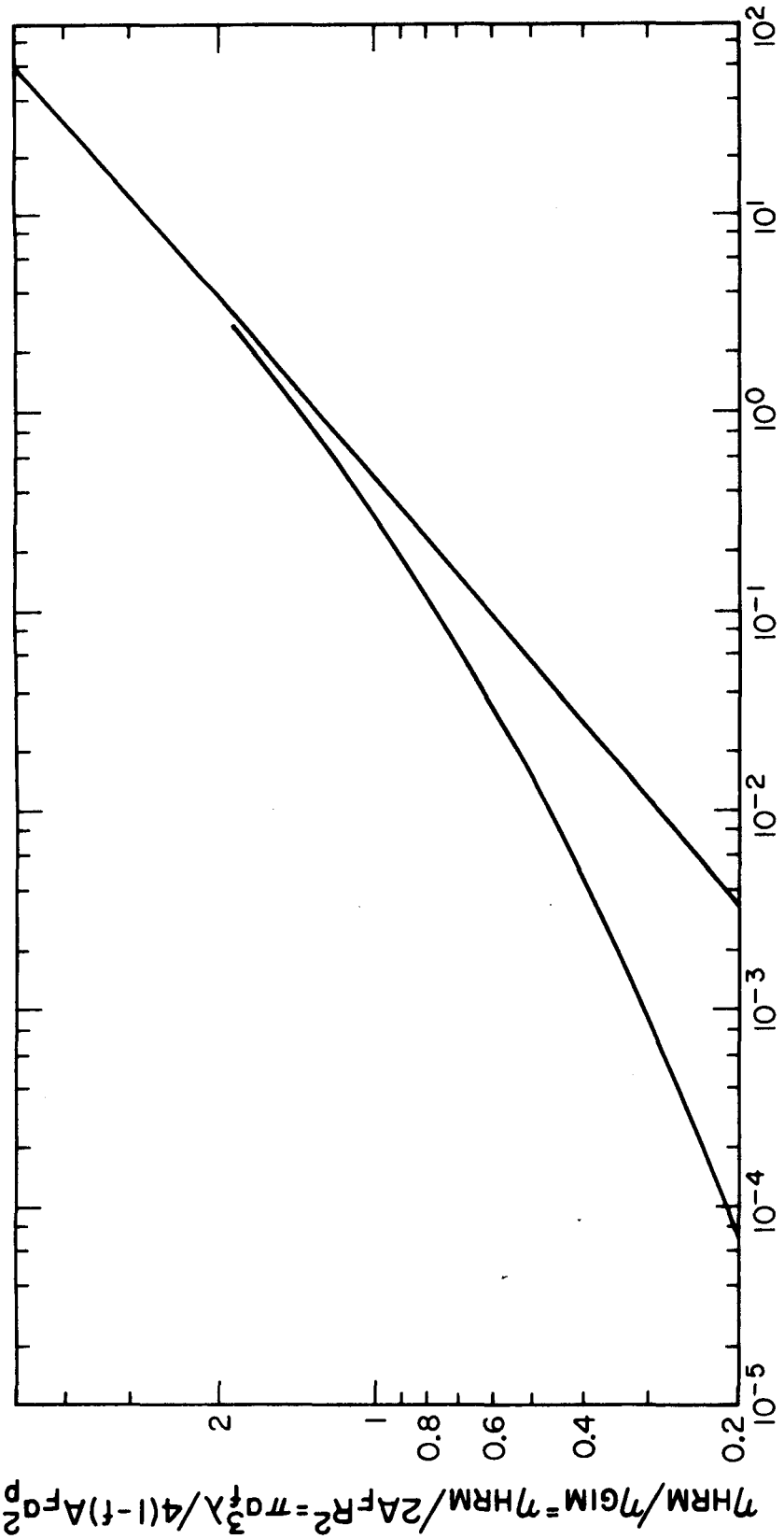

Figure II-A-1 Ratio of HRM to GIM Transport Efficiency versus Adhesion Number

variables may be clearly seen,

$$\eta_{HRM} \propto \frac{Q^{1/4} A_F^{3/4} a_p}{\mu^{1/4} U^{1/4} a_f^{3/2}} \cdot \qquad \text{(II-A-13)}$$

Note the weak dependence upon the flow ($\mu^{-1/4}$, $U^{-1/4}$) and the material composition ($Q^{1/4}$), absent in the GIM. Also note the moderate effect of the flow geometry ($A_F^{3/4}$) and particle size (a_p), and most interesting, the effect of fiber size ($a_f^{3/2}$). In contrast with transport by sedimentation, there is a strong increase in efficiency by decreasing the collector size.

The media size in sand filters (400 μm to 2,000 μm) has been limited by the media stratification which occurs with backwashing. As a result, sedimentation dominates interception for the flowrates under which typical sand filters are operated. Multi-media filters with increased efficiency have extended the size range to about 150 μm by using high density materials. Fibrous media filters are not subject to the same limitation and can be made more efficient by decreasing fiber diameters, the ultimate limitation being either fiber strength or manufacturing costs.

One does not usually think of diffusion as a significant transport mechanism outside the sub-micron range where it dominates (Cookson, 1967b, 1970 and Yao et al., 1971). Yet Yao et al. (1971) calculate that for a single spherical collector diffusion is non-negligible compared to transport by the GIM mechanism for particle diameters approaching 2 or 3 μm. Its role in removing particles in the micron size range is considered here.

The expression for the transport of point particles diffusing to cylinders from low speed flows has been derived independently by Friedlander (1957) and Natanson (1957b),

$$\eta_D = \pi C_1 A_F^{1/3} \left(\frac{D_p}{d_f U} \right)^{2/3} = \pi C_1 A_F^{1/3} N_{Pe}^{-2/3} \qquad \text{(II-A-14)}$$

where D_p is the diffusion coefficient of the particle, and d_f is the diameter of the fiber. The Peclét number, N_{Pe}, appearing in the above expression is a measure of convective to diffusive transport. Both Natanson and Friedlander utilize the fact that even though a hydrodynamic boundary layer does not exist, a concentration boundary layer does. The coefficient C_1 was calculated to be 1.17 by Natanson using "thin" concentration boundary layer approximations while a value of 1.035 was found by Friedlander using an integral boundary layer method.

The diffusion efficiency is seen to increase with decreasing particle size, i.e., higher diffusion coefficients, decreasing fiber diameter and decreasing velocity.

Spielman and Friedlander (1973) have included the effects of double layer forces on the diffusion of point particles to spherical and cylindrical collectors. By including the gradient of the potential energy of the particle in the convective diffusion equation, an analytic solution was obtained (in the form of an integral) for the collection efficiency as a function of a single parameter, β. Using their notation, the collection efficiency is given by

$$\eta = \frac{I}{2a_f U n_\infty} = 2.2955179\ A_F^{1/3}\left(\frac{Ua_f}{D}\right)^{-2/3}\left(\frac{\beta}{\beta+1}\right) C(\beta) \quad . \quad \text{(II-A-15)}$$

The parameter, β, depends upon the ratio of the potential to the thermal energy of the particle. The effect of β on the collision efficiency, $\alpha \equiv I/I_\infty$, has been reproduced from their work in Figure II-A-2.

The potential energy can be calculated from the Verwey-Overbeek, Derjaguin-Landau (VODL) theory. The results of an approximate calculation are shown in Figure II-A-3 using values from experiments with 2.0 μm latex particles depositing on glass fibers. An assumed value of the Hamaker constant of 3×10^{-20} joules was used. Increasing the Hamaker constant slightly displaces the curve in the direction of lower concentrations. Details of the calculation are given in Appendix B. Interestingly, the curve does not exhibit the discontinuous behavior of the interception solution. The distribution of particle energies is subtly accounted for in the theory.

A-2-c. Relative contribution of transport mechanisms

Figure II-A-1 shows that for large adhesion numbers, $N_{Ad,f}$, the HRM efficiency becomes greater than the GIM efficiency. The particles must therefore be displaced from their original streamlines toward the collector. Physically, it is difficult to imagine dispersion forces moving particles the distances needed (on the order of microns $\sim$ 10,000 Å) to increase the efficiency by factors of 2 to 10. Schenkel and Kitchener (1960) state that an electromagnetic retardation

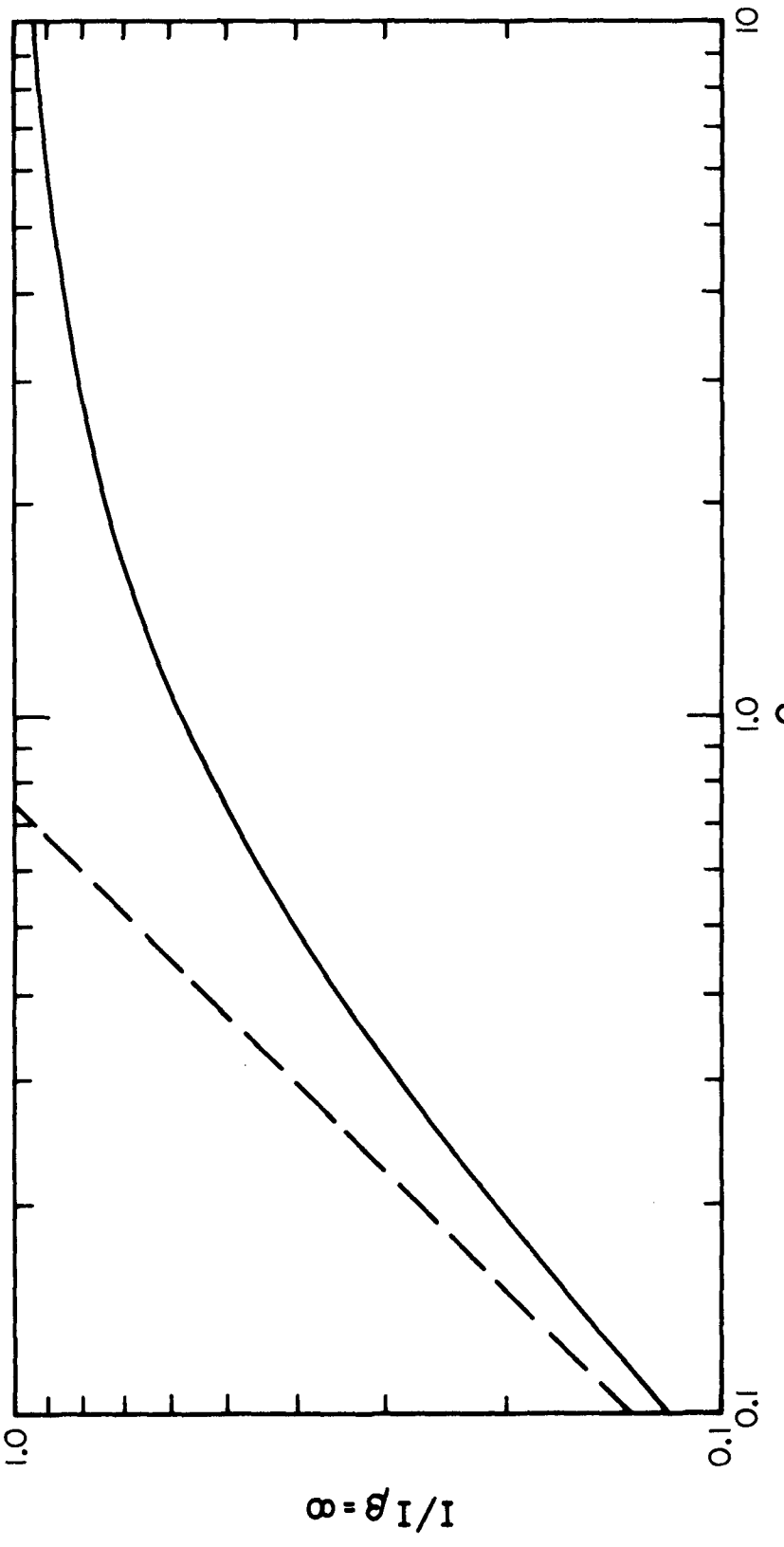

Figure II-A-2 Ratio of Rate of Diffusion of Point Particles Through an Energy Barrier to Diffusion without Barrier versus Barrier Strength Parameter β, for Cylindrical Collectors

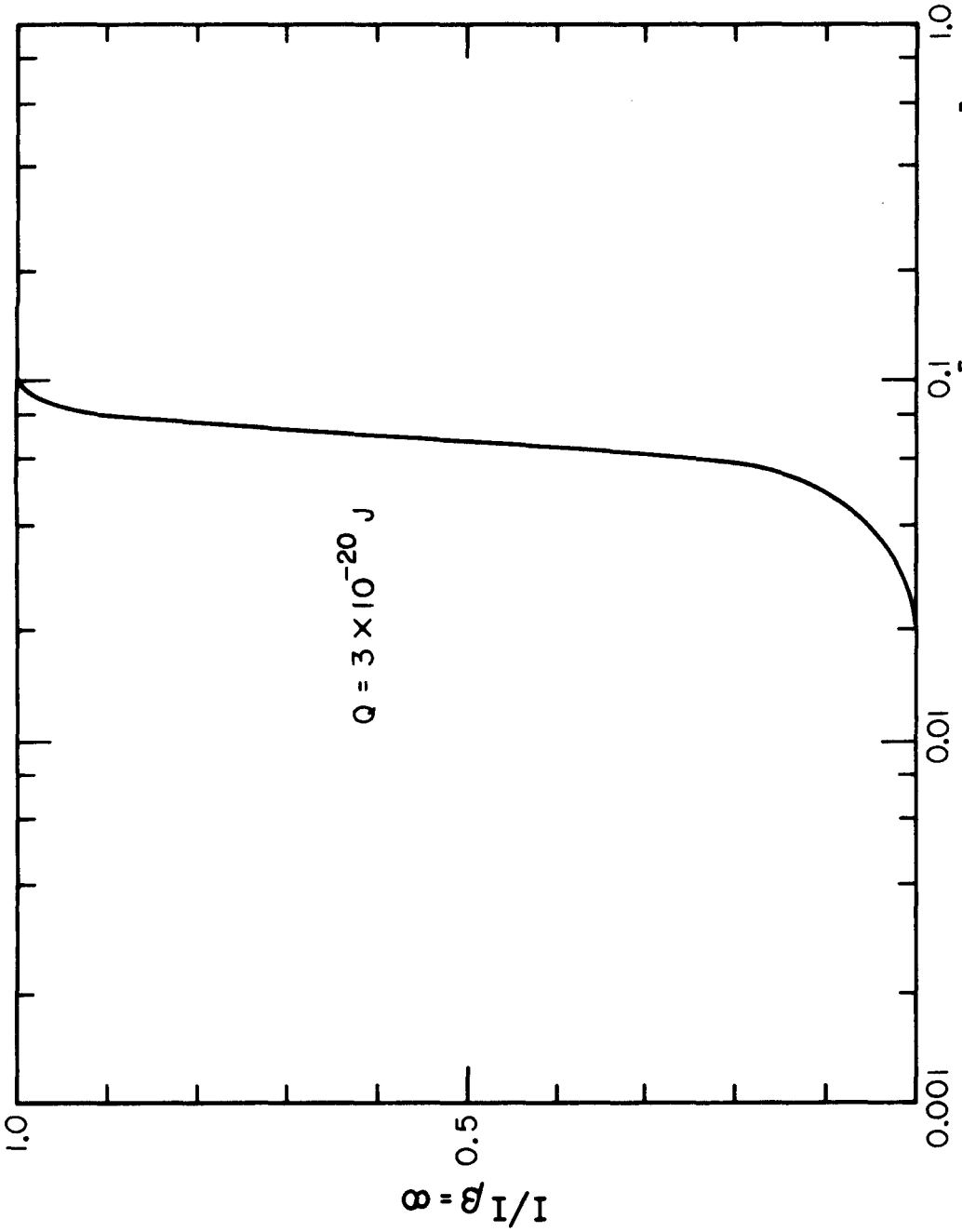

Figure II-A-3 Ratio of Rate of Diffusion Through Energy Barrier to Diffusion without Barrier versus 1:1 Electrolyte Concentration for Hamaker Constant of 3×10^{-20} J.

correction must be applied to particles of microscopic dimensions at separations less than 2×10^{-2} μm (< 200 Å). The correction increases the power dependence of the attractive force. Therefore, it is unlikely that the HRM efficiency calculated neglecting electromagnetic retardation is correct in the large $N_{Ad,f}$ region and agreement with experimental data in this region must be regarded as fortuitous.

Fitzpatrick and Spielman (1973) correlated data for packed beds of spheres in the high $N_{Ad,s}$ region using the unretarded dispersion expression for the force and neglecting diffusion. However, all of the experimental data with $\eta_{HRM}/\eta_{GIM} > 1$ were gathered under conditions where the single collector diffusion efficiency was at least comparable if not greater than η_{HRM}. The neglect of diffusion was justified for some data points on the basis that the flow geometry, A_F, in packed beds or fibrous mats, increases the interception contribution ($\eta_{HRM} \propto A_F^{2/3}$ to $A_F^{3/4}$) relative to diffusion ($\eta_D \propto A_F^{1/3}$). In single fiber experiments, there is no uncertainty about the flow model used to correlate the data. If the experimentally determined efficiency should be appreciably larger than the GIM efficiency, then this must be attributed to diffusion since all other mechanisms are negligible by experimental design.

Comparing the dependence of η_D, η_{HRM}, and η_G on particle size, it is apparent that there exists a particle size with minimum contact opportunity (Friedlander, 1967a; Yao et al.,1971). A plot of the sum of the efficiencies contributed by the three mechanisms is shown in Figure II-A-4. The minimum occurs for particles about 1 or 2 μm in

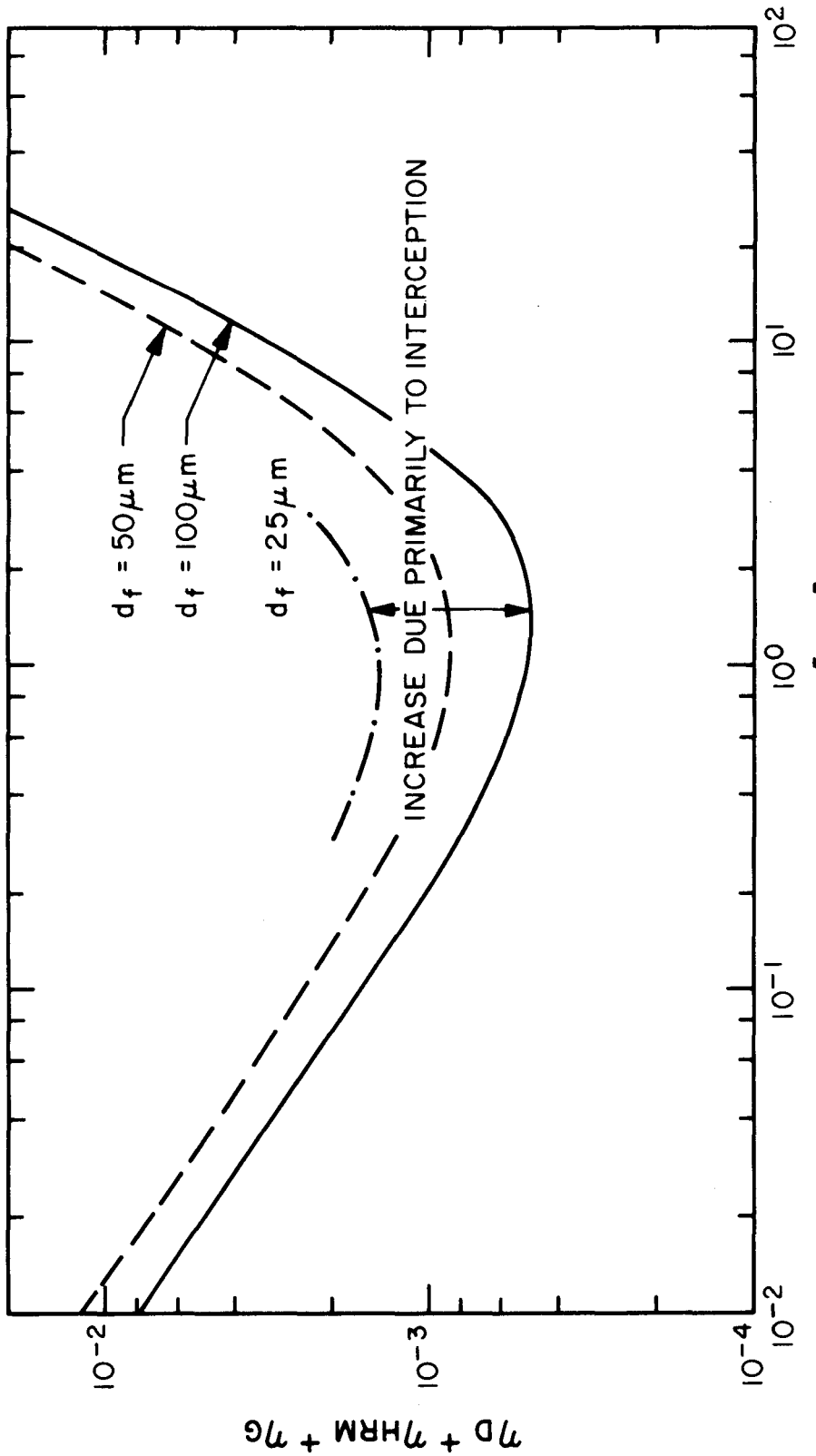

Figure II-A-4 Effect of Decreasing Fiber Diameter on Transport Efficiency for U = 0.15 cm/sec, ρ_p = 1.05 gm/cm^3, and μ = 0.01 dyne-sec/cm^2

diameter depending upon the collector diameter. The magnitudes of diffusion and interception are about the same for that size range.

Particle suspensions found in practice generally have broad size distributions so that more than one removal mechanism may be important. Yao et al. (1971) found fair agreement with measured filter efficiencies by simply summing the theoretical efficiencies. Friedlander (1967a,b) presented an empirical correlation for combined diffusion and interception based upon convective diffusion theory, incorporating interception in the boundary condition. No rigorously correct technique for combining the various efficiencies exists. Summing the individual efficiencies, properly weighted by the size distribution, appears to be the best practical technique for predicting the initial filtration efficiency.

B. Attachment Processes

In aqueous media, surfaces become charged by a number of different mechanisms including chemical reaction, lattice imperfections and substitutions, and specific ion adsorption (Stumm and Morgan, 1970). The presence of clouds of counterions in solution shields the charged surfaces so that charge effects are only appreciable at close approach. The diffuse electrical double layer proposed by Verwey-Overbeek, Derjaguin-Landau (VODL) attempts to describe the interaction energies of surfaces, taking into account charges and dispersion forces.

The VODL theory is analyzed in detail by Verwey and Overbeek (1948), Kruyt (1952), and Adamson (1967) among others. Its role in

the attachment step for both hydrophobic and hydrophilic particles is discussed here.

B-1. The VODL model predictions

Hogg et al. (1966) have derived an expression for the repulsive potential energy due to like charges on two dissimilar spheres,

$$V_R = \frac{4\pi\epsilon_0\epsilon a_1 a_2 (\psi_{01}^2 + \psi_{02}^2)}{4(a_1 + a_2)} \left[\frac{2\psi_{01}\psi_{02}}{(\psi_{01}^2 + \psi_{02}^2)} \ln\left(\frac{1 + \exp(-\kappa h)}{1 - \exp(-\kappa h)}\right) + \ln\left(1 - \exp(-2\kappa h)\right) \right], \quad \text{(II-B-1)}$$

where the subscripts refer to particle 1 or 2 and ψ_0 is the surface potential, κ is the reciprocal of the double layer thickness, h is the separation between sphere surfaces along a line joining their centers, ϵ is the dielectric constant, and $4\pi\epsilon_0$ is a constant used to convert electrostatic units to S.I. units.[1] The sphere-plate energy is readily derived by taking the limit as one radius tends to infinity,

$$V_R = 4\pi\epsilon_0\epsilon a_p \left(\frac{\psi_{01}^2 + \psi_{02}^2}{4}\right) \left[\frac{2\psi_{01}\psi_{02}}{(\psi_{01}^2 + \psi_{02}^2)} \ln\left(\frac{1 + \exp(-\kappa h)}{1 - \exp(-\kappa h)}\right) + \ln\left(1 - \exp(-2\kappa h)\right) \right]. \quad \text{(II-B-2)}$$

These approximations are believed to be accurate for thin double layers ($\kappa a_p \gg 1$) and low to moderate potentials ($< 50 - 60$ mv).

---

[1] ϵ_0 is the permittivity constant of "free space" and has the value 8.85×10^{-12} farad/meter.

The attractive energy caused by the unretarded dispersion forces are given by Adamson (1967) for the case of two unequal spheres,

$$V_A = -\frac{Q}{6}\left\{\frac{2a_1a_2}{h^2-(a_1+a_2)^2}+\frac{2a_1a_2}{h^2-(a_1-a_2)^2}+\ln\left[\frac{h^2-(a_1+a_2)^2}{h^2-(a_1-a_2)^2}\right]\right\} \quad \text{(II-B-3)}$$

Again, taking the limit as one sphere grows indefinitely one obtains

$$V_A = -\frac{Q}{6}\left\{\frac{2a_p(a_p+h)}{h(2a_p+h)}-\ln\left(\frac{2a_p+h}{h}\right)\right\}^{1}, \quad \text{(II-B-4)}$$

which for $h \ll a_p$ becomes

$$V_A = -\frac{Qa_p}{6h}. \quad \text{(II-B-5)}$$

Equations II-B-2 and II-B-5 were added to give the total potential energy of interaction of a sphere and plate

$$V_T = -\frac{Qa_p}{6h}+4\pi\epsilon\epsilon_0\left(\frac{\psi_{01}^2+\psi_{02}^2}{4}\right)\left[\frac{2(\psi_{01}\psi_{02})}{(\psi_{01}^2+\psi_{02}^2)}\ln\left(\frac{1+\exp(-\kappa h)}{1-\exp(-\kappa h)}\right)+\ln\left(1-\exp(-2\kappa h)\right)\right]. \quad \text{(II-B-6)}$$

Typical curves of the potential energy versus separation are shown in Figures II-B-1 and II-B-2. They were calculated to correspond to conditions used in 2.0 μm polyvinyltoluene latex particle (PVTL) and 100 μm glass fiber experiments and will be referred to again in the

---

[1] There are typographical errors in the expression given by Adamson (1967) for the sphere-plate interaction.

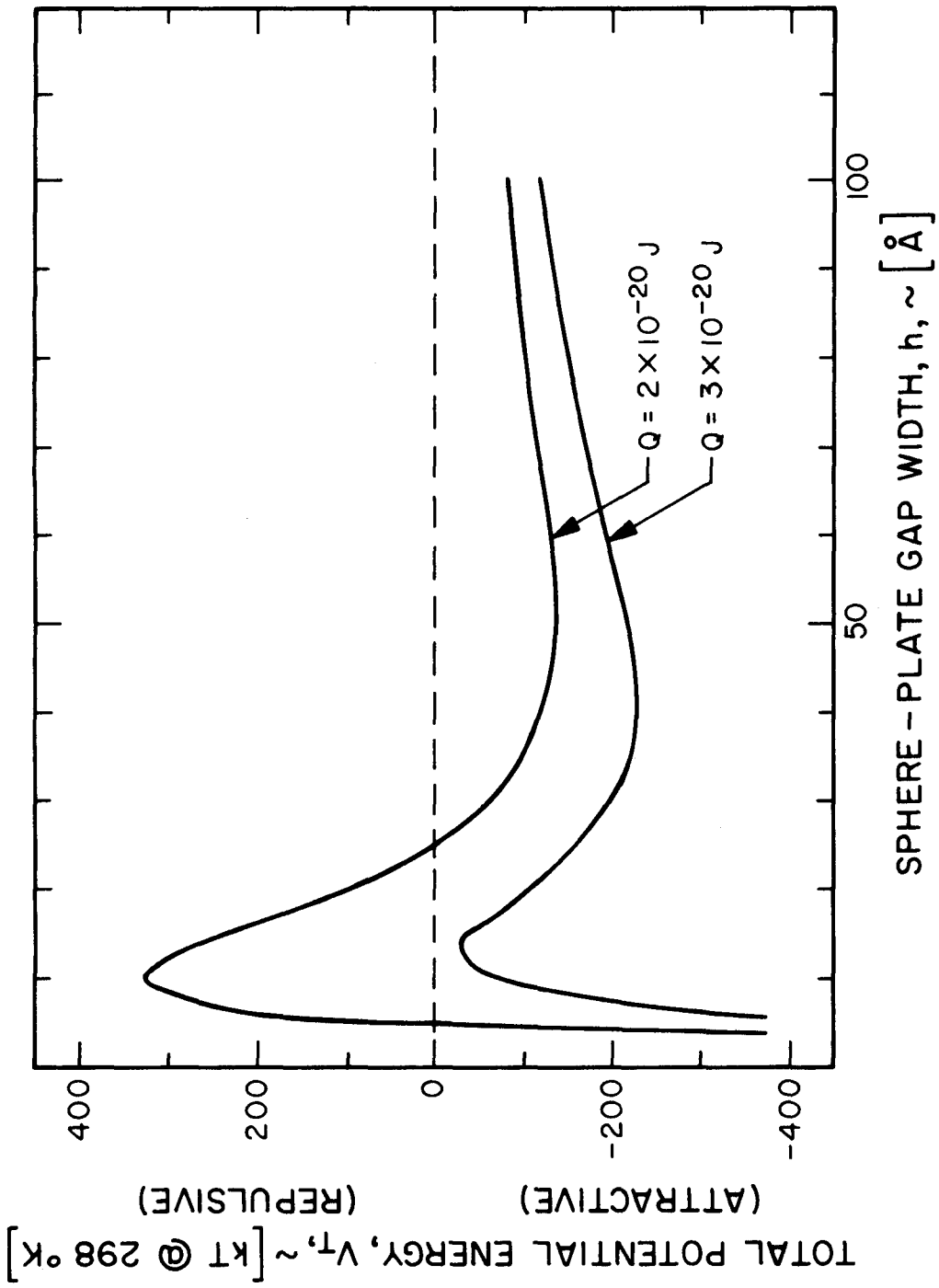

Figure II-B-1 Sphere-Plate Potential Energy versus Separation for 1:1 Electrolyte Concentration = 0.08 M

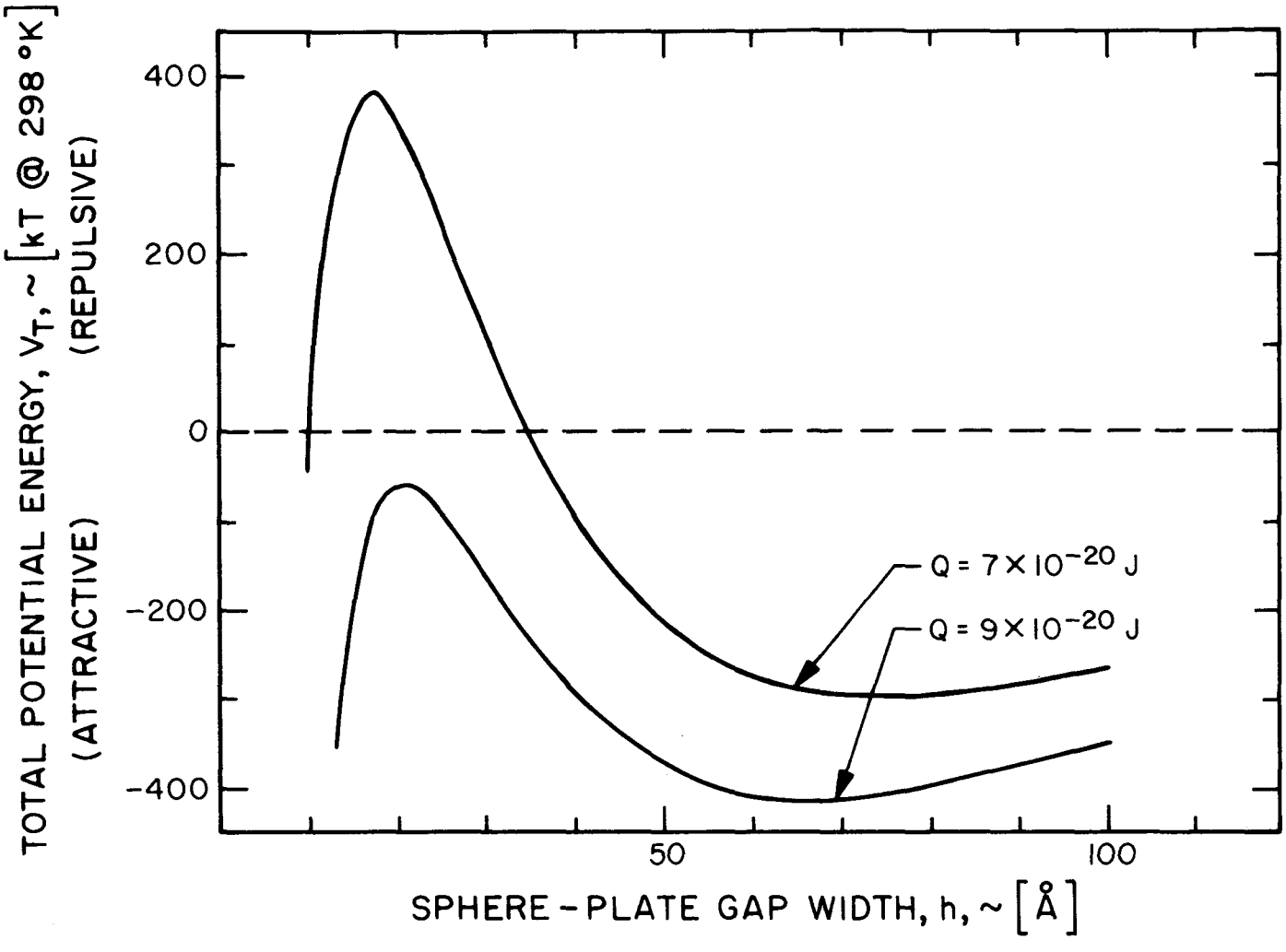

Figure II-B-2 Sphere-Plate Potential Energy versus Separation for 1:1 Electrolyte Concentration = 0.03 M

discussion of experimental results.[1]

The zeta potentials, ζ, based on mobility measurements were used in place of the surface potential, ψ_o, in the above calculations.[2] This corresponds to assuming that the total repulsive energy is adequately represented by the zeta potential. Justification for such an assumption comes from earlier coagulation studies (Watillon and Joseph-Petit, 1966; Ottewill and Shaw, 1966; Hunter and Wright, 1971) where the same assumption has been successful in some cases. Equation II-B-2 is an expression of double layer interaction at constant potential. The question of whether constant charge or constant potential should be used is still open to debate. Spielman and Cukor's (1973) numerical calculations show that they are qualitatively the same. The constant charge assumption makes the repulsive energy decay slightly faster with distance.

Figures II-B-1 and II-B-2 show definite secondary potential energy minima. Although the minima occur at distances less than 100 Å when ion concentrations are high, it is likely that they are overestimated. The large attractive energies result from the sphere-plate geometry assumed for micron-sized particles without electromagnetic retardation corrections. If the minima truly are as deep as

---

[1] In calculating the double layer thickness, κ^{-1}, the usual assumption was made that the counterion contribution dominates, since the electrolyte was not of the 1:1 variety.

[2] Calculation of the zeta potential was performed using the Helmholtz-Smoluchowski equation for large particles with large radii of curvature (Abramson, 1964). Diffuse double layer relaxation and retardation corrections were not applied since they are small ($< 10\%$ for $\kappa a > 100$) (Wiersma et al., 1966).

those calculated from Equation II-B-5, particles would be expected to be captured in a secondary minimum and dragged by the fluid toward the rear stagnation point of a cylindrical collector. It is not known whether the secondary minima are deep enough to "accelerate" particles over the potential energy barriers into primary minima.

B-2. Stern model corrections

Where interaction energies other than those due to charge and dispersion are significant, the Gouy-Chapman model of the double layer cannot be directly applied. Such systems include those where specific ion adsorption or chemical binding occurs or where the surfaces are hydrophilic (e.g., polyelectrolytes, complex forming species, and hydrated metal oxides, respectively). The experiments reported here confirm that the diffuse double layer model predicts the approach of particles reasonably well, but not their attachment to the surface. Further refinements such as the Stern model of the double layer must be incorporated into the VODL theory if advances are to be made.

Basically, the Stern model accounts for the finite size of ions and their specific sorbability. The number of available adsorption sites in the Stern layer is a function of the chemical nature of the surface and the size of the adsorbing species. The distribution of sorbable species between the surface sites and solution is assumed to be governed by a Boltzmann distribution of the free energy of that species. In turn, the Gibbs free energy is composed of a coulombic and chemical term

$$\Delta G = ze\psi_\delta - \varphi \qquad \text{(II-B-7)}$$

where z is the valence of the species, e is the electronic charge, ψ_δ is the electric potential of the Stern layer, and φ is the chemical energy of adsorption. Difficulties in the experimental evaluation of the chemical energy, number of adsorption sites, effective ion size, and dielectric constant within the Stern layer have been drawbacks to this approach. However, the amount of available data has been growing. Stumm et al. (1970) outlined a method for treating hydrated metal oxide surfaces, Kasper (1971) treated destabilization of particles by polyelectrolytes of opposite charge using the Stern model, and James and Healy (1972) have calculated adsorption energies of ions at oxide-water interfaces.

The VODL theory, even with Stern-type corrections applied, does not take into account several other phenomena which may influence deposition. The fluid mechanical behavior of the interfacial region as two surfaces intimately contact one another is not described. This might depend upon whether there is energetically significant structuring of the liquid phase in the region near the surface (Derjaguin, 1966; Johnson et al., 1966). Heterogeneity of surfaces and surface roughness on the order of interaction distances (< 100 Å) may also be important, even for apparently uniform surfaces (Marshall and Kitchener, 1966; Hull and Kitchener, 1969). The first two phenomena can present barriers which appear to be present in studies reported by Swift and Friedlander (1964), Marshall and Kitchener (1966),

Hull and Kitchener (1969), Fitzpatrick and Spielman (1973) and in the current study.

Although the VODL theory was not designed to answer all the questions posed above, it has provided a successful semi-quantitative approach to understanding a larger class of surface interactions than purely hydrophobic ones.

Chapter III

The Hollow Fiber Filter

A. The Hollow Fiber Concept

Hollow fibers with permeable membrane walls are relatively new products. Selective separations of both gas and liquid phases have been achieved using hollow fibers (Cole and Genetelli, 1970; Salyer et al., 1971; Cohen et al., 1972; Chemical Engineering, 1971). In solid or solute-liquid separations, e.g., reverse osmosis, the bulk of the liquid to be treated is passed through one side of a membrane wall; the "purified" product appears on the other. For solid-liquid separations of dilute suspensions, treatment of the bulk liquid by "ultrafiltration" is economically unwarranted unless exceptionally particle-free liquids are demanded.

Particles can be removed efficiently without processing the bulk of the flow through the fiber wall by using hollow fibers of small diameter. These can be used to construct a filter mat of high specific surface area, similar to conventional fibrous filters. The flow of liquid around the individual filter elements transports the particles to the fiber surface; the novel feature is the use of the permeability of the fiber's membrane wall to increase the collection efficiency of the fiber.

The basic idea behind using the permeability of the fibers to increase the collection efficiency is to allow ionic species to diffuse from the concentrated electrolyte solution inside the fiber through the membrane wall (Figure III-A-1). Thus, a high concentration of

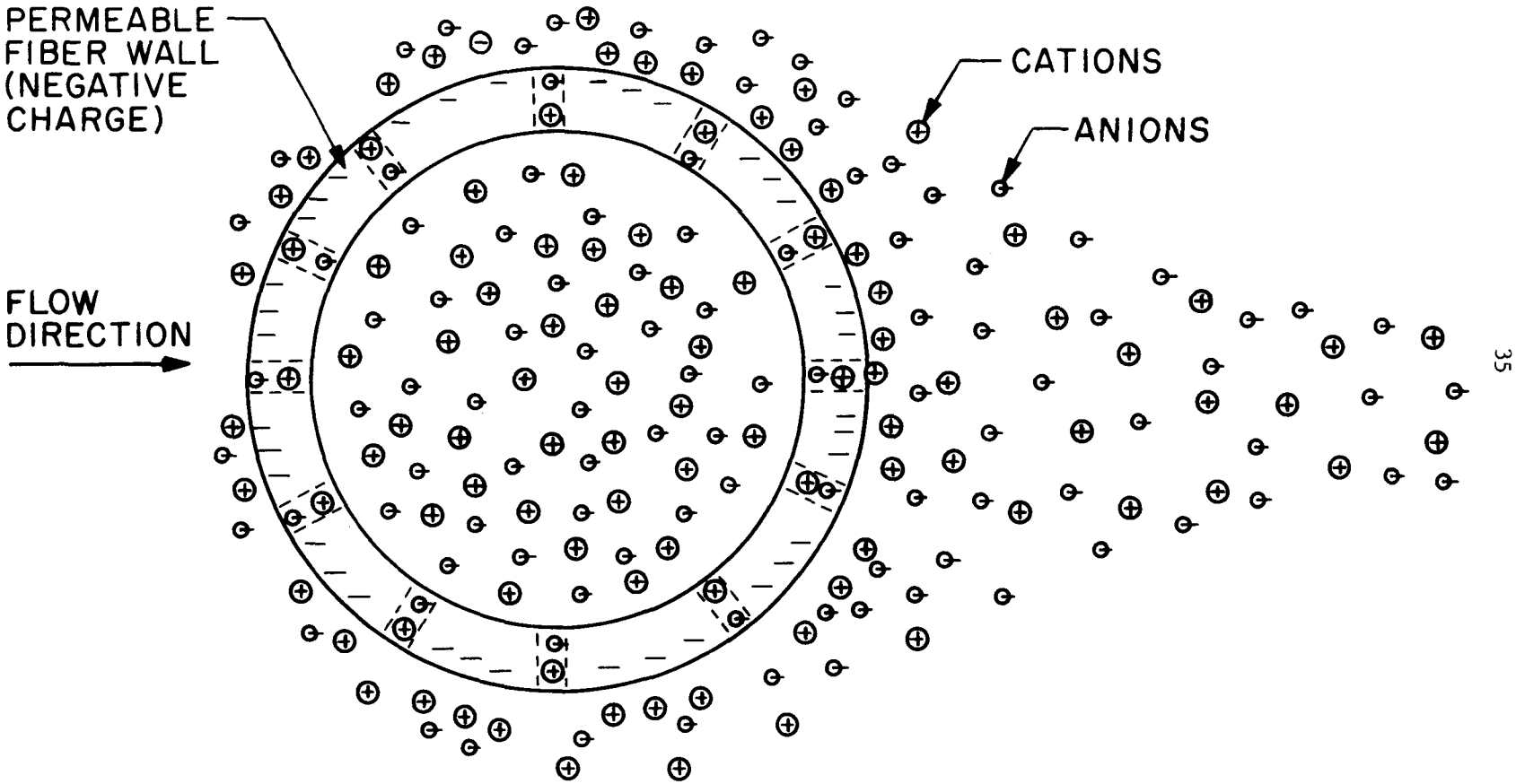

Figure III-A-1 Schematic of Hollow Fiber Operation Depicting Growth of Concentration Boundary Layer

ions is obtained at the fiber surface where it has the greatest effect. The osmotic pressure imbalance which arises from the concentration gradient forces the solvent between the particle and fiber surface through the wall into the fiber interior, thereby reducing the resistance to motion in the radial direction. The solution within the fiber is constantly renewed by pumping a fresh electrolyte through the fiber interior. With more porous membranes, polyelectrolytes of high molecular weight could be allowed to diffuse outwardly through the walls and adsorb onto the surface. In that case a mechanically induced pressure imbalance can be used to drive the fluid through the walls.

A chemical feed system of this design not only increases the collection efficiency of the fiber, but could potentially reduce the amount of chemical needed to destabilize the particles and the amount escaping in the effluent stream. It might also serve to eliminate problems of "overdosing" with specifically sorbable ionic species. Overdosing can result in charge reversal of both surfaces, and hence, restabilization. Only the fiber surface should reverse its charge if hollow fibers are used.

B. Hollow Fiber Theory

To evaluate the effectiveness of hollow fibers, the rate of transfer of electrolyte to solution and of particles to surface must be estimated for a single fiber. Then the total amount of electrolyte added can be calculated for a desired particle removal by summing the contributions of each fiber over the entire filter. If the total

amount of electrolyte approaches that amount which would be needed to destabilize the bulk suspension, the advantage of using hollow fibers is diminished.

As the electrolyte diffuses from the membrane surface, it is convected by the flow toward the rear of the collector, forming a concentration boundary layer. A design goal is to keep the boundary layer as thin as possible, while allowing enough time for a particle approaching the surface to have its double layer compressed by the high ion concentration. In this manner a minimum amount of chemical destabilizing agent would be added.

The convective diffusion equation

$$\frac{\partial n_\ell}{\partial t} + \vec{v} \cdot \nabla n_\ell = \nabla \cdot D_\ell \nabla n_\ell \qquad \text{(III-B-1)}$$

governs the mass concentration n_ℓ of species "ℓ". The velocity field $\vec{v}$, for an incompressible fluid is given by the solution of the Navier-Stokes equation

$$\frac{\partial \vec{v}}{\partial t} + \vec{v} \cdot \nabla \vec{v} = - \frac{1}{\rho_f} \nabla p + \frac{1}{\rho_f} \nabla \cdot \mu \nabla \vec{v} \qquad \text{(III-B-2)}$$

where p is the pressure and μ is the absolute viscosity. The Navier-Stokes equations are subject to the boundary conditions

$$\vec{v}_r = \vec{J}_w \bar{V} \quad \text{on the collector surface,}$$

$$\vec{v}_\theta = 0 \quad \text{on the collector surface,}$$

$$\vec{v} = \vec{U} \quad \text{far from the collector,}$$

where $\vec{v}_r$ is the radial velocity, $\vec{v}_\theta$ is the tangential velocity, $\vec{J}_w$

is the flux of solvent and $\bar{V}_w$ is the molar volume of the solvent.[1] Equations III-B-1 and III-B-2 are coupled through the boundary conditions which depend upon the activity of the solvent and hence upon the concentrations of the species "ℓ". The solution of this system of equations is difficult, and the following simplifying assumptions are employed to arrive at an estimate of the mass transfer coefficients:

1. The two dimensional steady solution is sought.
2. The Reynolds numbers, N_{Re}, of the flow is small so that the solution of the Oseen equations gives the velocity field around the cylinder.
3. The concentrations of dissolved species are low so that the fluid properties may be assumed constant (μ, ρ_f).
4. The osmotic flow of solvent is small so that its effect on the flow field and ion distribution may be neglected, thereby decoupling the Navier-Stokes equations from the convective diffusion equation.
5. The Peclét number, N_{Pe}, is large so that thin concentration boundary layers of particles and ionic species are formed around the fibers.

The justification for assumptions 2, 3 and 5 is that the operating conditions of liquid filters generally satisfy the stated restrictions. Assumption 4 can be justified on the basis that the fluid withdrawal rate of all fibers must be small compared to the total

---

[1] See Appendix F for a discussion of the boundary conditions.

flowrate in order to achieve efficient operation of the filter. The withdrawal rate will be determined by a combination of membrane permeability and driving force (concentration or pressure gradient) which can be controlled by proper membrane design and filter operation.

The simplifying assumptions lead to the following set of equations and boundary conditions for the fluid with the coordinates described in Figure III-B-1:

$$\vec{U} \cdot \nabla\vec{v} = -\frac{1}{\rho_f}\nabla p + \nu\nabla^2\vec{v} \qquad \text{(III-B-3)}$$

and boundary conditions

$$\vec{v} = 0 \quad \text{on } r = a_f$$
$$\vec{v} = \vec{U} \quad \text{as } r \to \infty \ .$$

The solution has been given by Lamb (1932) in terms of the stream function.[1] For the thin concentration boundary layer analysis only the first term, describing the flow near the cylinder, is retained

$$\Psi = 2A_F U \frac{(r-a_f)^2}{a_f} \sin\theta \ . \qquad \text{(III-B-4)}$$

The convective diffusion equation takes the form:

$$\vec{v}\cdot\nabla n_\ell = D_\ell \nabla^2 n_\ell \qquad \text{(III-B-5)}$$

---

[1]The velocity field is defined by the stream function by the relations:

$$v_r = \frac{1}{r}\frac{\partial\Psi}{\partial\theta}$$
$$v_\theta = -\frac{\partial\Psi}{\partial r}$$

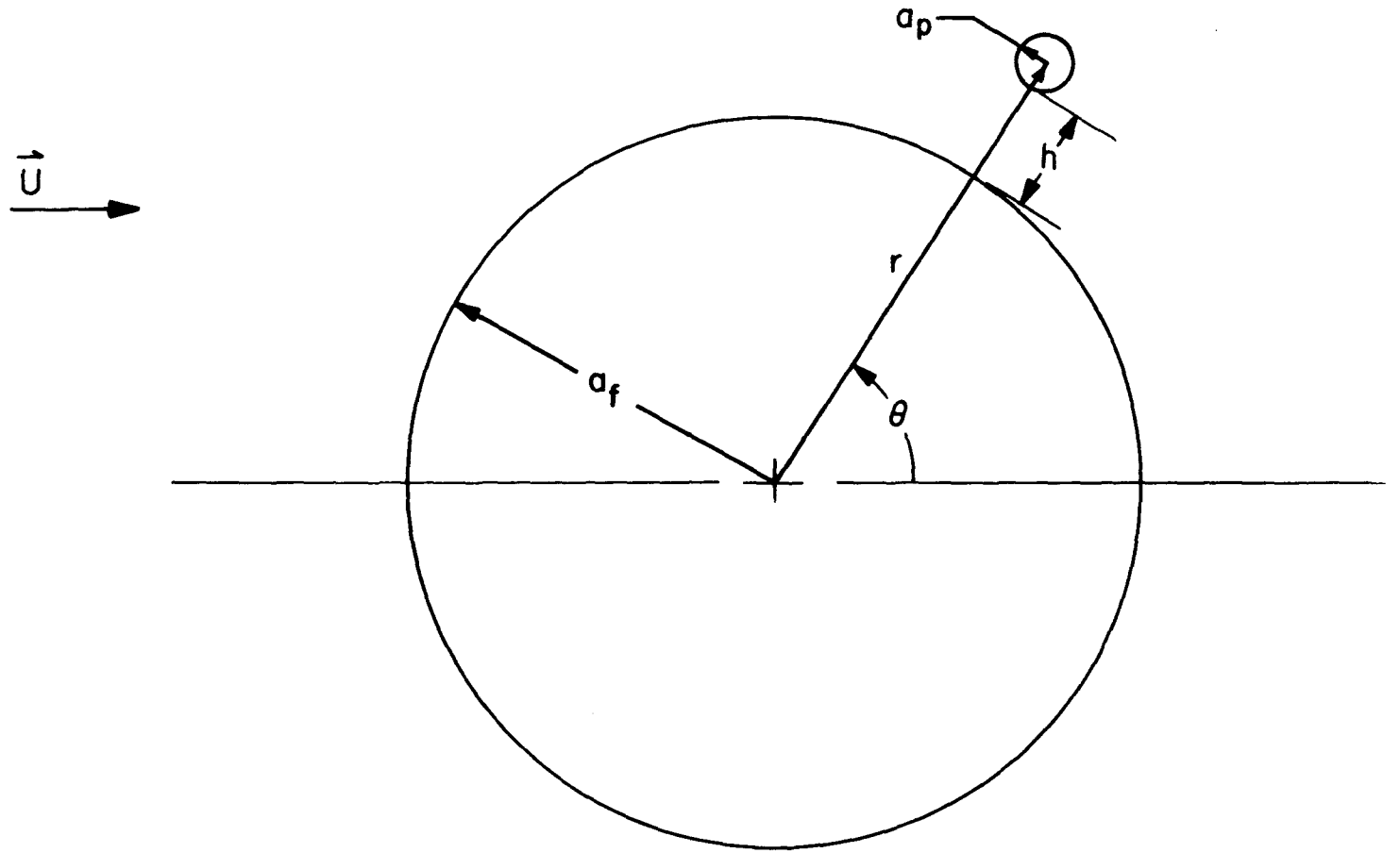

Figure III-B-1 Polar Coordinate System

and the boundary conditions

$$n_\ell = n_{\ell,\infty} \quad \text{as } r \to \infty$$

$$J_\ell(\theta) = -D_\ell \frac{\partial n_\ell}{\partial r} = \frac{\varphi_{m,\ell}}{\delta_m} \Delta n_{m,\ell} \quad \text{at } r = a_f ,$$

where $\varphi_{m,\ell}$ is the permeability of the membrane, δ_m the thickness of the membrane and $\Delta n_{m,\ell}$ the concentration difference across the membrane wall. The flux can readily be controlled by varying wall thickness, permeability and internal ion concentration.

The second boundary condition causes difficulty in obtaining an analytic solution since it is determined by the solution of the concentration field. Two special cases will be considered here which permit evaluation of the functional dependence of the ratio of the mass transfer coefficient of the particles to that of the electrolyte.

Consider the case when the flux through the surface is a known constant, J_ℓ. This corresponds to the situation where the major resistance to diffusion of the electrolyte is contributed by the membrane. Define an average mass transfer coefficient, $k_{\ell,av}$, by the equation

$$J_\ell = k_{\ell,av} \Delta n_{bl,\ell} , \qquad \text{(III-B-6)}$$

where $k_{\ell,av}$ is the average transfer coefficient and $\Delta n_{bl,\ell}$ is the concentration difference across the boundary layer. J_ℓ must be large enough to maintain a minimum value of the surface concentration to destabilize the entire surface of the fiber. Therefore the mass transfer coefficient can be estimated by

$$k_{\ell,av\ minimum} = \frac{J_{\ell,minimum}}{\Delta n_{bl,\ell}} = \frac{-D_\ell}{\Delta n_{bl,\ell}} \frac{\partial n_\ell}{\partial r} \propto \frac{D_\ell}{\delta_{bl}} \qquad \text{(III-B-7)}$$

where δ_{bl}, the concentration boundary layer thickness, is approximately proportional to

$$\delta_{bl} \simeq \frac{d_f^{2/3} D_p^{1/3}}{A_F^{1/3} U^{1/3}} \quad .$$

The mass transfer coefficient for the particles is proportional to

$$k_{p,av} \propto \eta \cdot U \quad . \qquad \text{(III-B-8)}$$

Therefore, the ratio of the two coefficients when interception is important (using η_{GIM}) is

$$\frac{k_{p,av}}{k_{\ell,av}} \propto \frac{d_p^2 A_F^{2/3} U^{2/3}}{d_f^{4/3} D_\ell^{2/3}} \quad . \qquad \text{(III-B-9)}$$

For efficient operation the goal is to maximize the ratio while maintaining a minimum concentration of "ℓ" at the surface of the fiber. This can be done by choosing less rapidly diffusing electrolytes, smaller fiber diameters and higher flow velocities.

The second case to be considered is that of a constant concentration surface as the boundary condition in Equation III-B-5. This corresponds to the case where the membrane has very low resistance to diffusion compared to diffusion to the the bulk solution. A solution to this problem has been given by Friedlander (1957) for the conditions assumed here. Only the result is presented. Friedlander found that the Nusselt number, N_{Nu}, a dimensionless transfer coefficient, was given by

$$N_{Nu} = 1.035 \ (A_F \cdot N_{Pe}^{1/3}) \quad . \qquad \text{(III-B-10)}$$

Since the average mass transfer coefficient is related to the Nusselt number by

$$N_{Nu} = k_{\ell,av} \cdot \frac{d_f}{D_\ell} \quad ,$$

then

$$k_{\ell,av} = 1.035 \left(A_F \frac{d_f U}{D_\ell}\right)^{1/3} \cdot \frac{D_\ell}{d_f} \quad . \qquad \text{(III-B-11)}$$

The ratio of particle to electrolyte transfer in this case is

$$\frac{k_{p,av}}{k_{\ell,av}} \propto \frac{d_p^{\,2} \, A_F^{\,2/3} U^{2/3}}{d_f^{\,4/3} \, D_\ell^{\,2/3}} \quad . \qquad \text{(III-B-12)}$$

The behavior of the real system should be between the two extremes represented by Equations III-B-9 and III-B-12. The functional dependences do not differ so that the following criterion may be established:

> When the ratio of mass transfer coefficients is large, (as given by Equations III-B-9 and III-B-12) the use of hollow fibers will decrease the amount of electrolyte which needs to be added to the solution and increase the collection efficiency.

Presumably, the membrane permeability can be tailored to meet the requirements of the destabilizing agent. For simple electrolytes, membranes with low molecular weight cutoffs would be needed to prevent rapid loss of electrolyte. For heavier polyelectrolytes more porous membranes could be used. An advantage of a more porous membrane is that it might reduce manufacturing costs, since membrane defects would be less critical.

Chapter IV

IV. Experimental Design, Apparatus and Procedures

A. Design of Experiments

A test section was designed to permit control of the hydrodynamic and chemical conditions of the experiments. The flow past a single fiber mounted in the test section approximated that of a uniform stream past an isolated cylinder of infinite length, with the fiber axis oriented transverse to the direction of flow. Flow conditions were laminar. During particle deposition experiments the fiber Reynolds number was maintained less than unity to prevent circulating eddies and vortex shedding on the downstream portion of the fiber.

Red blood cells (RBC) were chosen as the bioparticle because of their interest in blood filtration. Styrene-divinylbenzene copolymer latex (SDVBL) spheres of approximately the same size (7.6 μm) were used for comparison. Both types of particles were deposited from dilute suspensions on the single fiber collectors under a variety of surface chemical conditions.

The hydrodynamics of single collectors has been thoroughly studied, hence the transport efficiencies could be calculated (see Section II-A) without the additional assumptions needed for packed beds or arrays. Fibers were used because they are inherently easier to handle and are a common filter material.

Dilute suspensions prevent complicating interactions of particles with one another and the flow. Dilute suspensions are of interest

because they represent the usual conditions under which filters are operated. In the case of whole blood, however, the volume fraction of the cells is about 40% so that dilute suspensions are a large departure from reality. The primary interest in RBC here was the effect of surface chemistry on deposition rates.

The particle deposit was counted with a microscope as a function of time in situ. This prevented changes in the deposit which occurred if the fiber was removed from the test section for counting. The particle concentration was simultaneously measured with a Coulter Counter. Experimental collection efficiencies could then be calculated and compared with theoretical values. The effects of changes in surface chemistry were reflected in the deposition data. Visual observation of the particles depositing also provided information about the transport and attachment mechanisms.

The VODL theory was tested using 2.0 μm polyvinyltoluene latices (PVTL) depositing on a flint glass fiber. A simple electrolyte (cation Na^+) was used to vary the ionic strength of the solution at fixed pH (phosphate buffer). Deposition rates were measured and concentrations determined as in the previous experiments. The zeta potentials of the glass and PVTL surfaces were determined from mobility measurements and checked against the range of reported literature values. Using the zeta potentials, total potential energy curves were calculated by the method described in Section II-B. It should be possible to relate the experimental data to theory if the VODL model applies.

The 2.0 μm PVTL spheres were used because they have smooth surfaces compared to the SDVBL spheres (Figure IV-B-8). This should permit them to conform to the theoretical assumptions more closely. A pH of about 7.0 pH units was chosen since at this pH the ionizable groups of the latices are believed to be fully dissociated (Kasper, 1971;Ottewill and Shaw, 1967). A phosphate buffer which did not appear to interfere with the surface properties of either material was used to maintain constant pH.

Hollow fiber experiments were designed to study the effect of simple electrolyte (NaCl) addition, through the membrane wall, on the deposition rate of a variety of latex particles (2.0 μm PVTL; 3.5, 5.7, 7.6, 9.5 and 25.7 μm SDVBL). Two different cellulose-acetate fibers were used. One had a low molecular weight cutoff, 200-300 MW (CA-a), while the other had a higher value 30,000 MW (CA-c). The low molecular weight fiber allowed slow diffusion of the electrolyte to the particle suspension. Concentrations of electrolyte on either side of the membrane were varied systematically to study the effects of concentration differences on the flow field as well as on the double layer. The CA-c fiber was used to study the effect of the flow field on deposition and to provide a vivid demonstration of the importance of surface chemical effects (see Section V-C-1 and Figure V-C-3). The accumulated deposit was measured as a function of time in similar fashion as previous experiments. The distribution of particles over the fiber surface was also noted as a qualitative test of the boundary layer model.

Data from the experiments with negligible double layer repulsion could be used to check the HRM. The adhesion number could be calculated using a value for the Hamaker constant based on VODL theory and the 2.0 μm PVTL experiments. The Hamaker constant could be checked against the range of values reported by Gregory (1969). The plot of efficiency ratio, η_{EXP}/η_{GIM}, versus adhesion number, $N_{Ad,f}$, could be compared with the theoretical curve of η_{HRM}/η_{GIM} versus $N_{Ad,f}$, as a test of the correctness of the theory. Additional data points gathered under a variety of conditions by varying the flowrate and pH of the suspension could also be used to test the HRM.

The CA-c hollow fiber was used to test whether hydrodynamic resistance truly is a factor in retarding the deposition rate of particles. This was accomplished by withdrawing fluid into the fiber interior at a known rate and measuring the change in the deposition rate. An increase in the deposition rate, above that which could be accounted for by particles convected to the surface by fluid withdrawal, would be evidence for hydrodynamic retardation.

B. Description of Experimental Apparatus and Materials

B-1. The test apparatus

A transparent water tunnel (Figure IV-B-1) was constructed entirely out of plexiglass. Its depth was governed by the working distance of the microscope objectives used (Leitz UMK 32X "high dry" objective; American Optical 10X objective). The length and breadth of the tunnel were adequate to ensure fully developed Poiseuille flow

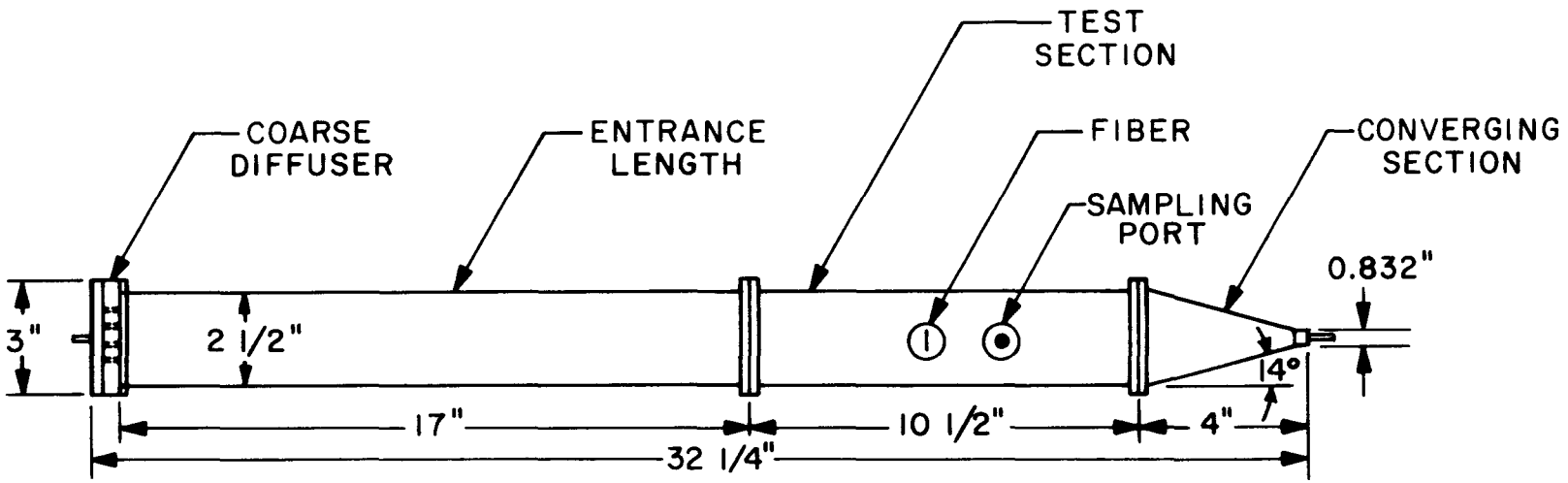

TEST SECTION INTERIOR CROSS-SECTION: 5/16" DEEP × 2" HIGH
COARSE DIFFUSER ~ 4 HOLES 1/4" DRILL SPACED 3/4" APART

Figure IV-B-1 Schematic of Plexiglass Water Tunnel Showing Overall Dimensions

in the test section.[1] A coarse diffuser was placed at the entrance of the tunnel to prevent jets from propagating into the test section. By throttling the flowrate from a constant head tank, the maximum velocity at the mid-depth of the test section could be smoothly varied or maintained constant.

Rotameters were calibrated volumetrically and placed between the constant head tank and the tunnel. The centerline velocity in the test section could then be calculated from the assumed Poiseuille velocity profile. An independent check of the centerline velocity was performed using a hydrogen bubble marker technique.[2] The tests gave results consistent with the calculations (less than 2% difference).

A fixture for holding the fibers was constructed from plexiglass and copper wire or stainless steel tube supports (Figure IV-B-2). Glass fibers were mounted through holes drilled in the "0.027" diameter copper wires and tacked in place with a diluted solution of "Liquid-Tape".[3] Teflon fibers were threaded through 0.025" (outside) diameter hypodermic needle tubing and tacked in place with "Liquid-Tape". Hollow fibers were mounted in 0.028" (outside) diameter annealed stainless steel (304) tubing. A watertight seal was formed using

---

[1] Entrance lengths were computed from formulae given by Schlicting (1968).

[2] Details of the technique are given by Schraub et al. (1965).

[3] Liquid insulating material, a product of G. C. Electronics, Rockford, Illinois.

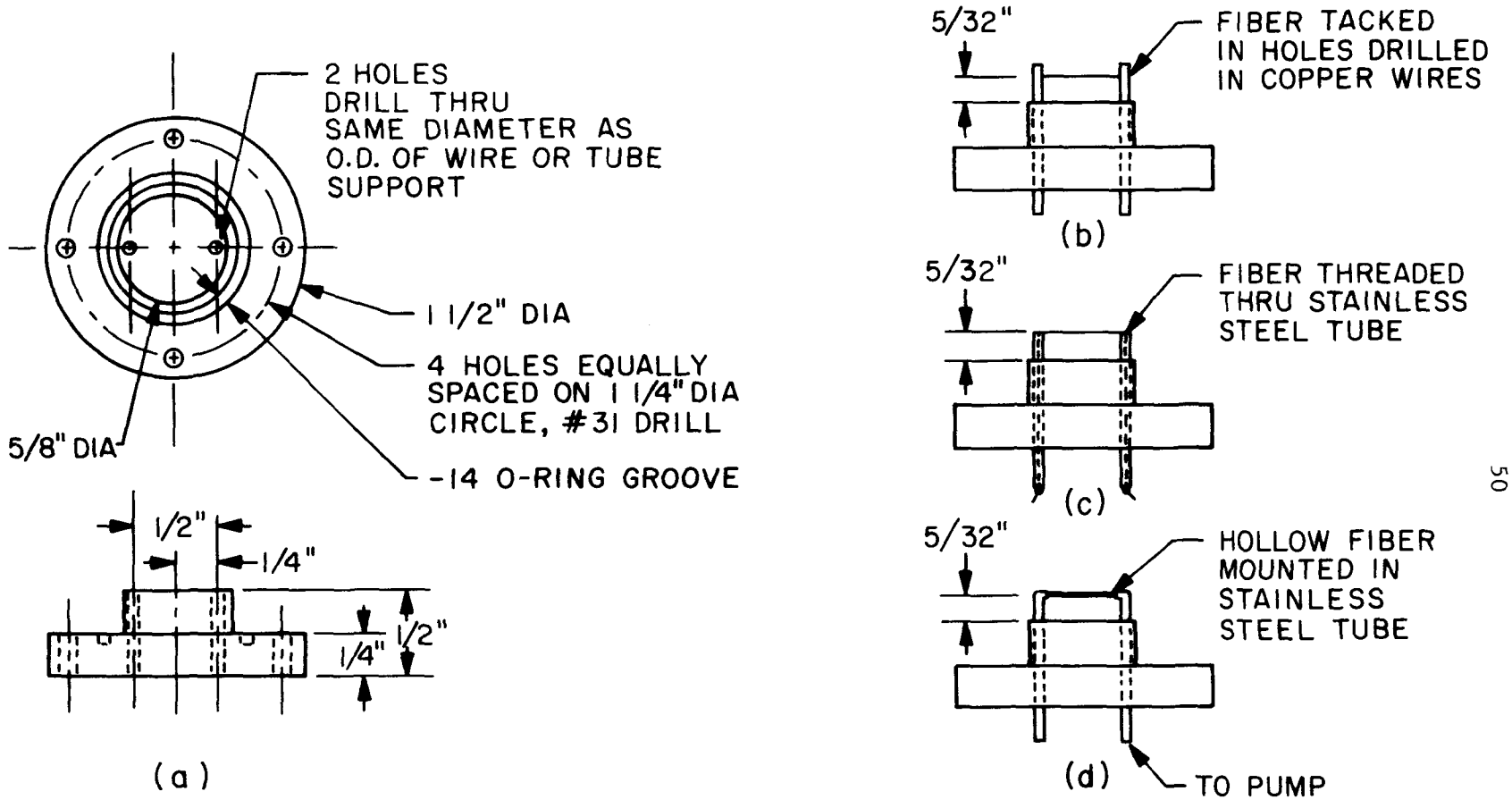

Figure IV-B-2 Schematic of Fiber Supports

a) Overall Dimensions of Support b) Glass Fiber Through Copper Wires c) Teflon Fiber Through Stainless Steel Tube d) Hollow Fiber Through Stainless Steel Tube

"Silastic 140" silicone rubber adhesive.[1]

The fixtures were mounted in ports drilled in the test section and fit flush with the test section wall. The fibers were positioned at the mid-depth of the test section. They were oriented with their axes parallel to the apex of the parabolic velocity profile. Since the fiber diameters were much smaller than the depth of the test section and the velocity gradients low at the apex of the parabola, the flow approximated that of uniform flow past a cylinder (Figure IV-B-3).

The tunnel itself was clamped to the microscope stage with the test section containing the fiber in the field of view of the microscope (Figures IV-B-4 and IV-B-5). The microscope was tilted 90° relative to its normal orientation so that the action of gravity was along the fiber axis. A system of counterweights balanced the weight of the tunnel so that the stage could be positioned freely. A microscope illuminator built into the base provided adequate back lighting. This could be supplemented by external lighting when needed.[2] Convection due to heating was negligible when the fluid was flowing, but was noticeable when the flow was stopped. As a precaution, the

---

[1]The hollow fibers had to be kept moist or else they would dry and shrivel up irreversibly. The silicone rubber adhesive has the advantage of being able to cure under water. "Silastic 140" is a product of Dow Corning, Midland, Michigan.

[2]The fibers used all had refractive indices close to that of water so that they appeared transparent.

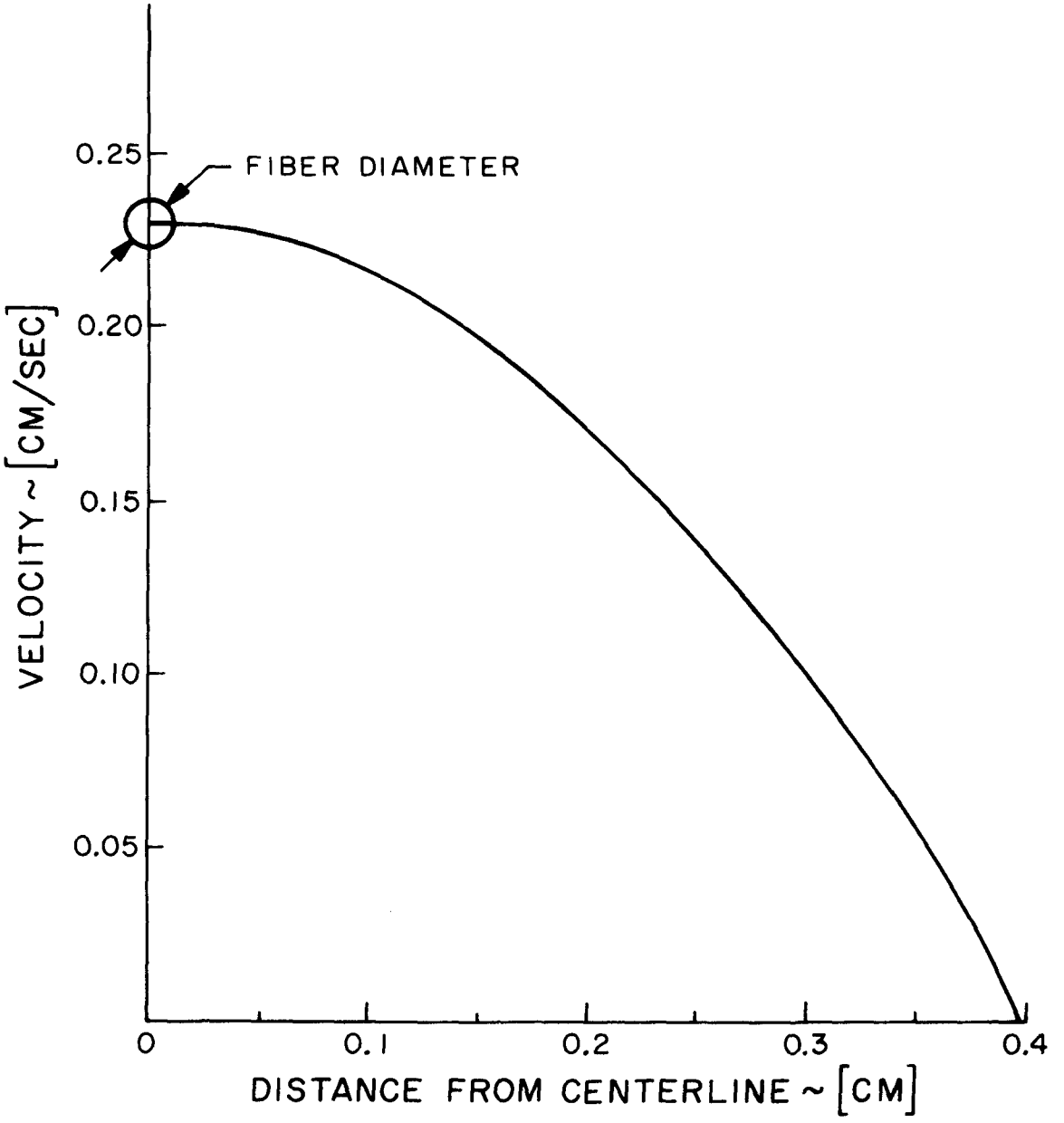

Figure IV-B-3 Comparison of Typical Undisturbed Poiseuille Velocity Profile to Hollow Fiber Diameter 230 μm

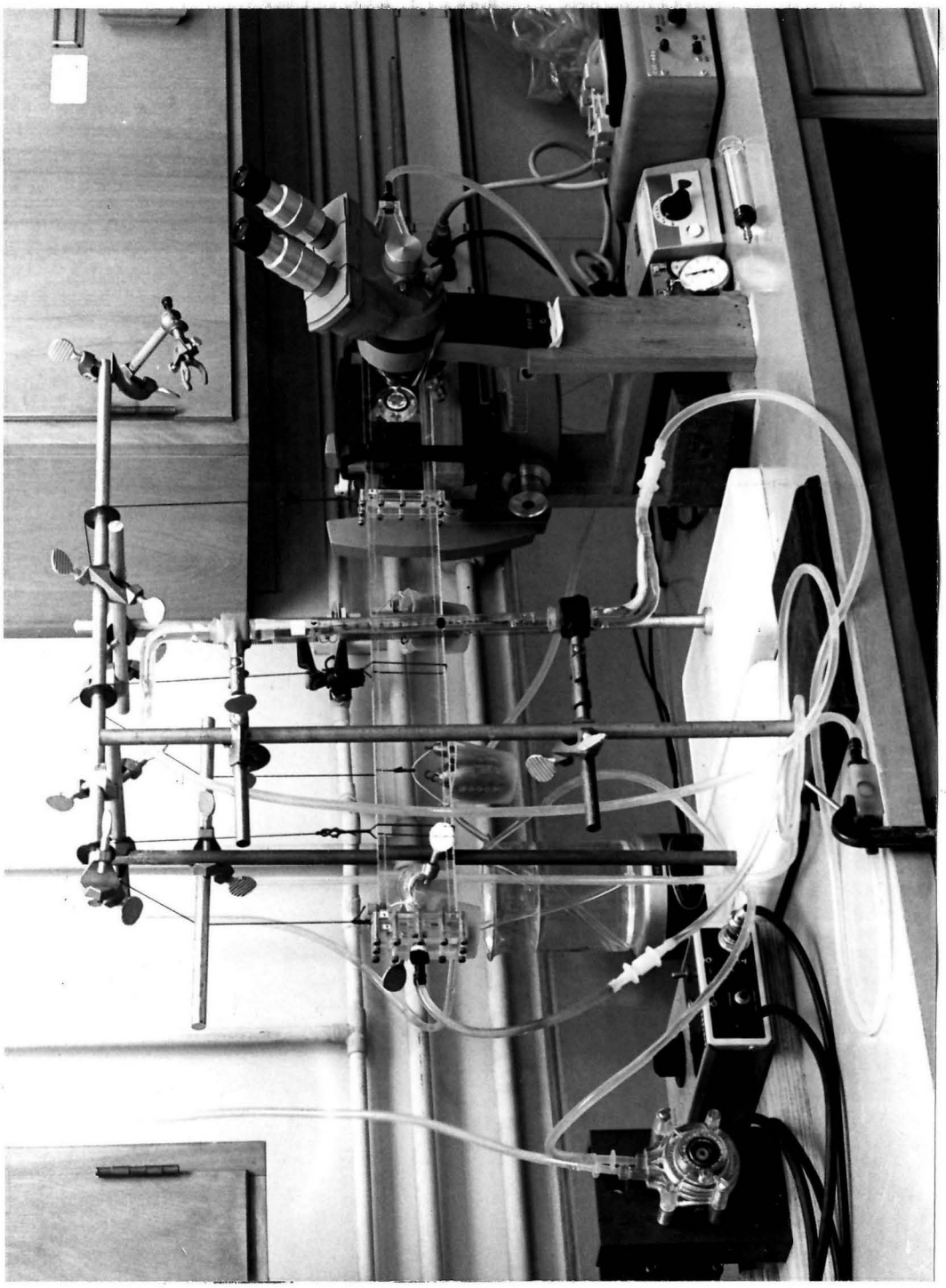

Figure IV-B-4 Photograph of Experimental Apparatus

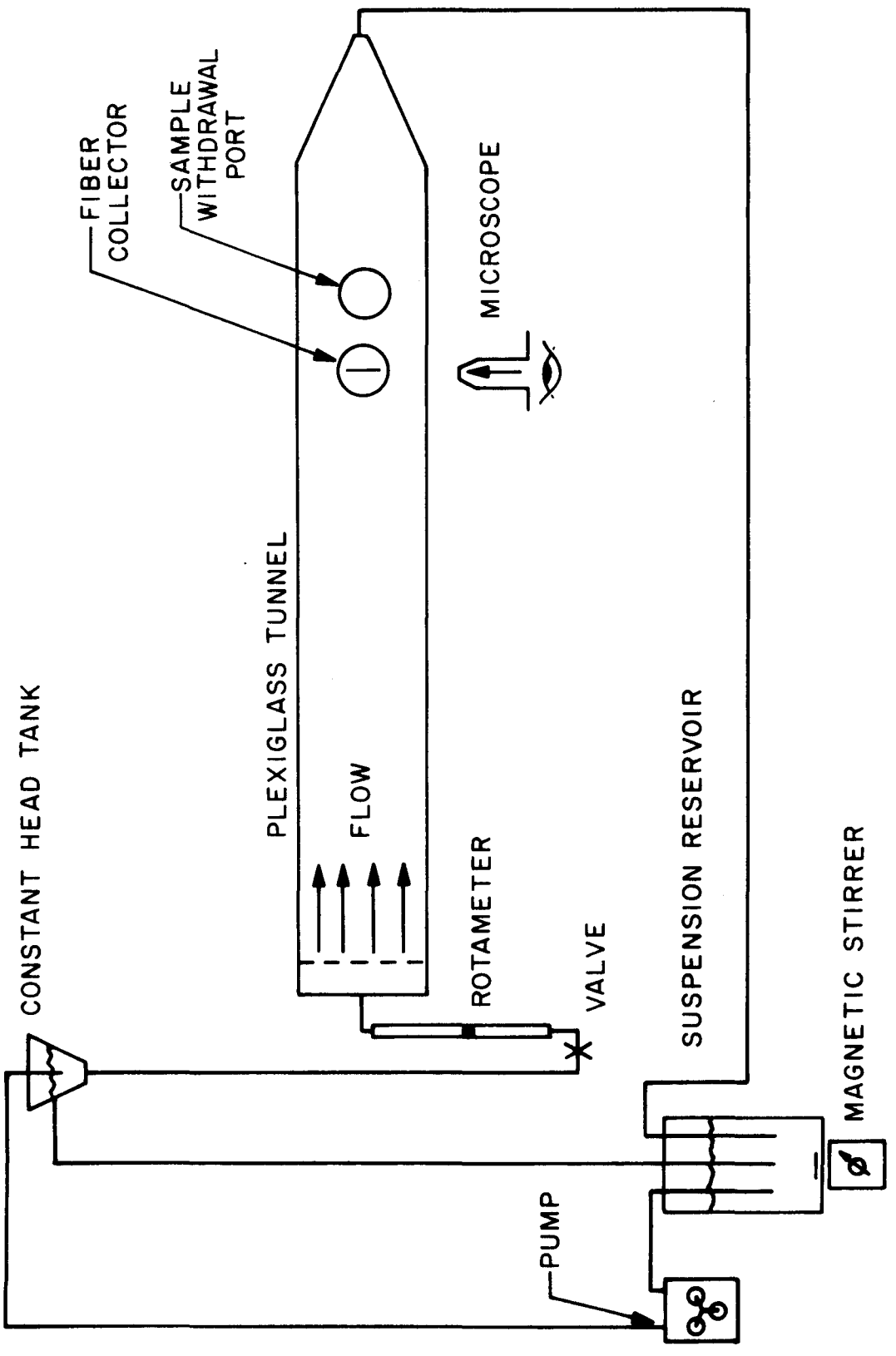

Figure IV-B-5 Schematic of Experimental Apparatus

illuminator lamp was turned off between observations. Particle counts were made normal to the direction of flow over a region which was not influenced by the fiber supports.

A peristaltic pump[1] transported the particle suspension from the magnetically stirred reservoir to the constant head tank. From there, the suspension either passed through the rotameter and tunnel back to the reservoir or directly back to the reservoir through the overflow line. The tunnel, tubing, constant head tank and reservoir formed a closed recirculating system. It was possible to thermostat the reservoir, but this was found to be unnecessary since the reservoir temperature did not change by more than one or two degrees centigrade.

A second variable speed peristaltic pump[2] was connected to the hypodermic needle supports to pass electrolyte through the hollow fiber interior. The electrolyte was pumped from a reservoir at a high rate to minimize concentration differences between the inner surface of the membrane wall and the bulk electrolyte. The mechanical pressure difference was small compared to the osmotic pressure difference. In cases where the interior and exterior electrolyte concentrations were equal, pumping was discontinued.

---

[1]The Masterflex tubing pump head was driven by a Bodine speed reducing motor with Minarik speed control.

[2]Holter Company, Bridgeport, Connecticut.

B-2. Suspension characteristics

The suspension pH was measured with a Beckman Model G pH-meter standardized against commercial buffers of known value.[1] Conductivity was measured with a Radiometer conductivity meter of known cell constant. These samples were taken from the reservoir. The pH measurements indicated no significant changes during the course of any runs. The conductivity measurements were made during hollow fiber runs to estimate the rate of addition of electrolyte. This also served as a check against leaks in the fiber-support system and incorrect preparation of solutions.

The osmolarity of the buffer solution used for maintaining red blood cells (RBC) was determined with a freezing point depression osmometer. The Osmette 2007[2] was calibrated against commercial standards of 100 and 500 milliosmols. Reproducibility to ±3 milliosmols was achieved routinely. With special care better precision can be achieved.

Electrophoretic mobilities were measured using the procedure of Black and Smith (1962). Palladium electrodes described by Neihof (1969) were used in the horizontal rectangular Briggs cell. The palladium electrodes have the advantage of not giving off gas bubbles even with high ionic strength solutions. Mobilities were measured as a function of time lapsed after preparation of the particle

---

[1] Calomel and glass electrodes were used. The pH values reported are the raw readings.

[2] A product of Precision Systems.

suspensions. The glass fibers were ground with a mortar and pestle in order to obtain glass particles whose mobilities could be measured.

Concentration samples were obtained from a point immediately downstream of the fiber. Sampling was accomplished using a hypodermic needle and syringe. The sampling rate was slow enough to prevent break-up of any aggregates by shearing forces in the needle. The samples were diluted and counted with a model B Coulter Counter (Figure IV-B-6). The Coulter Counter was initially checked against hemocytometer measurements and gave excellent agreement.

The large particles were sized optically with a filar micrometer eyepiece (American Optical 10X) calibrated against a stage micrometer (Edscorp 0.01 mm divisions). This was done primarily to check the particle manufacturer's specifications. Generally, the geometric mean size[1] agreed with the stated size within the limits of statistical error, but the geometric standard deviations were somewhat larger.[2] Late in the study, a particle sizing amplifier and multichannel analyzer were added to the Coulter Counter. Size distributions obtained using this system agreed with the optical measurements. They could be approximated by a log-normal distribution

---

[1]The size distributions were fitted by a log-normal size distribution.

[2]Inquiries into the method of measurement used by the manufacturer suggest that particles "obviously" differing in size from the mean are not included in the distribution. This included doublets and larger aggregates. These were found to constitute roughly 5-10% of the particles. The reason for this is presumed to be because the latices are used for electron microscope calibrations. In that case the mean size must be accurately known. Singlets of the same apparent size would be used as the standard.

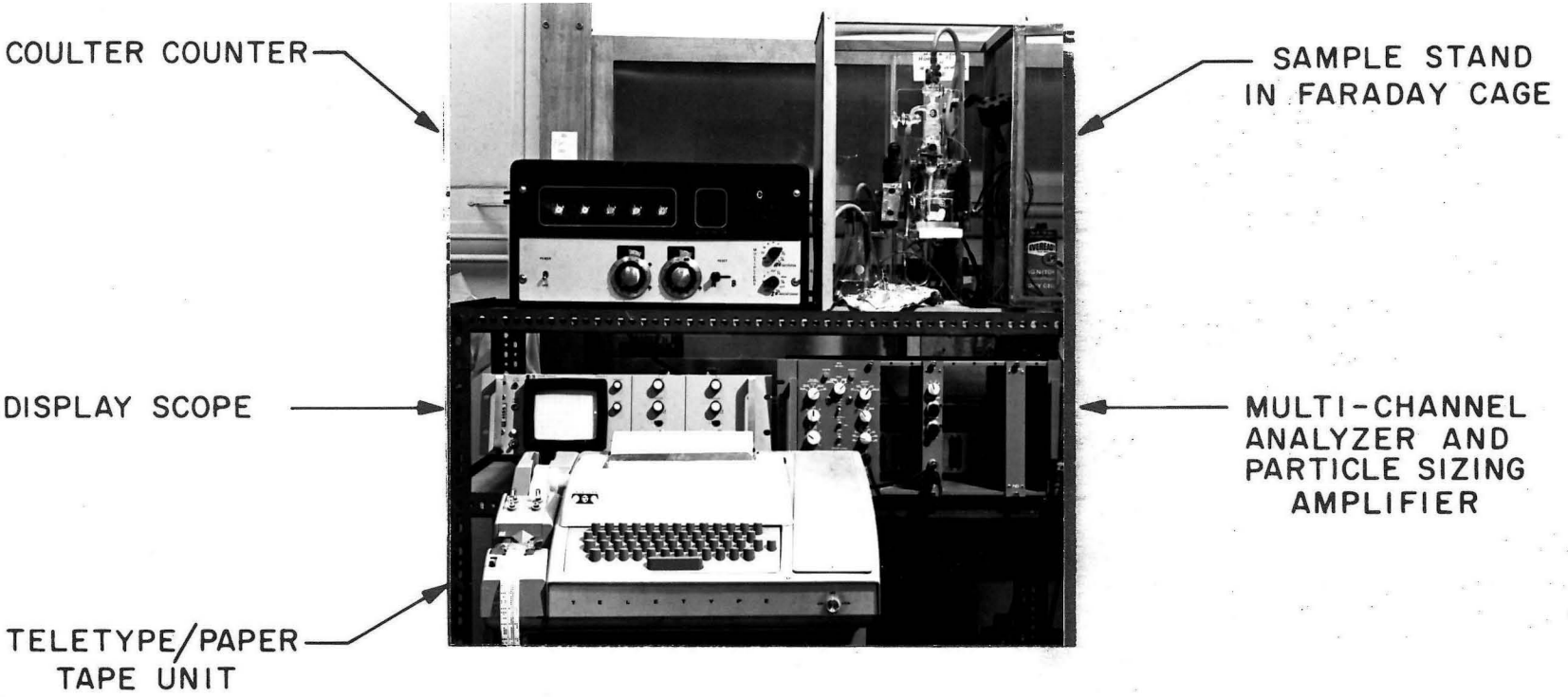

Figure IV-B-6 Particle Counting System

except in the upper tail of the distribution. The mean size of the latices was taken to be that given by the manufacturer because they reported a larger number of measurements. However, the standard deviations used to estimate size distribution effects were taken to be those measured optically and by the Coulter Counter.

B-3. Cellulose Acetate-c permeability measurement

To conduct the fluid withdrawal experiment, it was necessary to measure the flux of solution through the CA-c membrane as a function of the applied pressure difference. A convenient means for doing this proved to be to seal a section of fiber between two pieces of polyethylene tubing (0.023" inside diameter). One piece of tubing was closed off while a vacuum was applied to the other. The exposed fiber was immersed in solution in a plastic petri dish mounted on a microscope stage (Figure IV-B-7). An air bubble trapped in the polyethylene tube served as a marker. The advance of the bubble was measured as a function of time using a filar micrometer eyepiece and a stopwatch. Knowledge of the fiber dimensions and polyethylene bore permitted calculation of the flux. A mercury manometer was used to measure the pressure differential.

This technique requires a few precautions in order to achieve accurate reproducible results. First, the fiber and all associated tubing must be allowed to equilibrate under the applied pressure before making any measurements. Second, dissolved gases should be removed either by boiling or reduced pressure before the solution is used. Third, "cold" lighting should be used to prevent thermal

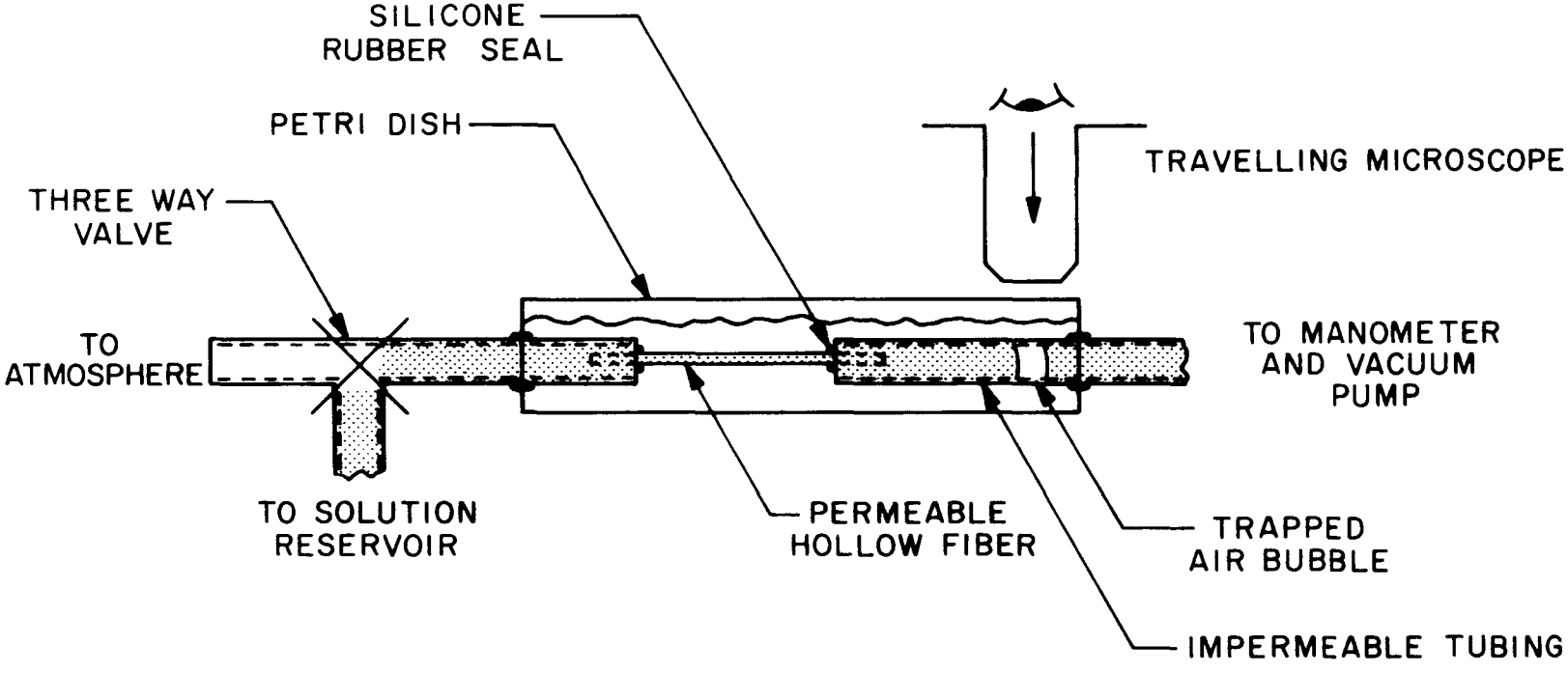

Figure IV-B-7 Schematic of Hollow Fiber Permeability Measurement Apparatus

expansion effects. The advantage of the apparatus described was that single fibers could be measured, then mounted in the test section. As it turned out, sampling of the fibers indicated that the permeability was uniform within the experimental error of the measurement.

B-4. Materials

All chemicals used in the study were of analytical reagent grade. All solutions were prepared with distilled deionized water (DDH_2O) and subsequently filtered with 0.45 μm millipore filters. The RBC buffer ingredients and proportions are listed in Table IV-B-1. The buffers used in the varying cation concentration experiments were equimolar solutions of sodium phosphate, di-hydrogen (NaH_2PO_4) and sodium phosphate, monohydrogen (Na_2HPO_4). They are reported in terms of the total cation concentration.

The source of red blood cells was either banked blood preserved with acid citrate dextrose and refrigerated at 4^{o} C or fresh blood drawn by finger puncture. The fresh blood was diluted with the isosmolar,pH 7.4 buffer during collection in order to prevent coagulation. The cells were centrifuged and the buffy coat removed. They were then mixed with at least ten times their volume of buffer, shaken and centrifuged after which the supernatant was drawn off. This was repeated five times.[1] The washed cells were allowed to stand

---

[1]The washing procedure caused the particles to become crenated. Incubation with adenosine was found to restore their shape; however, the treatment was abandoned as it was feared that it might affect the surfaces of the cells and fiber.

Ingredient	Amount*
NaCl	17.60 gms
KH_2PO_4	5.40 gms
Na_2HPO_4	32.15 gms

*To make 4 liters of isosmolar buffer, 294 milliosmols; pH ~7.4.

Table IV-B-1 RBC Isosmolar Buffer Recipe

at room temperature until they were needed (normally less than a few hours).

All but one of the latices used in these experiments were obtained from the Dow Chemical Company, Midland, Michigan. The 9.5 μm SDVBL was obtained from Duke Standards, Palo Alto, California. The known properties of the latices and RBC are listed in Table IV-B-2. The method employed to grow the PVTL and SDVBL particles to their final size differs,[1] and this results in a difference in the surface roughness as determined by electron microscopy (Figure IV-B-8). The latices were not dialysed before use. This may have resulted in the latices acting as hydrophilic rather than hydrophobic surfaces.

Several different fibers were employed in the deposition experiments. The 4-mil teflon monofilaments are a copolymer of tetrafluoroethylene and hexafluoropropylene (FEP).[2] The glass fibers were drawn from soft glass rod (flint glass). Hollow fibers were composed of cellulose acetate with different molecular weight cutoffs.[3] The fiber properties are summarized in Table IV-B-3.

The order of the roughness of the teflon fiber was about a few microns. Whether the surfaces were smooth between rough spots was

---

[1]The PVTL are believed to be grown by emulsion polymerization (Vanderhoff, 1972) whereas the SDVBL are probably grown by a combination of coagulation and polymerization (Wiley, 1954).

[2]A product of DuPont, Wilmington, Delaware.

[3]Osmolyzer (CA-a,200 MW) and Ultrafilter (CA-c, 30,000 MW) are products of Dow Chemical Company distributed by Bio-Rad Laboratories, Richmond, California.

Particle	Shape	Density $\sim [gm/cm^3]$	Diameter $\sim [\mu m]$	Surface
RBC	Biconcave disc	1.11	7.5	anionic - carboxyl groups
PVTL	sphere	1.03	2.0	anionic - possibly sulfate, sulfonate or hydroxyl[1]
SDVBL	"	1.06	3.5	Triton X-305[2] non-ionic
"	"	1.05	5.7	anionic - possibly sulfate, sulfonate or hydroxyl
"	"	"	7.6	" " "
"	"	1.06	9.5	Triton X-305 non-ionic
"	"	1.05	25.7	anionic - possibly sulfate, sulfonate or hydroxyl

[1]Private communication with J. W. Vanderhoff, 1972.

[2]Private communication with Duke Standards Co., Palo Alto, California.

Table IV-B-2 Properties of Particles Used in Experiments

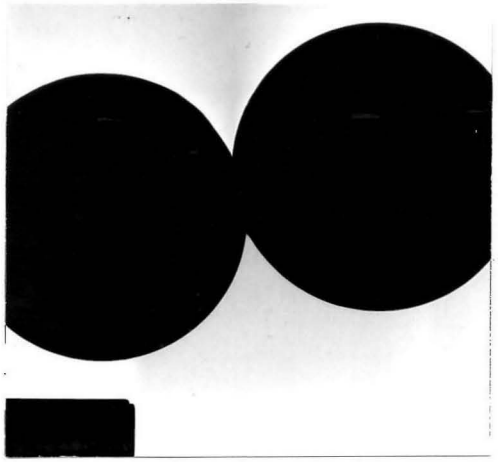

2.0 μm PVTL

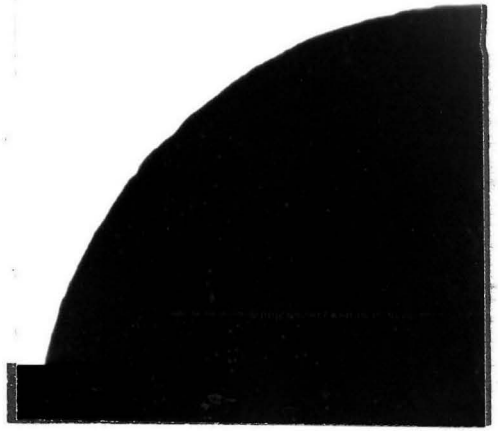

5.7 μm SDVBL

Figure IV-B-8 Electronmicrograph of 2.0 μm PVTL and 5.7 μm SDVBL at Magnification 18,800 Times

Fiber material	Diameter	Refractive Index	Surface Roughness	Permeability to H_2O
Flint Glass	~ 100 μm	~ 1.6	Subject to surface tension, < 1 μm	Impermeable
Teflon[1]	~ 100 μm	~ 1.3 - 1.4	(1 μm)	" "
Cellulose Acetate-a[2]	~ 230 μm	~ 1.4 - 1.5	Solution spun, < 1 μm	MW cutoff~200
Cellulose Acetate-c[2]	~ 230 μm	~ 1.4 - 1.5	" " "	MW cutoff~30,000

[1]Supplied courtesy of Mr. H. P. Bodenstab, Textile Fibers Dept., DuPont, Wilmington, Delaware.

[2]Cut from Beaker Osmolyzer CA-a and Beaker Dialyzer CA-c, Dow Chemical distributed by Bio-Rad Laboratories, Richmond, California.

Table IV-B-3 Properties of Fibers Used in Experiments

not known. The glass and cellulose-acetate fibers appeared to be smooth down to the limit of resolution of the optical system[1] employed ~ 0.5-1.0 μm. They are expected to be smooth because they are formed under the action of surface tension forces. The pores in the cellulose-acetate fiber were less than 100 Å in diameter.[2]

C. Experimental Methods and Procedures

C-1. Preparation of particle suspensions

The particles were suspended in the appropriate solutions with concentrations of the order of 10^3- 10^5 particles per cubic centimeter (see Section IV-B-4 for recipes). The buffered RBC were transferred to the reservoir (capacity ~ 1.7 liters for RBC and 2.0 μm latex experiments, ~ 0.9 liters for hollow fiber experiments) by pipette while the latex particles were added directly from their 10%-solids solutions either by dipping a clean glass rod into the solution or adding drops. The particles were quickly dispersed and the reservoir slowly stirred to prevent settling. No appreciable coagulation occurred during this step or during the course of the run.

C-2. Preparation of fibers

Teflon and glass fibers were cleaned overnight by soaking in a concentrated chromic-sulfuric acid solution. The glass fibers

---

[1] American Optical 45X objective N. A. 1.25 with condenser N. A. 1.25.

[2] Private communication with Mr. J. Davis, Dow Chemical Co., Walnut Creek, California.

were rinsed with copious amounts of DDH_2O and oven dried at $> 100^{\circ}C$. Then they were carefully mounted in the fixture with clean stainless steel tweezers, handling the fibers only by their ends. The teflon fibers were cleaned on their fixtures. On one occasion a teflon fiber was cleaned in a boiling nitric acid reflux apparatus to remove residual metal ions. The fiber was mounted after cleaning because the nitric acid fumes attacked the plexiglass fixture. It was impossible to thread the fiber into the stainless steel supports without handling extensive regions of the surface.

Hollow fibers were too fragile for acid cleaning and it was feared that normal solvents might change their properties in an unknown way. As an alternative, they were cleaned, after mounting, by prolonged soaking in a 1% solution of DDH_2O and formaldehyde (added as a bacteriocide). Then they were placed in an ultrasonic bath[1] with DDH_2O for final cleaning about an hour before the run.

There was a maximum power which could be applied to an intact fiber without causing it to crack. This proved to be an effective means for detecting damaged fibers since the "fractures" propagated from the damaged sites at much lower power levels. It was necessary to have several fibers ready for use since only about one in two survived the ultrasonic treatment. The fibers cleaned by this procedure appeared to be clean under the 45X objective.

---

[1] L and R Manufacturing Company, Kearney, New Jersey.

C-3. Preparation of Coulter Counter

The procedure followed for counting the particles was that detailed in the Coulter manual.[1] Spielman and Goren (1968b) have pointed out that finer resolution can be achieved in size distribution measurements by "hydrodynamic focusing," but for counting purposes this was not necessary. A Faraday cage surrounding the sample stand was helpful in decreasing noise generated by the vacuum pump. Disconnecting the stirring motor also helped reduce stray noise. Samples were swirled between counts with the largest particles used to prevent settling losses. Enough counts were taken so that in the worst case (25.7 μm SDVBL) a 4% standard deviation might be expected. Usually the accuracy was better than 1%.

Dilutions of the samples withdrawn from the test section were used to prevent large coincidence corrections and to increase solution conductivity if it was low. The particles were counted in ~ 1% NaCl solutions. The 70 μm aperture was used for all but the 25.7 μm latex particle runs in which case a 140 μm aperture was used.

A blank of the filtered solution used to prepare the particles was run, then the initial reservoir concentration was counted followed by samples at 10, 20, 35, and 50 minutes after the start of the run. Samples were taken at twenty minute intervals thereafter for the duration of the run.

---

[1] Coulter Electronics Industrial Division, Hileagh, Florida.

C-4. Preparation of tunnel and flow circuit

The tunnel was filled and stored with deionized water between runs. Before each use it was vigorously shaken and flushed with deionized water several times followed by a final rinse with the solution used to make the particle suspension. The ends were stoppered and the tunnel filled with solution through the test section port. The mounted fiber was replaced sealing the tunnel. The tunnel was then clamped to the microscope stage, counterweighted and given a very slight tilt. The seal was removed from the entrance line and connected to the rotameter. Trapped air bubbles could be removed with a hypodermic needle and syringe through a serum bottle stopper located at the entrance to the test section. The tunnel was dismantled and cleaned with a test tube brush whenever particle sizes were changed.

The constant head tank and rotameter were also kept immersed in deionized water between runs. They were flushed with solution and filled prior to each run. On occasion, incomplete rinsing after a run resulted in algal growths. A 50% ethanol - 3N hydrochloric acid solution was effective in killing the growths. The system was flushed for extended periods before the run to prevent loose filaments from entering the tunnel. Thorough rinsing of all components of the circuit with deionized water was practiced thereafter.

C-5. Deposited particle counts

A section of the fiber free from the influence of the supports was selected for counting. The length of this region was measured by the filar micrometer eyepiece. The background count on the fiber

was duly noted. Particles caught by the fiber were counted while the suspension was flowing. The midpoint of the period required to count the particle was recorded with the number deposited. The transparency of the fibers used permitted the total deposit to be counted by focusing back and forth through the fiber.

Doublets depositing on the fiber were counted as single particles since their presence could be accounted for by the size distribution data.[1] Distinguishing between doublets and two singlets apparently in contact with one another was not difficult during the initial stages of filtration. (It was possible to "remember" whether a doublet was formed from two single particles by their position on the fiber.) As the surface coverage became greater (more than a hundred particles in the field viewed) doublets posed a problem because the probability of two particles depositing in the same place increased as well as the difficulty in "remembering" whether a particle was originally a singlet. This may have resulted in a slight decrease in the counts as a function of time. Fortunately, the initial rates could be determined before this became a severe problem.

C-6. Initiation of the experiment

After all the preparatory steps and flow circuit connections had been completed, the run was started. The throttling valve was opened fully to allow particles to reach the test section in a

---

[1] The HRM comparison (Figure V-D-1) does not have size distribution corrections applied. They are probably 10-20% high as indicated by the unequal length error bars.

minimum amount of time. As soon as the particle "front" was observed at the location of the fiber, a stopwatch was started and the flow-rate set to the desired value. Particle deposits, concentration counts and suspension properties were measured as previously noted. In the event hollow fibers were being used, an initial period of deposition with no internal flow through the fiber was allowed. Then the Holter pump was turned on and electrolyte pumped through the fiber interior. Runs were terminated after a sufficient number of particles for drawing meaningful conclusions had been deposited.

The entire sequence of events has been listed in Appendix C. This sequence was generally followed with the appropriate changes in procedure where noted.

Chapter V

Experimental Results, Discussion and Conclusions

The data were collected in three groups of experiments. The goal of the first group was to compare the deposition of red blood cells (RBC) and 7.6 micron (μm) styrene divinylbenzene copolymer latex (SDVBL) suspensions on 4-mil teflon fibers (tetrafluoroethylene-hexafluoropropylene copolymer, FEP). In the second group, a study was made of the effect of varying the cation concentration of an electrolyte on the collection of 2.0 μm polyvinyltoluene (PVTL) spheres by glass fibers. In the last set of experiments, permeable hollow fibers were employed to study the effect of modifying the solid-solution interface on deposition. The results of each of the three groups of experiments are discussed separately. In addition, the experiments from each group applicable to the hydrodynamic retardation model (HRM) are dealt with as a separate unit. A summary of conclusions appears at the end of the chapter.

A. Comparison of RBC and 7.6 μm Latex Deposition

A-1. Experimental results

The original motivation for the experiments with red blood cells was to compare RBC with "inert" particles and to determine the applicability of double layer concepts to blood filtration. This goal was modified after it was realized that protein adsorption by the fiber markedly complicated the system.

Initial experiments were conducted with RBC and 7.6 μm latex suspensions flowing past a 4-mil teflon fiber collector in the test section. Although the estimated errors range from ±10 to ±50%[1], significant trends can be discerned.

Differences between the RBC and 7.6 μm latex particles were observed even though both particles have negative electrophoretic mobilities and comparable major dimensions (Table IV-B-2). Data are plotted in Figures V-A-1 through V-A-3 as the logarithm of the deposit per unit length of fiber normalized to a concentration of 1000 particles per cubic centimeter of suspension[2], versus the logarithm of the time. A slope of 45^{o} indicates constant deposition rate. Theoretical values calculated for the geometric interception model (GIM) without size distribution corrections are drawn in the same figures. Table V-A-1 shows the conditions corresponding to the different runs.

RBC deposition rates on both glass and teflon decrease sharply with time (Figure V-A-1). Changing the acid used to clean the teflon fiber from chromic-sulfuric to nitric acid resulted in a lower deposition rate. The nitric acid treatment should have removed any traces of metal ions. The time dependence observed with both treatments suggested that substances, probably protein in nature, were depositing

---

[1] See Appendix A for a discussion of the errors of measurement.

[2] This particular normalization permits some "physical feeling" for real situations.

Run #	Particle/age	Surface	$d_f \sim$ [cm]	$d_p \sim$ [cm]	$U \sim$ [cm/sec]	$\eta_{GIM} = 2A_F R^2$
1	RBC/30 days	Teflon-chromic	0.0106	0.00075	0.140	0.00130
2	RBC/<1 day	" "	"	"	0.116	0.00123
3	RBC/61 days	" -plasma	"	"	0.150	0.00132
4	RBC/<1 day	" -nitric	0.0108	"	"	0.00128
5	SDVBL/<1 day	" -plasma	"	0.00076	"	0.00131
6	SDVBL/<1 day	" -chromic	"	"	"	"
7	RBC/<1 day	" -Purifloc	"	0.00075	"	0.00128
8	RBC/<1 day	" "	"	0.00076	"	0.00131
9	RBC/<1 day	Glass-chromic	0.0105	0.00075	"	0.00134

ν = 0.0096 cm^2/sec; pH = 7.5 ± .05 (uncorrected for ionic strength); univalent cation concentration = $[Na^+ + K^+]$ = 0.198 M; T = 22°C ± 1°C

Table V-A-1 Summary of RBC-Latex-Solid Fiber Experiments

Run #	Particle	Surface	$\eta_{EXP} \times 10^3$	$\eta_{GIM} \times 10^3$	η_{EXP}/η_{GIM}	η_{EXP}/η_{GIM} *
1	RBC	Teflon-chromic	0.671	1.3	0.52	---
2	"	" - "	0.754	1.23	0.61	---
3	"	" -plasma	0.0155	1.32	0.012	---
4	"	" -nitric	0.053	1.28	0.041	---
5	SDVBL	" -plasma	1.39	1.31	1.06	0.94
6	"	" -chromic	0.41	"	0.313	0.28
7	RBC	" -Purifloc	1.32	1.28	1.03	---
8	"	" - "	1.01	1.31	0.77	---
9	"	Glass -chromic	0.50	1.34	0.37	---

*7.6μ SDVBL size distribution correction factor 1.13

Table V-A-2 RBC-Latex-Solid Fiber Efficiencies Compared to GIM

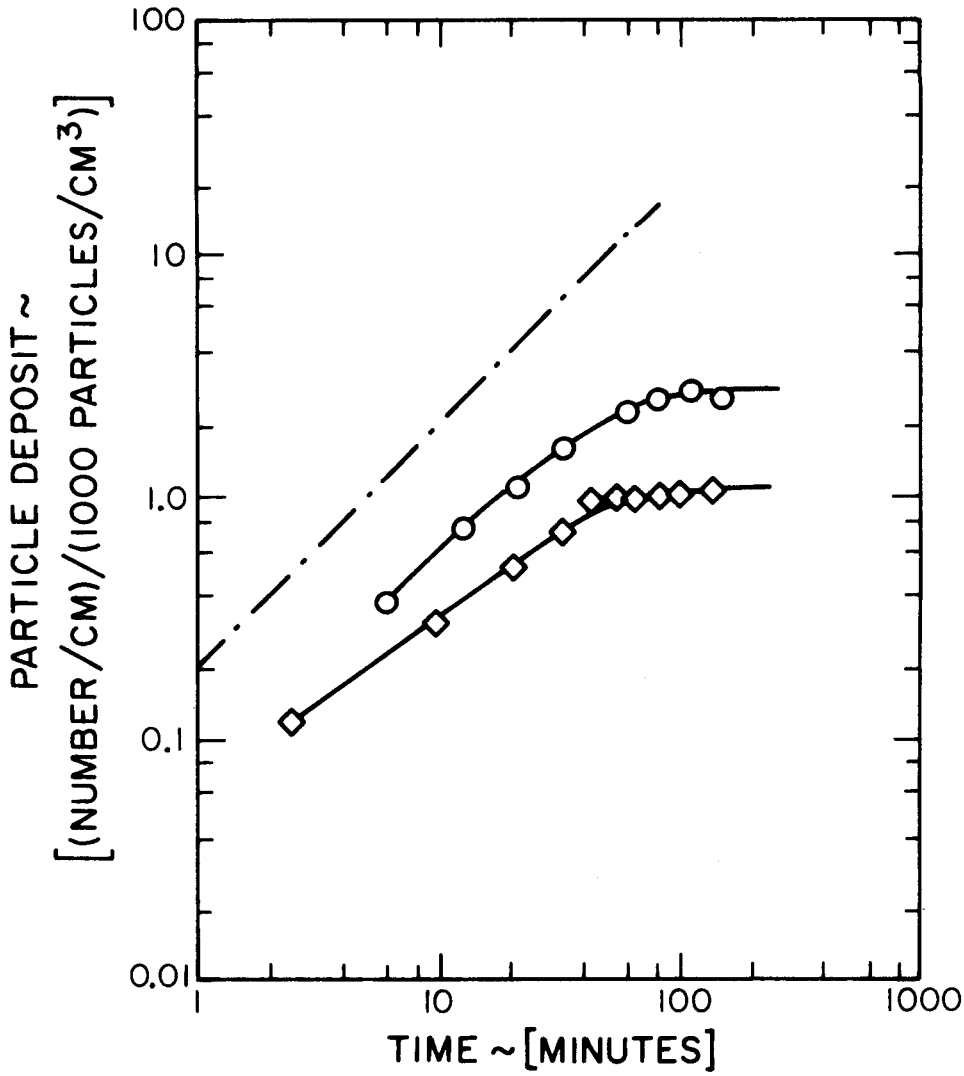

Figure V-A-1 RBC Deposition on Chromic-Sulfuric Acid Cleaned Teflon and Glass Fibers

○ RBC on Teflon, Run 1

◇ RBC on Glass, Run 9

—.—.— GIM Value for 7.5 μm Sphere

on the teflon surface. To check this, the teflon fiber was dipped into a dilute plasma solution and rinsed with a filtered, buffered, isotonic saline solution before the run. The low deposition rate obtained supports that hypothesis (Figure V-A-2).

When a comparison run was made with the 7.6 μm latex particles and a plasma-coated teflon fiber, a low deposition rate was expected because of the similar charge characteristics of the particles. Instead, the rate was much higher, reaching the maximum rate predicted by the interception theory (Figure V-A-3).

To test the effects of a positively charged surface with RBC, the teflon filter was coated with Purifloc C-41[2], a high molecular weight cationic polymer. The collection efficiency increased to roughly the value predicted by the GIM for spherical particles with 7.5 μm diameters, and the time dependence was much less pronounced.

A-2. Discussion

The initial collection efficiencies were calculated from the first data points obtained in each run. The tabulation appears in Table V-A-2 along with the theoretical efficiencies predicted by the GIM, assuming 7.5 μm diameter for the RBC and 7.6 μm diameter for the latex. Correction for size distribution was applied to the latex particles only.[1] The correction for the RBC was not significant because of its narrower size distribution. Comparison with the HRM

---

[1] See Appendix D.

[2] A high molecular weight polymer, product of Dow Chemical Co.

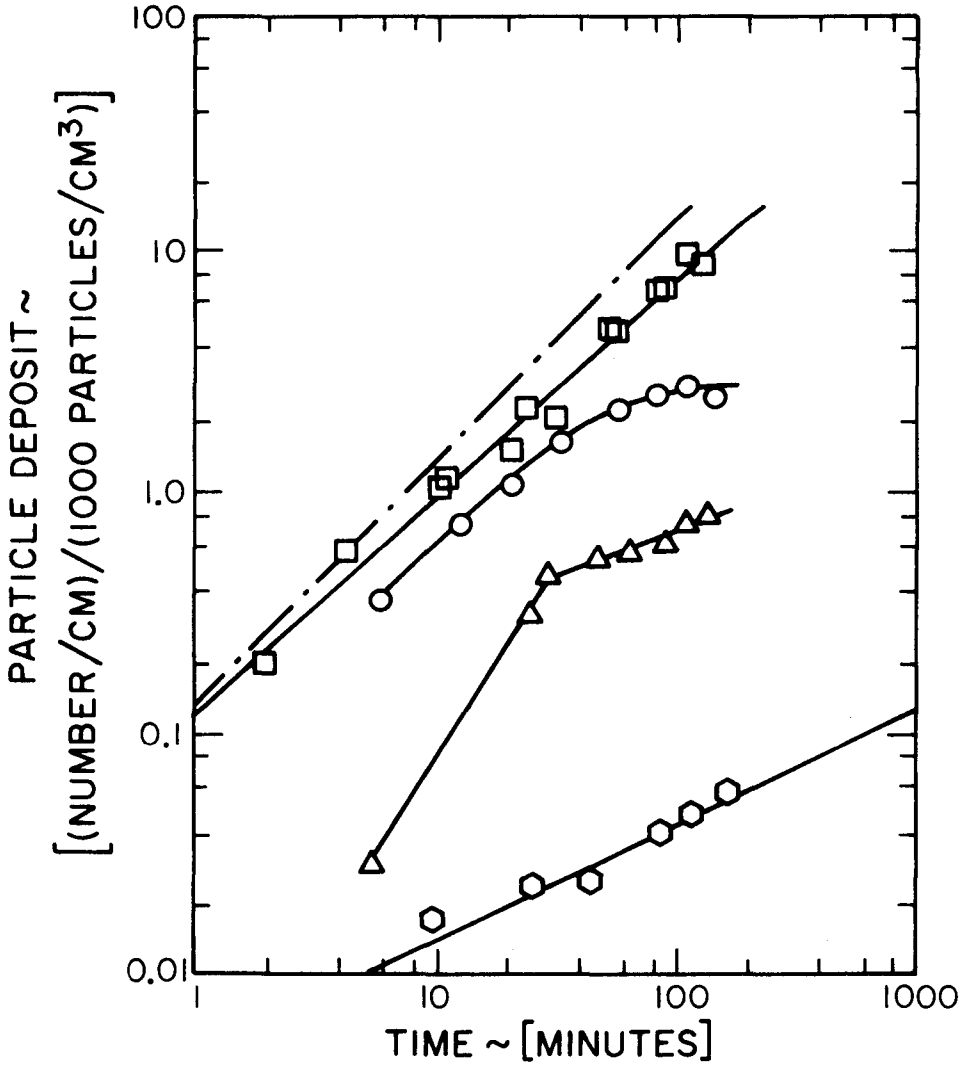

Figure V-A-2 RBC Deposition on Teflon Fibers with Different Surface Treatments

○ RBC, Chromic-Sulfuric Acid Cleaned, Run 1

△ RBC, Nitric Acid Cleaned, Run 4

□ RBC, Purifloc Coated, Runs 7, 8

⬡ RBC, Plasma Coated, Run 3

—.—.— GIM Value for 7.5 μm Sphere

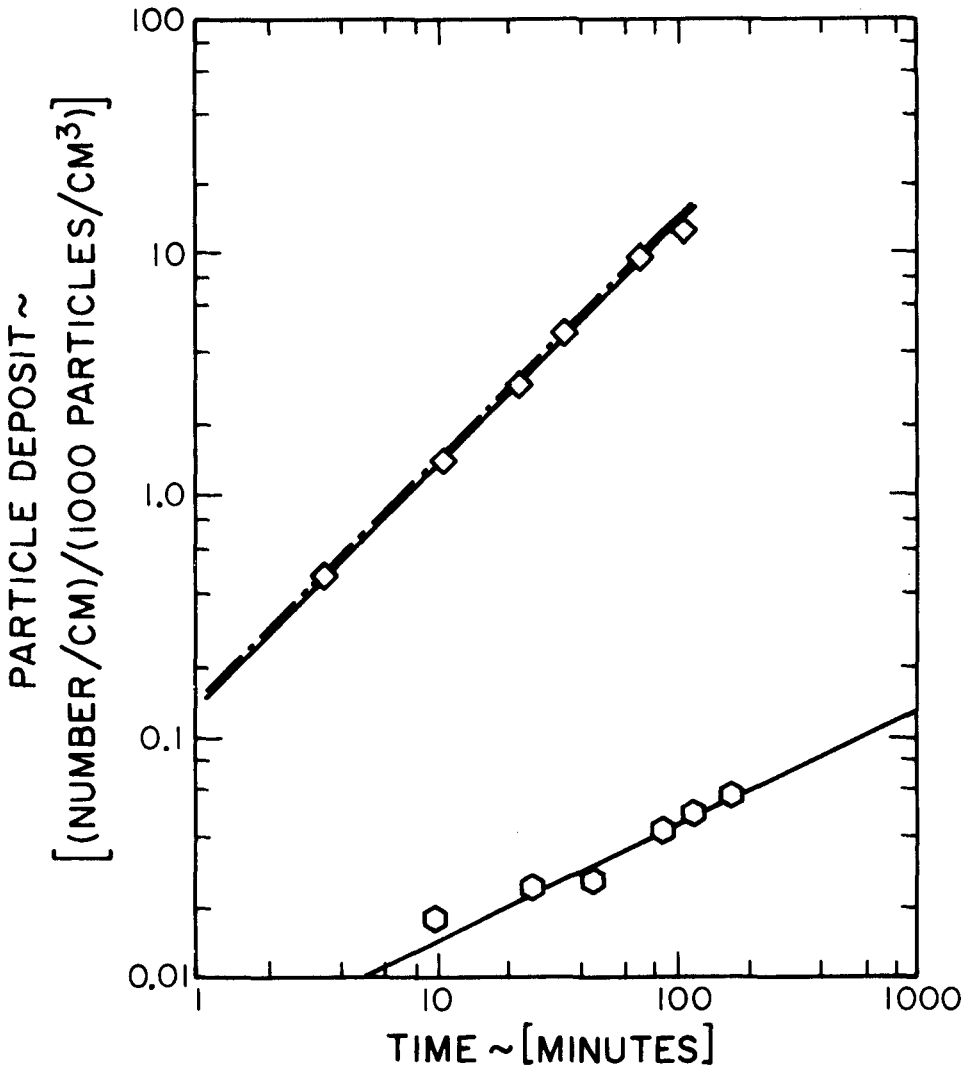

Figure V-A-3 Particle Deposition on Plasma-Coated Teflon Fiber

⬡ RBC, 7.5 μm, Run 3; ◇ SDVBL 7.6 μm, Run 5;

—.—.— GIM Value for 7.6 μm Sphere

efficiency for 7.6 μm mono-sized particles is made only for latex particles because the RBC have varying radii of curvature. The RBC radius that is significant in hydrodynamic interactions with the surface is not known.

The nature of the solid-solution interface plays a major role in determining the efficiency of a collecting surface. This is so even under conditions of high ionic strength (thin double layers and theoretically negligible repulsion energies). Tenney and Stumm (1965) have discussed the significance of this fact as it applies to hydrophilic biocolloids such as bacteria, algae, and RBC. Experiments with RBC corroborate the finding that non-coulombic energy barriers are important with hydrophilic surfaces. On the other hand, other studies indicate that double layer concepts are applicable to biocolloids. These include:

a. Boddy, et al. (1965), who deposited RBC on platinum and gold electrodes by controlled polarization of the electrodes;
b. Brooks et al. (1967), who hypothesize aggregation of RBC in secondary minima;
c. Cookson (1967a,b), who studied virus adsorption on activated carbon;
d. Rubin and Hanna (1968) and Rubin et al. (1969), who found that E. coli follow the Schulze-Hardy rule for coagulation.

The apparent contradiction can be explained if one takes into account the specific adsorption energy of ions and the hydration energy of water molecules at the surface of hydrophilic solids. The

hydration energy must be added to the double layer repulsion energy and is expected to act at molecular distances ($\mathcal{O}$(1-10 Å)), whereas the specific ion adsorption energy will alter the ion distribution and surface potential. The latter can be described by modified Stern models of the double layer. Therefore, at distances greater than about 10 Å the VODL theory can still be expected to apply.

Secondary minima predicted by VODL theory exist at distances greater than 10 Å and could explain the applicability of theory to the biocolloids studied, particularly in light of the reversibility of aggregation reported by each of the investigators. Coagulation into primary minima would preclude reversibility.

According to VODL theory, without additional energy barriers, the high electrolyte concentration (0.198 M cations) of the RBC suspensions should compress the double layer sufficiently for deposition into primary minima. The deposition rate should approach the maximum predicted by interception theory (Table V-A-1). However, for both chromic-sulfuric and nitric acid cleaned runs the data do not support this view. Some deposition did occur but not at the predicted rate. Evidently favorable sites for deposition, possibly of reduced or opposite charge, did exist. Other investigators (Hull and Kitchener, 1969) have found similar behavior even on apparently uniform surfaces. If currently predicted VODL interactions are the only ones allowed, the entire surface should have been suitable for deposition.

The chromic-sulfuric acid cleaned fibers were cleaned on the plexiglass holder by dipping only the fiber into the acid. Chromium

ions either adsorbed or permeating from the fiber interior probably enhanced deposition on chromic-sulfuric acid cleaned teflon. Subsequent boiling of the teflon fiber with nitric acid in a reflux apparatus to remove residual metal ions reduced the deposit, but it remained non-zero. Handling of the fiber when it was mounted after cleaning probably resulted in some surface contamination which may have enhanced the deposition.

Plasma adsorption by the teflon markedly reduced RBC collection, but significantly increased latex collection, indicating that the RBC can chemically distinguish the surface coating. Rapid adsorption of plasma proteins by surfaces has been reported by Vroman et al. (1971). Experiments conducted by Edmark et al. (1970) with different blood proteins adsorbed on glass indicate that the surface potential of the teflon would have been lowered but not reversed. However, they also found that gamma globulin could reverse the surface charge making it positive. The strong collection of latex suggests that both positively and negatively charged plasma elements were adsorbed.

Using the experimental value for the Hamaker constant calculated from the 2.0 μm PVTL-glass system[1], 3×10^{-20} joules, the theoretical collection efficiency calculated from the HRM (Figure II-A-1) is approximately 75% of the GIM value. The corresponding experimentally observed efficiency was 106% of the GIM value for 7.6 μm SDVBL particles depositing on plasma coated teflon. The agreement is better than could

---

[1] See Section V-B-2.

be expected considering the experimental uncertainties. In contrast, deposition of 7.6 μm SDVBL particles on uncoated teflon was considerably lower, 28% of the GIM value. This low value cannot be explained by experimental uncertainty. This suggests that there was a barrier to deposition even under conditions of negligible double layer repulsion.

Design of these experiments permitted direct observation of the depositing particles. Several qualitative observations having direct bearing on the results of the experiments should be pointed out. The RBC, upon entering the shear field generated by the fiber, began to tumble. The tumbling action caused the effective size for collection to coincide with the major dimension of the cell. Collection of RBC by a Purifloc-coated fiber approached the GIM efficiency predicted for a 7.5 μm sphere, the major dimension of the RBC employed. Furthermore, the adhering RBC appeared to be oriented by the flow with the disc face parallel to the surface. Happel and Brenner (1965) reported that a disc near a wall in Couette flow (uniform shear field) experiences a torque when the edge is normal to the wall. In whole blood the high concentrations of cells will cause complicating interactions, but for dilute suspensions of non-spherical particles, the RBC result suggests a method for predicting the proper size for use in interception calculations, namely using hydrodynamic predictions for the envelope of the particle motion.

RBC and 7.6 μm SDVBL particles deposited primarily on the forward half of the fiber, a few being caught on the rear half. On one

occasion a latex particle which was apparently adhering to the surface, broke loose and rolled around to the back half of the fiber. To be consistent with the low Reynolds number GIM model, deposition must occur only on the front half of the fiber. Deposition on the rear cannot be explained without assuming local asymmetries of the fiber, radially directed force fields such as the London-van der Waals attraction or significant Brownian diffusion.

B. 2.0 μm PVTL-Glass Fiber Experiments

B-1. Experimental results

Varying surface characteristics greatly affected the deposition rate of suspended particles in the RBC-latex experiments, but the result could not be explained completely by diffuse double layer theory. For this reason a series of experiments was designed with a system in which double layer theory should apply. The quantitative data gathered from such a system would test whether double layer theory could be applied to particles larger than a micron.

PVTL particles 2.0 μm in diameter were deposited on flint glass fibers approximately 100 μm in diameter to determine the effect of electrolyte concentration on the deposition rate. Figure V-B-1 summarizes the results of those experiments and Table V-B-1 the run conditions and GIM predictions. The ordinate represents the ratio of the experimental to the GIM value of the collection efficiency while the abscissa gives the logarithm of the sodium ion concentration. The sodium phosphate buffer concentration was varied over the range

Run #	$d_p \sim$[cm]	$d_f \sim$[cm]	U~[cm/sec]	N_{Re}	pH*	$[Na^+] \sim [M]$	η_{EXP}	η_{GIM}	η_{EXP}/η_{GIM}
14	.0002	0.0098	0.15	0.149	7.08	0.0025	9.02×10^{-6}	1.15×10^{-4}	0.0784
15	"	0.0113	"	0.177	7.03	0.0025	3.07×10^{-6}	0.854×10^{-4}	0.0359
17	"	"	"	"	7.02	0.005	6.21×10^{-6}	"	0.0727
16	"	"	"	"	7.04	0.01	1.66×10^{-5}	"	0.195
18	"	"	"	"	6.97	0.02	2.25×10^{-5}	"	0.264
21	"	"	"	"	6.94	0.03	3.25×10^{-5}	"	0.381
19	"	"	"	"	6.91	0.04	5.58×10^{-5}	"	0.654
22	"	"	"	"	6.88	0.06	1.28×10^{-4}	"	1.50
23	"	0.0119	"	0.182	6.6	0.359	1.26×10^{-4}	0.779×10^{-4}	1.62
46	"	0.0096	0.23	0.224	1.19	0.0	$2.5\text{-}4.3 \times 10^{-4}$	1.28×10^{-4}	2-3.4

*pH uncorrected for ionic strength

Table V-B-1 Summary of 2.0 μm - Glass Fiber Experiments

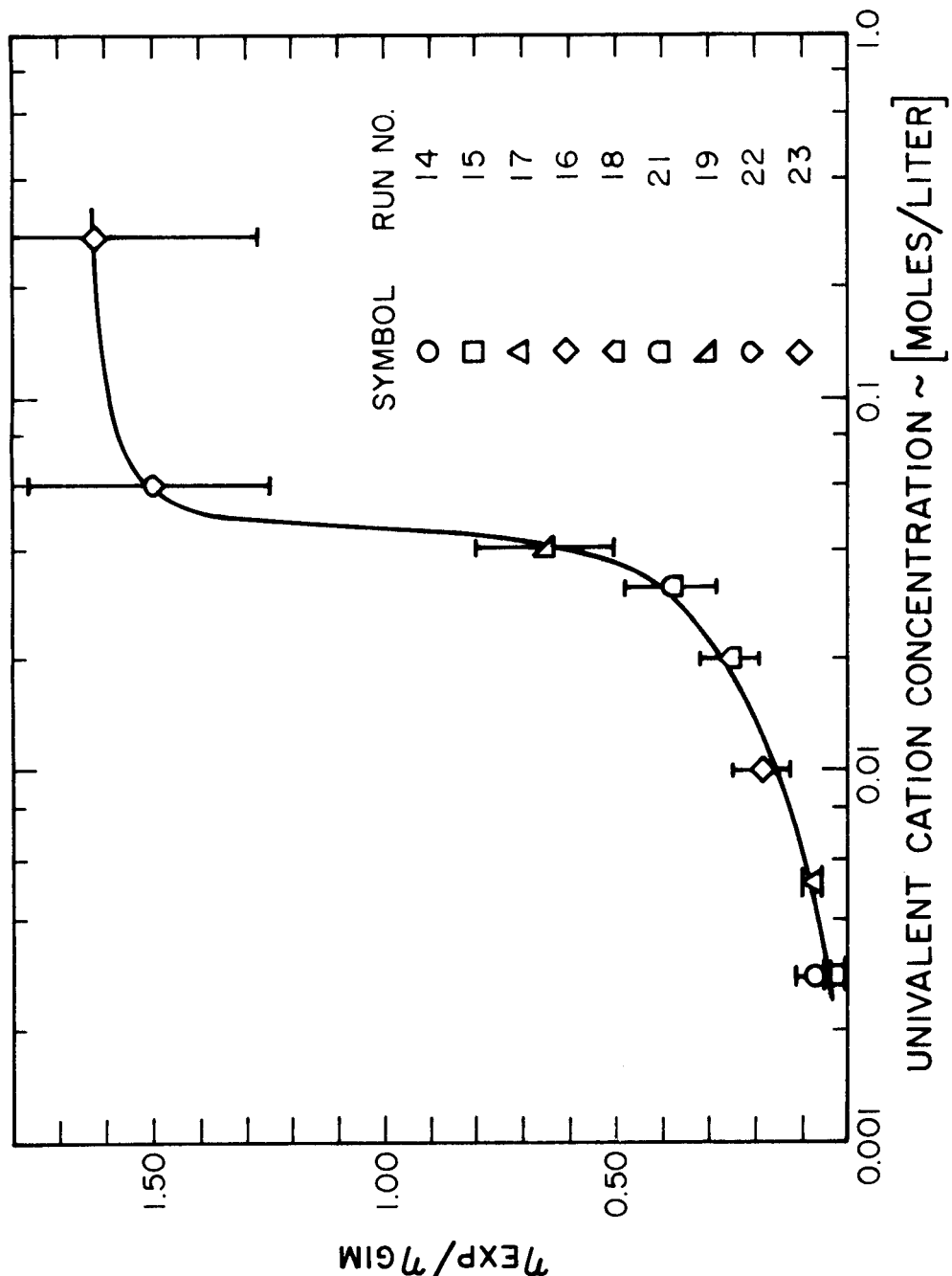

Figure V-B-1 Effect of Cation Concentration on the Collection Efficiency of 2.0 μm PVTL Particles

$\sim 10^{-3}$ M to 10^{-1} M while pH was maintained at $\sim$ 7.0. In one run the pH was lowered to 1.19 to test the effect of that variable. Separate measurements of the PVTL particles and ground-up glass fibers' mobilities were made using the Briggs cell previously described (Chapter IV-B-2). Zeta potentials (ζ) were calculated from mobility measurements using the Helmholtz-Smoluchowski equation. No attempt was made to correct for double layer relaxation or retardation effects which were small. The values obtained are compared with the range of literature values obtained for similar materials and various electrolytes in Figures V-B-2 to V-B-5.

The mobility of the latex particles decreases with time after initial dilution (Figure V-B-2), probably because of desorption of emulsifier. To calculate zeta potentials, the mobility of the particles one hour after the initial dilution was used. Glass particles from ground up fibers had constant mobilities.

The particle deposit over the entire surface of a known length was periodically counted in situ with a microscope. Figure V-B-6 presents data from a typical run; the ordinate gives the deposit per unit length of fiber normalized to a particle concentration of 1000 particles per cubic centimeter on a logarithmic scale, while the abscissa gives the time on a logarithmic scale.

The time dependence of the deposition rate probably results from adsorption of the latex emulsifier at the glass surface. The initial deposition rates were calculated from the deposit at ten minutes, a period long enough for the effects of initial mixing to

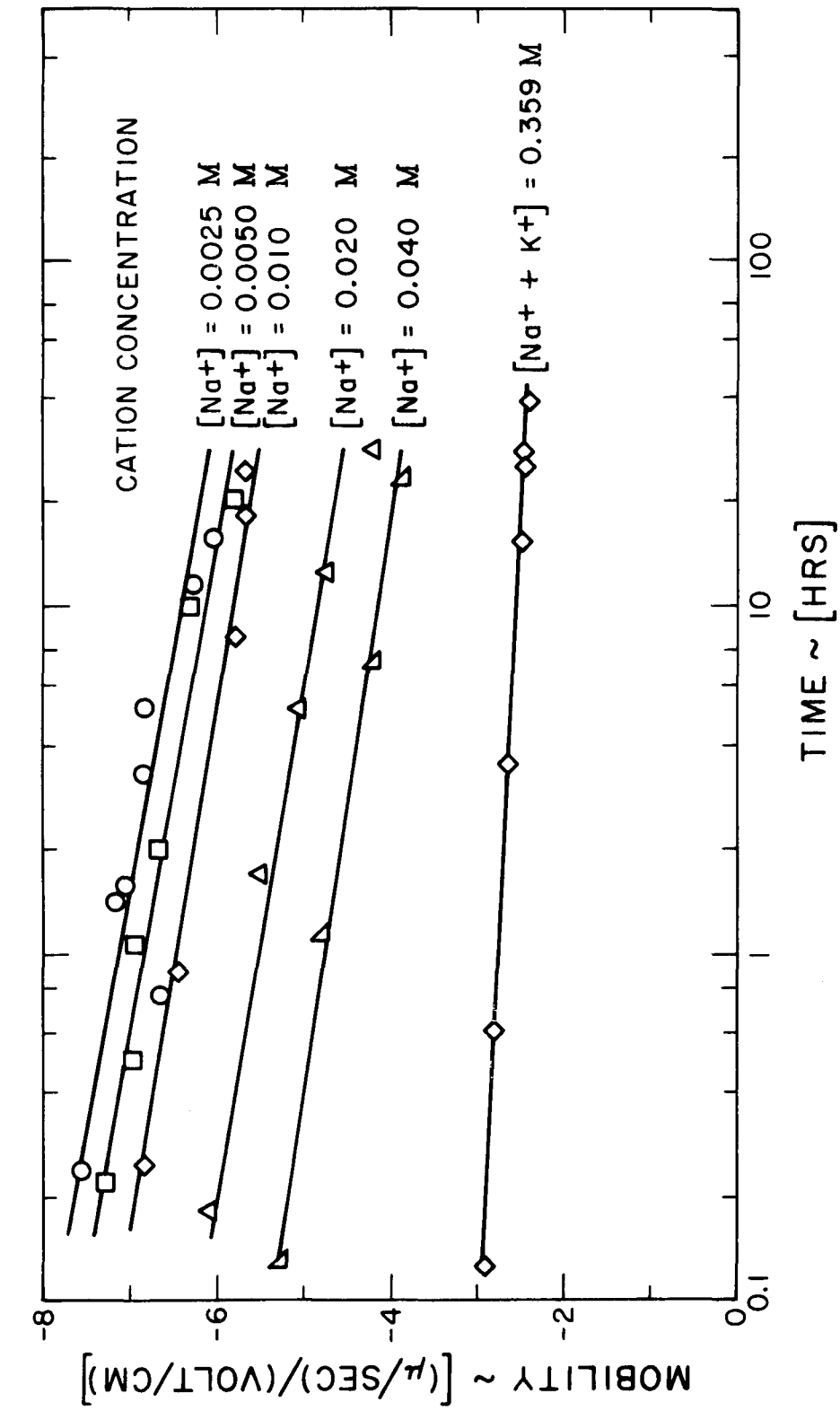

Figure V-B-2 2.0 μm PVTL Mobility versus Time

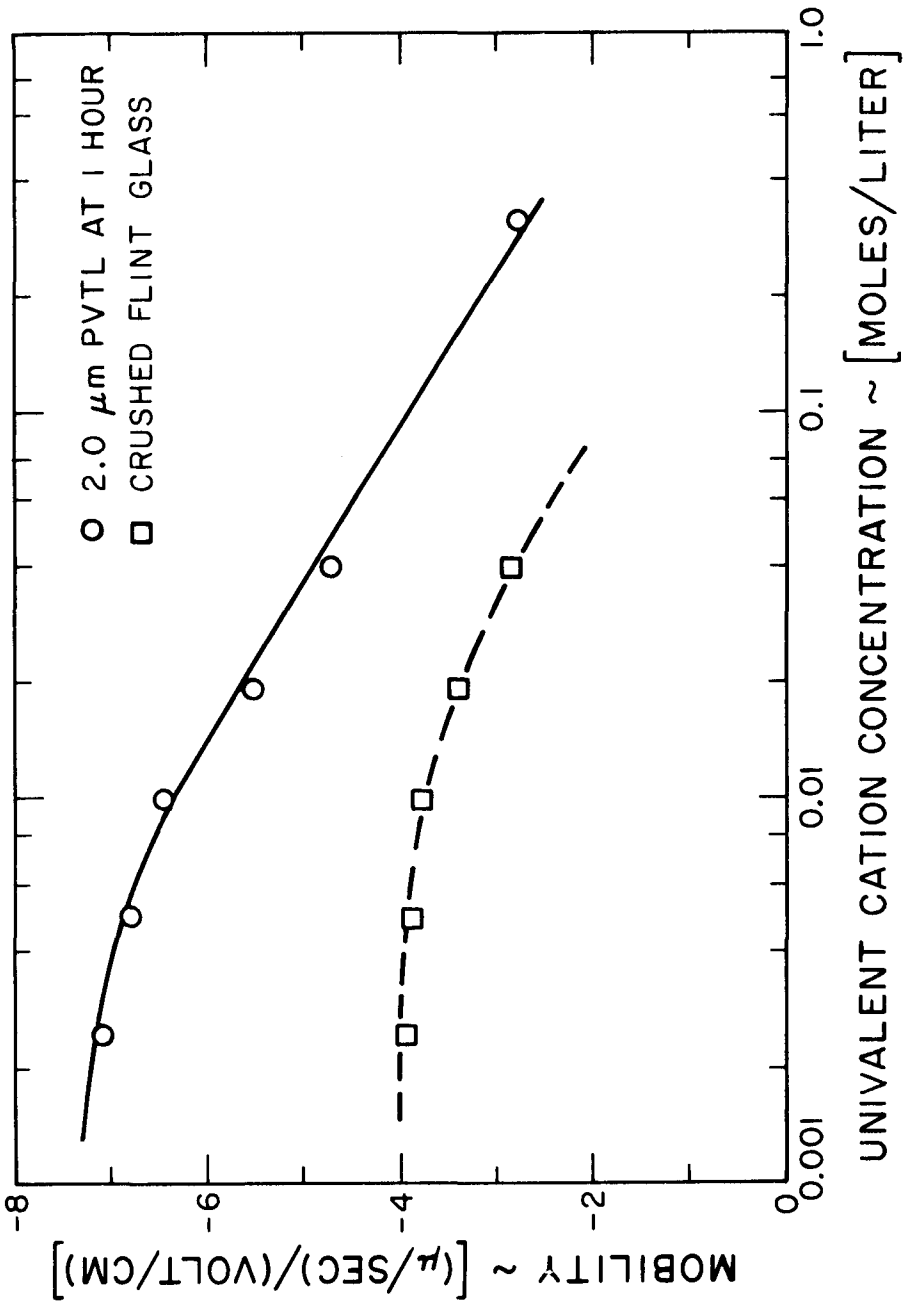

Figure V-B-3 2.0 μm PVTL and Crushed Flint Glass Particles Mobility versus Concentration

Measured at pH 7.0

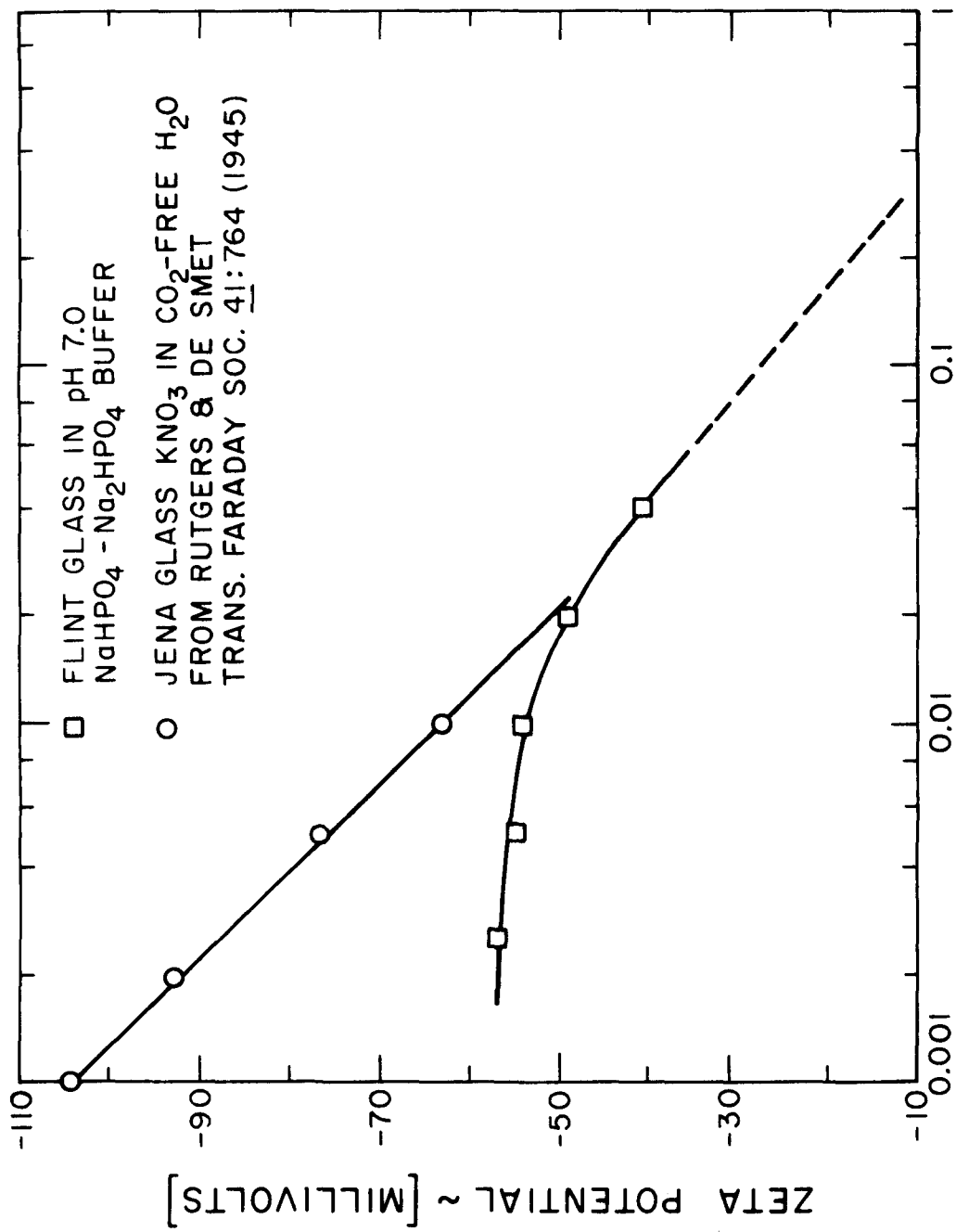

Figure V-B-4 Effect of Counterion Concentration on Zeta Potential of Glass, Measured and Literature Values

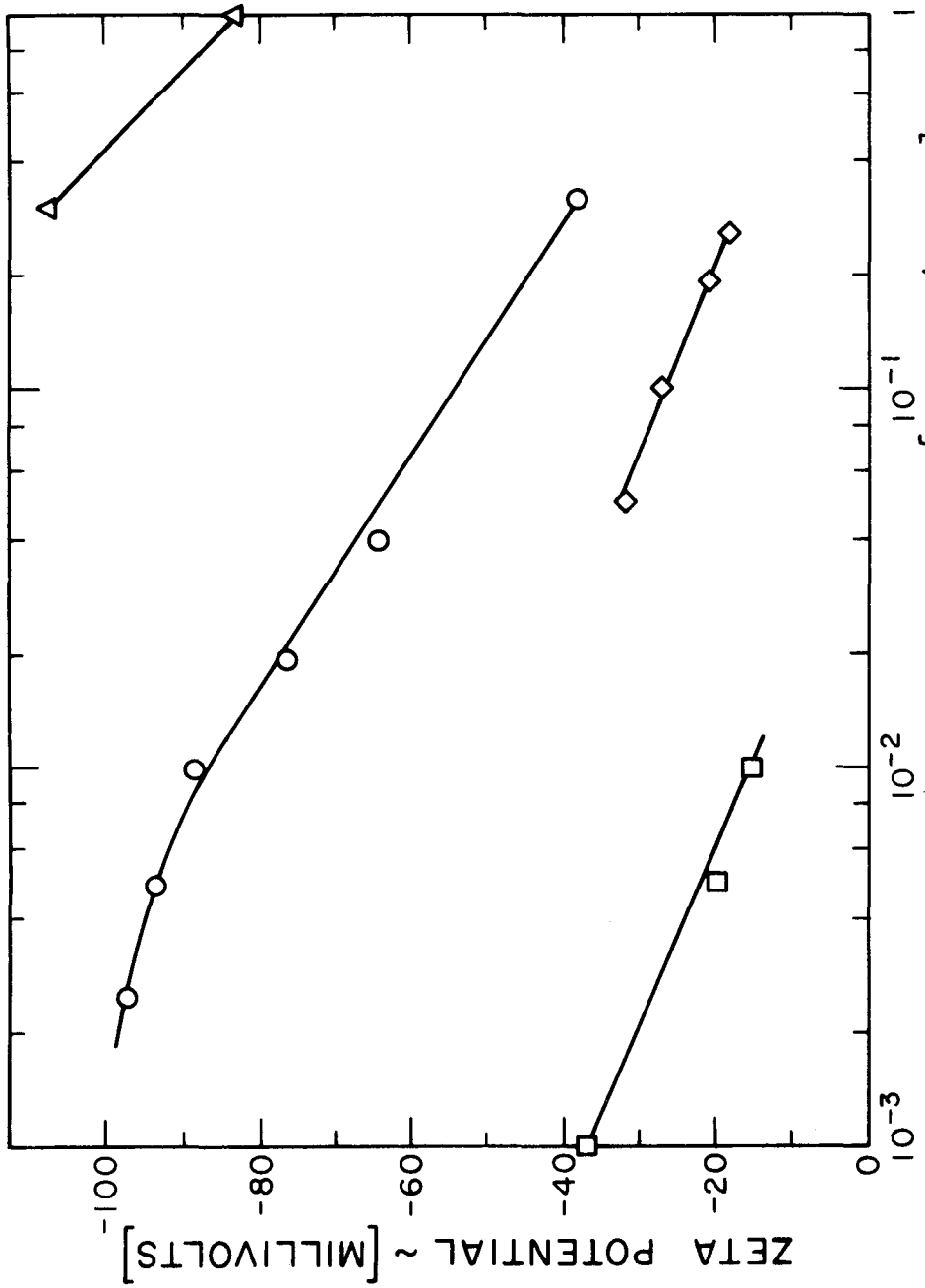

Figure V-B-5

Effect of Counterion Concentration "x" on Zeta Potential of Latices
○ 2.0 µm PVTL, x = Na^+, pH ~ 7.0; □ 0.2115 µm Carboxylated Latex, x = Ba^+, pH ~ 8.0 Ottewill and Shaw (1966); ◇ 0.175 - 0.188 µm Polystyrene Latex, x = Na^+ in 10mM $HClO_4$, Watillon and Joseph-Petit (1966); △ Polystyrene Latex-Sodium Lauryl Sulphate, x = Na+, Schaller and Humphrey (1966).

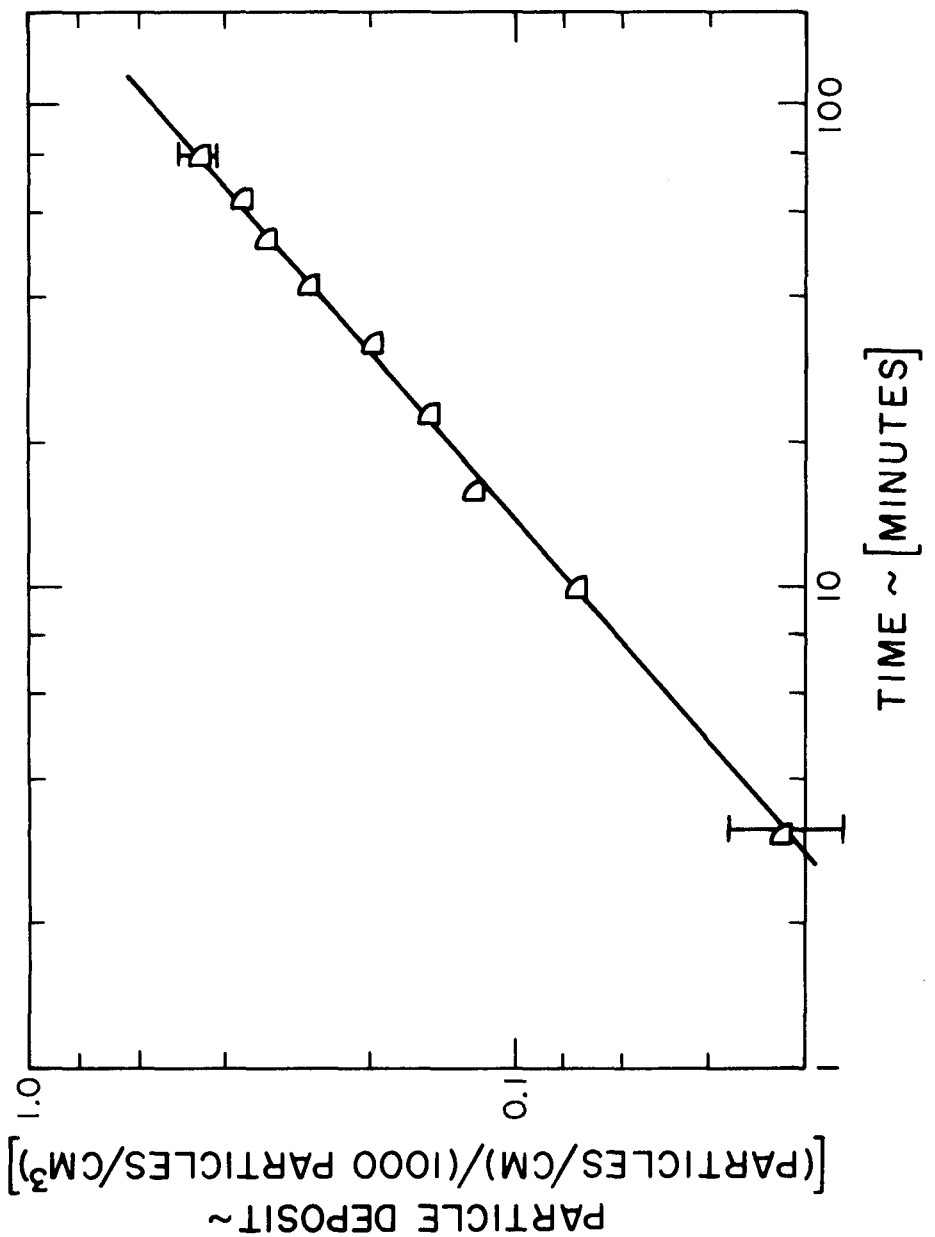

Figure V-B-6 Typical Data from 2.0 μm PVTL Experiment

Cation $[Na^+]$ = 0.04 M

disappear, yet short enough so that the rate did not diminish appreciably. Error bars appearing on the data points are an estimate of systematic, personal and random errors of measurement.

Deposition of the particles occurred over the entire surface of the fibers. In contrast with the case of the 7.6 μm SDVBL and RBC, only a few percent of the larger particles deposited on the downstream half of the fiber, whereas the smaller 2.0 μm PVTL particles were distributed much more evenly over the forward and rear.

B-2. Discussion

The marked dependence of the collection efficiency on counterion concentration qualitatively agrees with the VODL theory of the electrical double layer. Quantitative agreement with the VODL theory was not obtained using measured mobility data and a value for the Hamaker constant calculated from refractive index data. However, the calculation of Hamaker constants is not known to better than an order of magnitude.

The deposition rate increased sharply over the range of sodium ion concentrations from 0.03 M to 0.08 M. The corresponding measured zeta potentials of glass and PVTL without double layer retardation and relaxation corrections were found to be ζ_f = -44 mv, ζ_p = -70 mv, and ζ_f = -30 mv and ζ_p = -57 mv respectively. Using the values 0.03 M and 0.08 M as the limits of the range over which deposition into primary minima occurs, one can compute an effective value of the Hamaker constant needed to render deposition possible. This method parallels that discussed in Verwey and Overbeek (1948) for the

stability of flat plates except that sphere-plate interaction energies are used (see Appendix B). The "effective" Hamaker constants calculated by this method range from 3-8 x 10^{-20} joules. The theoretical Hamaker constants estimated from the method given by Gregory (1969) are about a factor of five lower. Considering that reported experimental values range from about 1 x 10^{-21} joules to 2 x 10^{-20} joules for polystyrene-polystyrene in water and 6 to 11 x 10^{-20} joules for quartz-quartz in air, the range of values calculated from the stability criterion agrees within the experimental error.

The curve shown in Figure V-B-1 for simple salt addition suggests that the maximum collision efficiency had almost been reached. This was not the case. In another experiment in which the pH was lowered the collision efficiency was about three times greater.

Using the lower value calculated for the Hamaker constant by the stability criterion, 3 x 10^{-20} joules, the HRM efficiency ratio, η_{HRM}/η_{GIM}, was equal to 2.5 for the low pH run (run #46 in Table V-D-1). The corresponding experimental efficiency ratio, η_{EXP}/η_{GIM}, was 3.4. The agreement is within the experimental error. On the other hand, the maximum experimental efficiency ratio obtained for indifferent electrolyte addition did not agree with theory within experimental error, but was about a factor of three lower. This suggests that there was a barrier to deposition at close range in addition to hydrodynamic retardation.

The existence of a barrier which prevents particles from adhering at maximum theoretical values has been reported by Swift and Friedlander (1964), Marshall and Kitchener (1966), Hull and Kitchener

(1969), and Fitzpatrick and Spielman (1973). The observation of Fitzpatrick and Spielman, that the latices destabilized by simple salts deposit at a lower rate than those destabilized by lowering pH, led to the pH experiment performed here.

Glass can serve as an ion-exchanger for sodium and hydrogen ions (Eisenman, 1965; Allen and Matejevic, 1969, 1970). Depending upon the exact composition of the glass, hydrogen ion more or less strongly dominates in the competition for available sites for pH lower than about 8. It is believed that under the conditions of the experiments hydrogen ion probably behaved as a potential-determining ion and the sodium ion as a relatively "indifferent" ion.

Although the exact nature of the barrier is not known, it appears to be connected with adsorbed layers on the surfaces. A plausible explanation for the effect of pH is that, lowering the pH lowered the charge on the latex and glass. Extrapolation of zeta-potential measurements from the literature (Rutgers and DeSmet, 1945; Fitzpatrick and Spielman, 1973) indicates that the zero point of charge for both substances occurs in the pH range 1 to 2. Hence at pH 1.19 there was less charge on the surfaces. Therefore, water and adsorbed counterions were less tightly bound.

At high pH, the surfaces were highly charged. Sodium ions used to destabilize the particles and water molecules were strongly adsorbed. These layers interfered with one another at close approach. Hollow fibers exhibited high collection efficiency (see Section V-C-1) with

sodium ion addition because of their porosity. The adsorbed layers did not interfere with one another. In fact, the adsorbed layer on the particle may have simply "fit" into a pore so that only a small amount of the adsorbed layer needed to be displaced!

Spielman and Cukor (1973) have made numerical computations for particle collection by single spherical collectors using the HRM, accounting for double layer forces. They found that for spherical collectors, particle deposition exhibits a sharp transition between conditions of collection and no collection with varying ionic strength. The change is practically discontinuous for large values of the adhesion parameter $N_{Ad,f}$. This means that the curve of theoretical efficiency versus ionic strength would look like a step function, rather than the S-shaped curve shown in Figure V-B-1. Similar numerical computations for a cylindrical collector neglecting hydrodynamic interactions indicate that the collection efficiency is practically discontinuous for the conditions of the present experiments.

Several factors may have contributed to the continuous variation of collision efficiency with cation concentration, rather than a step increase as might be expected from VODL theory. These include variability of surface charge on the latex particles and over the fiber surface, Brownian movement, and a distribution in the size of the particles. These factors can be expected to result in a distribution of repulsive energies and Brownian diffusivities, and hence, in a smooth dependence on cation concentration. In Section II-A-2, a smooth curve was observed when the VODL theory was applied to collection by diffusion.

Further investigation shows that for thin double layers, and moderate dispersion and double layer forces, the flow field plays a major role only in the integration of the particle trajectory, and not in the stability criterion. If collection of particles results from primary minima only, the criterion for collection reduces to requiring double layer repulsion to be negligible.

For particles larger than about 1 μm, pronounced secondary minima are predicted to occur under conditions of moderate to high ionic strength. Figures II-B-1 and II-B-2 show the depth of the minima in kT. Some coagulation experiments support secondary minimum capture (Brooks et al., 1967; Rubin and Hanna, 1968; Rubin et al., 1969). Particles trapped in secondary minima should be moved by hydrodynamic forces and should be swept to the rear of the collector. Spielman and Cukor (1973) point out that the theoretical collection efficiency does not change as one moves from primary minimum collection to secondary minimum collection.

Calculation of the tangential velocity of a particle trapped at a separation distance of 50 Å indicates that a slow movement should have been observed on the time scale of these experiments. Experimentally, the PVTL did not move toward the rear of the collector, but appeared to attach abruptly and remain attached. Furthermore, even after flushing with deionized water the particles continued to adhere. Had they been trapped in secondary minima, the low ionic strength should have caused them to be reversibly removed. Moreover, as the ionic strength was increased, no significant change in the way the particles were being caught was observed. VODL theory predicts

that at some point, secondary minimum collection should have been possible as the ionic strength was increased. At that point slow movement of the particles should have been observed. If VODL theory gives a correct description, then some mechanism, such as that proposed by Marshall and Kitchner (1966) or Hull and Kitchener (1969), which does not require surmounting an energy barrier must exist allowing particles to contact the fiber surface.

The zeta potential of the latex particles as well as the collection efficiency of the fiber decreased with time, perhaps because the emulsifier desorbing from the latex was adsorbed by the fiber. The time chosen to compute the collection efficiency does not affect the dependence on ionic strength, although it does affect the magnitude of the efficiency. The collection efficiencies in Figure V-B-1 were those measured at ten minutes. Choice of the ten minute period was based upon the highest observed deposition rate for which initial mixing did not play an appreciable role.

Deposition of particles on the downstream side of the fiber could have been due to attraction by dispersion forces, Brownian diffusion or a combination of both. The Brownian diffusion contribution can be estimated from the theoretical value calculated by Spielman and Friedlander (1973) for diffusion in a force field using Equation II-A-B. In the case of negligible replusion ($\beta = \infty$ in Equation II-A-15) the result reduces to that calculated by Friedlander (1957) and Natanson (1957a) for point particles diffusing to a cylinder. Assuming negligible repulsion, the calculated values for the diffusion

transport efficiency, η_D, cluster about 5.1×10^{-5} in these experiments. An estimate of the hydrodynamic retardation by the method of Spielman (1970) indicates that this value should be lowered by about 10-15%. The GIM efficiency on the other hand was 8.5×10^{-5} while the HRM efficiency with an assumed Hamaker constant of 3×10^{-20} joules results in a value about 30×10^{-5}. Therefore, it appears that diffusion probably contributed to the collection efficiency of the fiber but of itself cannot explain the observed results.

C. Experiments with Permeable Hollow Fibers

C-1. Experimental Results

Permeable hollow fiber membranes offer the possibility of reducing double layer repulsion and fluid resistance to particle deposition. Passing electrolyte solutions through the fiber results in outward diffusion of electrolyte and inward diffusion of solvent because of osmotic effects. The increased concentration in a thin layer near the fiber surface should compress the double layer, reducing the repulsive energy barrier and, simultaneously, the fluid suction should reduce the hydrodynamic retardation resulting from "squeezing fluid" out of the gap.

Commercially available hollow fibers made from cellulose acetate with a molecular weight cut off of about 200 (Osmolyzer-CA-a) were used in a series of experiments to study the effect of varying internal ion concentration.[1] Unbuffered sodium chloride solutions flowed

---

[1] See Section IV-B-4 for a description of materials used.

through the fiber interior while latex particles in deionized distilled water (DDH_2O) flowed past the fiber exterior. When calcium chloride was used as electrolyte, the flow of solvent into the fiber rapidly diminished indicating blockage of the membrane pores. This "blinding" was irreversible and did not occur when using DDH_2O alone. The latex emulsifier may have formed a complex or precipitate with Ca^{+2} ions on the membrane pores. There was no evidence of "blinding" when sodium chloride was used.

The data collected consisted of:

a. the total number of particles initially "captured" as a function of time and internal ion concentration
b. the regional distribution, that is forward stagnation, rear stagnation, or lateral surfaces
c. the total number of particles retained after flushing the interior of the fiber with DDH_2O and
d. the regional distribution of the retained particles.

Not all of the initially captured particles adhered to the fiber surface. Some were held solely because of the osmotic flow into the fiber. When the driving force was removed, that is, when the osmotic flow was stopped by flushing the interior of the fiber with DDH_2O, particles were released by the fiber. After flushing, the flowrate past the fiber was increased by about a factor of four rapidly and stopped completely in a cyclical manner twice, then reset to the original flowrate. Particles retained by the fiber "adhered firmly" and were recorded under category C.

From the initial capture rate, the fiber efficiency could be calculated and its ratio to the GIM efficiency computed as a function of ion concentration inside the fiber. These results are plotted in Figure V-C-1 and the run conditions summarized in Table V-C-1. By measuring the increase in the suspension conductivity and assuming constant surface concentration, an estimate of the surface concentration could be made from the mass transfer theory of Friedlander (1957). The resulting value was about 0.1 M NaCl at the fiber surface for 1 M NaCl fed through the fiber interior.

Scatter in the data resulted from an inability to clean the fragile fiber surfaces thoroughly enough to ensure uniformity of the surface. The cleaning procedure used is described in Section IV-C-2.

Deposition was defined in the above procedures as the percentage of particles firmly adhering. This was plotted as a function of ionic strength in Figure V-C-2. Most of the particles in the low adhesion region were collected at the rear of the collector and were released when the osmotic flow ceased. Some particles were captured on the lateral surfaces of the fiber. This number increased with cation concentration. Few of those particles adhering to the lateral or forward surface of the fiber were released when the osmotic flow ceased. This indicates strong capture does occur for some of the particles on favorable sites--an observation previously made with solid fibers.

A particularly striking example of this collection phenomena is plotted in Figure V-C-3. In this case the fiber used was a

Run #	$d_f \sim [cm]$	$[Na^+] \sim [M]$	pH	$\eta_{EXP} \times 10^3$	$^*\eta_{GIM} \times 10^3$	$^*\eta_{EXP}/\eta_{GIM}$	% Retained after rinse
26	0.0191	1.0	5.7	24	0.356	67	---
29	0.0275	0.5	5.6	22	0.198	110	82
31	"	0.1	5.7	9.8	"	50	---
30	"	0.01	5.6	3.8	"	19	---
33	0.0230	0.001	5.3	2.7	0.264	10	---
36	0.0226	0.3	5.5	12.5	0.272	46	40
35	"	0.03	5.5	7.2	"	26	5
34	"	0.001	5.5	4.5	"	16	4
37	0.0271	"	5.7	"	0.203	22	10
38	"	1.0	5.6	1.8	"	89	83

d_p = 0.00057 cm; U = 0.23 cm/sec; Exterior solution - DDH_2O

*5.7 μm SDVBL size distribution correction factor 1.11

Table V-C-1 Summary of Experimental Conditions for Varying Internal Electrolyte Concentration with CA-a Hollow Fiber

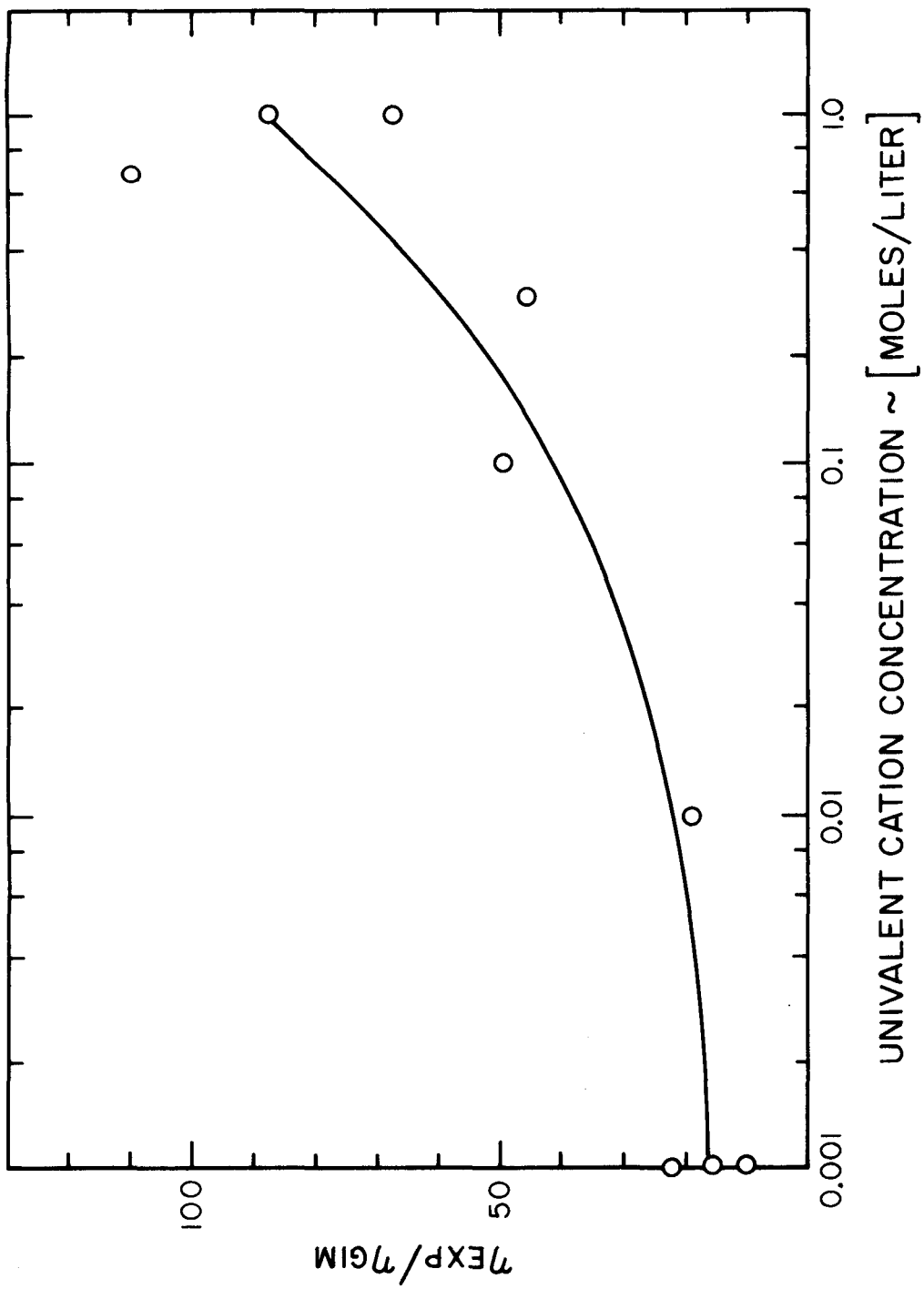

Figure V-C-1 Effect of Cation Concentration Within CA-a Fiber on Initial Capture Efficiency of 5.7 μm Latex Suspended in Distilled Deionized Water

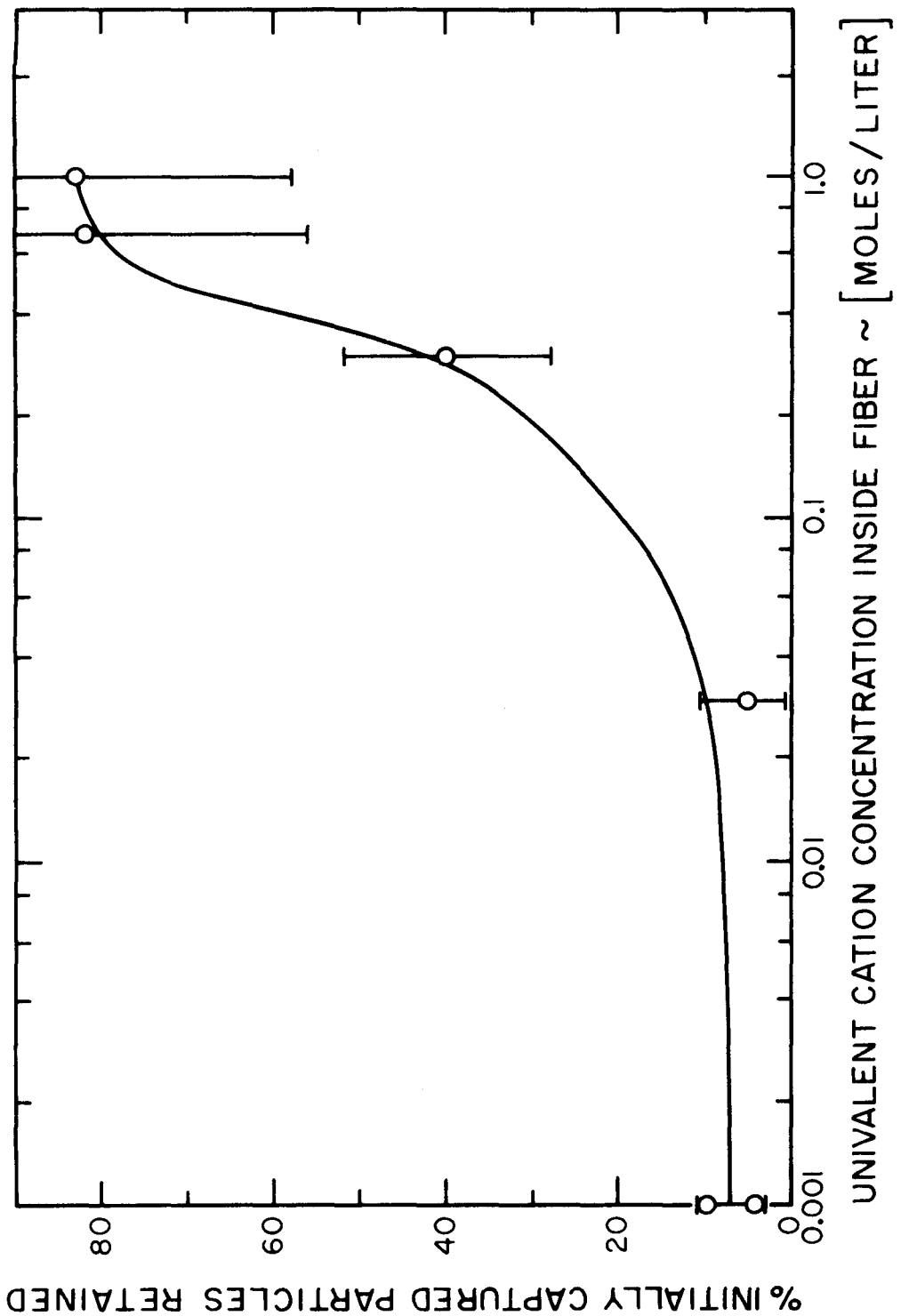

Figure V-C-2 Effect of Cation Concentration Within Osmolyzer Fiber on the Retention of 5.7 μm SDVBL Particles

commercial cellulose acetate fiber with a molecular weight cutoff of about 30,000 (Ultrafilter-CA-c)[1]. The 5.7 μm particles were suspended in DDH_2O. A pressure gradient was used to drive the fluid into the fiber. Collection occurred but primarily on the rear stagnation region. Under the microscope one could see a jerky zig-zag motion of the particles in close proximity to the fiber as they moved from the front to the rear of the fiber. When suction was released, the particles were released. However, when $CaCl_2$ was added[2], the particles were not released. This direct evidence of the importance of surface chemical forces for non-colloidal particles indicates that they must be considered in any comprehensive treatment of filtration.

Several sizes of latex particles were used in these high interior concentration runs. The 2.0 μm PVTL and 5.7 μm SDVBL deposited over the entire surface of fiber. However, the 25.7 μm SDVBL deposited almost entirely on the rear stagnation region with the remainder depositing near the forward stagnation line. In other suction experiments with 9.5 μm SDVBL particles, deposits were observed on the lateral surfaces as well. This indicated that hydrodynamic shearing forces were of significant magnitude to prevent the larger particles from adhering to the lateral surfaces.

---

[1] See Section IV-B-4 for description of materials used.

[2] $CaCl_2$ was permeable to the Ultrafilter Fiber and did not cause "blinding" of the larger pores.

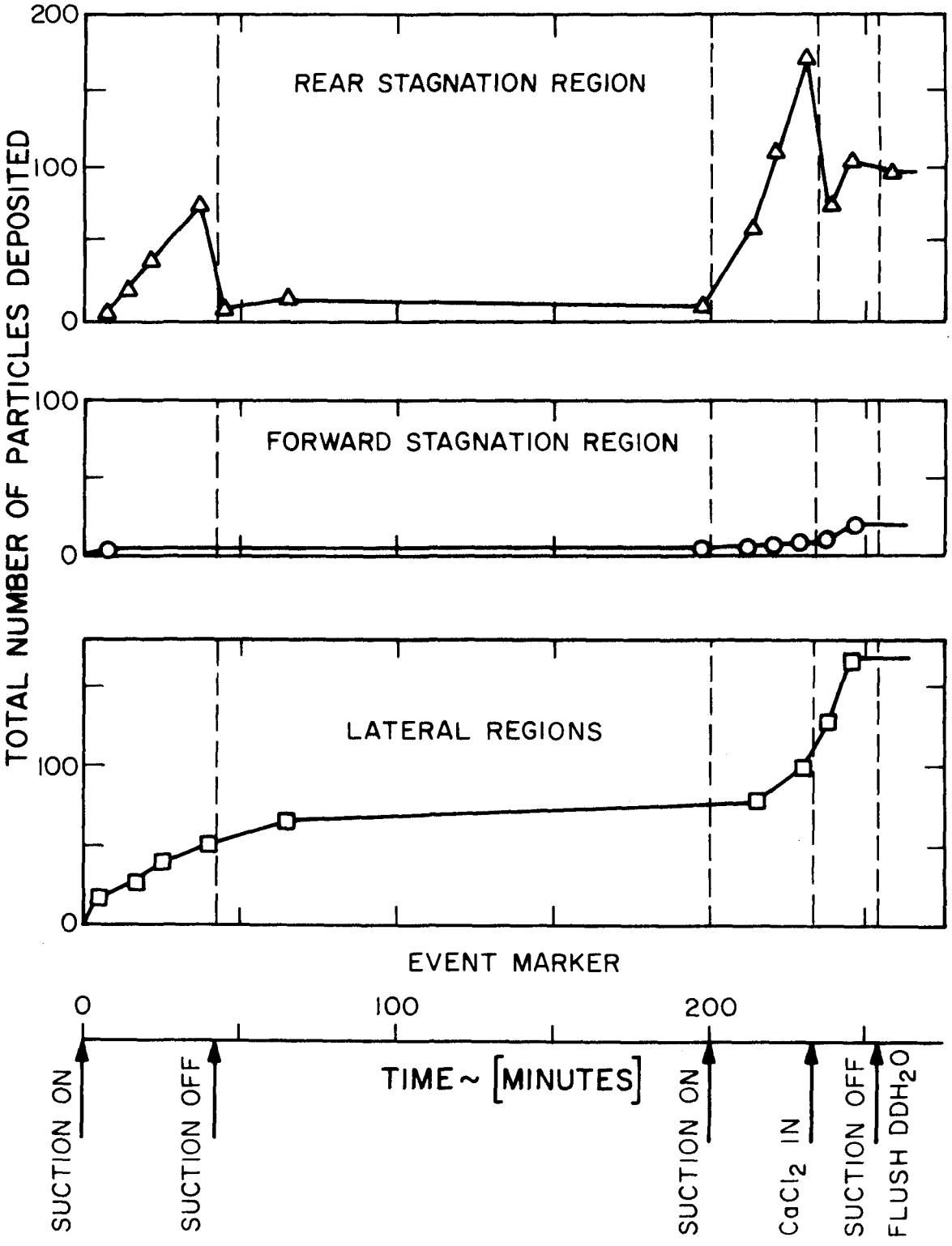

Figure V-C-3 Effect of Suction and Chemical Addition on Particle Capture by CA-c Hollow Fiber

A second series of experiments was performed in which the external ion concentration was varied while the internal ion concentration was maintained at 1 M NaCl. Those results are expressed as the ratio of the experimentally observed efficiency to the geometric interception efficiency versus the cation concentration in Figure V-C-4. The corresponding run conditions are given in Table V-C-2.

For tap water, the ion concentration is the value equivalent to the concentration of sodium chloride required to produce the conductivity of the tap water. The conductivity serves as a rough estimate of the ion concentration and, that in turn, of the driving force for the solvent through the membrane wall. The ionic species present in tap water, other than sodium and chloride, generally have higher mobilities and some carry multiple charges. Hence the conductivity overestimates their contribution to the osmotic pressure.

As the external ion concentration increased, the ratio of efficiencies decreased, leveling off at about unity. The runs with tap water exhibit greater variation. An analysis of water entering the distribution system on those two days was performed by the Caltech physical plant. For the 5.7 μm SDVBL tap water run, the total Ca^{+2} and Mg^{+2} content expressed as mg/liter of $CaCO_3$ was 240 mg/liter. The 2.0 μm PVTL tap water measured only 90 mg/liter. In view of the previous experience with membrane clogging, this might have been the cause of the difference observed.

The proportion of particles depositing on the forward half of

Run #	$d_p \sim$[cm]	$d_f \sim$[cm]	$[Na^+] \sim$[M]	Cation	pH	$\eta_{EXP} \times 10^3$	$\eta^*_{GIM} \times 10^3$	η_{EXP}/η_{GIM}
39	0.00057	0.0271	1.0	DDH_2O	5.6	18	0.199	90
24	"	0.0223	"	"	5.7	14	0.272	52
25	"	0.0271	0.0025	Na^+	7.1	1.3	0.199	6.5
26	"	0.0191	"	"	5.7	0.97	0.32	3.0
38	"	0.0271	Tap Water	Ca^{+2}, Mg^{+2}	8.2	0.19	0.199	0.95
40	0.0002	"	"	" , "	"	0.097	0.0225	0.43
32	0.00057	0.0275	0.125	Na^+	5.8	0.38	0.193	1.9

U = 0.23 cm/sec; Internal solution - 1.0 M NaCl

*5.7 μm SDVBL size distribution correction factor 1.11; no correction applied to 2.0 μm PVTL

Table V-C-2 Summary of Experimental Conditions for Varying External Electrolyte Concentration with CA-a Hollow Fiber

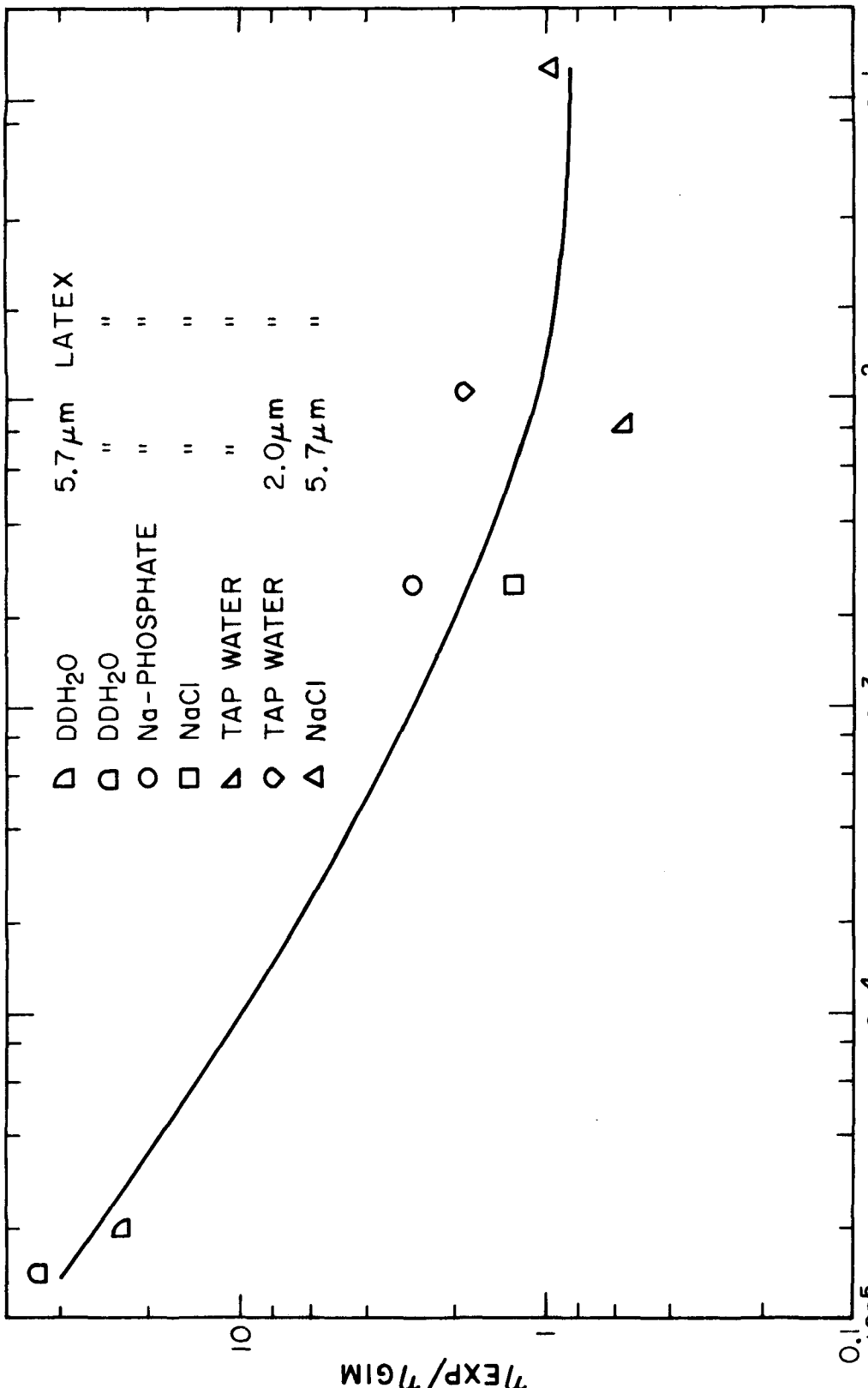

Figure V-C-4 Effect of External Cation Concentration on Initial Capture Efficiency of Latex Particles by CA-a Hollow Fiber with an Internal Concentration of 1M NaCl

the fiber increased with external ion concentration. This indicated that the concentration near the surface was greater toward the rear of the fiber.

C-2. Discussion

Figure V-C-2 strongly resembles Figure V-B-1 (for 2.0 μm PVTL particles and glass fibers), particularly if it is noted that the electrolyte concentration at the hollow fiber surface was about an order of magnitude lower than the concentration inside the fiber. This indicates that adhesion was controlled not by hydrodynamic forces generated by the osmotic gradient, but by double layer repulsion.

However, the primary mechanism for the initial capture of particles in the runs with varying internal ion concentration and (distilled deionized water, DDH_2O, particle suspensions) was the osmotic flow of solvent into the membrane. Essentially the membrane acted as a sieve. Under conditions of low ion concentrations, the double layer repulsion was strong enough to prevent adhesion except at a relatively small number of favorable sites. Therefore the flow swept the particles to the rear stagnation line where the hydrodynamic drag diminished and the particles were held in balance by the "suction" and double layer repulsion.

Simultaneously, a concentration boundary layer formed from ions diffusing out through the membrane wall. As the interior concentration increased, the concentration in the boundary layer region became sufficiently high to depress the double layer repulsion

allowing adhesion of the particles (Figure V-C-2). The concentration boundary layer thickens as one moves downstream. This explains why particles began to adhere at the rear of the fiber. The particles became unstable with respect to one another as well as to the fiber surface. As the concentration was increased the region of negligible repulsion moved toward the front of the fiber.

As the external ion concentration increased, the driving force for the solvent diminished. The ion concentration on the fiber surface was high enough for adhesion to occur and the proportion of particles caught on the forward half of the fiber increased. The total number of particles carried to the fiber surface decreased and the experimentally observed efficiency approached the interception value of the latex particles (Figure V-C-3).

The concentration boundary layer model described in Chapter III qualitatively describes the ion distribution outside the double layer. The model provides a means for determining the best operation of the fiber in terms of electrolyte species and flow parameters.

Dimensional analysis of the governing differential equation reveals that the relevant parameter describing optimum operation of the hollow fiber filter is the ratio of the mass transfer rate of the particles to the fiber versus the mass transfer rate of electrolyte to the suspension,

$$\frac{k_{p,av}}{k_{\ell,av}} \propto \frac{A_F^{2/3} d_p^{2} U^{2/3}}{d_f^{4/3} D_\ell^{2/3}} \quad . \qquad \text{(III-B-12)}$$

Here d_p is the diameter of the smallest particle in the interception

range whose removal is desired. This ratio should be maximized for high efficiency and low additive concentration. If the ratio is less than about one, then the use of hollow fibers will not substantially reduce the amount of electrolyte which needs to be added. Smaller fibers, smaller electrolyte diffusion coefficients and higher filtration rates improve collection by interception.

The hollow fibers should not be operated as sieves, or ultrafilters in the conventional terminology. In a filter bed, the total withdrawal by all fibers should be only a small fraction of the bulk flow; otherwise a significant energy expenditure to pump the fluid through the walls would be incurred. Only a small withdrawal of fluid at the wall is needed to diminish the hydrodynamic retardation, which builds up as the particle approaches the surface, before dispersion forces become effective.

D. Hydrodymanic Retardation Model Experiments

D-1. Experimental results

Data used to test the hydrodynamic retardation model (HRM) (Spielman and Fitzpatrick, 1973) are summarized in Table V-D-1. Teflon, glass, and both types of cellulose acetate fibers were used as the collecting surfaces. The particle sizes range from 2.0 μm PVTL to 25.7 μm SDVBL spheres. The ionic strength of the suspensions was kept high to reduce double layer forces to theoretically negligible values. Where hollow fibers were employed, the osmotic pressure was maintained constant across the fiber wall by having the same solution on both sides of the membrane.

Figure V-D-1 shows the data plotted as the ratio of the experimental (η_{EXP}) to geometric interception model (η_{GIM}) efficiency versus the adhesion number ($N_{Ad,f}$).[1] The error bars shown in the figure represent the statistical, systematic and personal errors of the experiment. The GIM efficiency has been calculated using the geometric mean diameter without correction for size distribution. The adhesion number, $N_{Ad,f}$, proposed by Fitzpatrick and Spielman (1973) requires that a value for the Hamaker constant, Q, be supplied. A value of 3×10^{-20} joules, determined from the stability criterion discussed in Section V-B-2, has been used throughout. This value lies above the range of values (0.3×10^{-20} - 0.7×10^{-20} joules) theoretically calculated from refractive indices by the method outlined by Gregory (1969)[2].

The solid curve in Figure V-D-1 represents the HRM theoretical correlation when diffusion and gravitational settling may be neglected, the solid straight line the asymptotic value for large adhesion numbers, and the dashed straight line the GIM efficiency. The data are seen to fall into two bands, one agreeing with the HRM theory closely, while the other band lies about a factor of three lower. All data in the lower band (open symbols) were collected using solid fibers and simple salts.

---

[1] Definition of the different transport efficiencies, collision efficiencies, overall collection efficiency, and filter coefficient have been given in Chapter II.

[2] See Appendix E for details of the calculation.

Run #	$d_p \sim$[cm]	$d_f \sim$[cm]	Surface	U~[cm/sec]	Cation~[M]	pH	$\eta_{EXP} \times 10^3$	η_{EXP}/η_{GIM}	$N_{Ad,f}$*
5	0.00076	0.0108	teflon-plasma	0.150	0.198	7.4	1.38	1.06	0.077
6	"	"	teflon-chromic	"	"	"	0.41	0.31	"
10	0.0002	0.0095	glass	0.966	0.359	6.6	0.124	0.57	1.01
11	"	0.0079	"	0.230	"	"	0.196	0.61	5.25
12	"	0.0095	"	0.054	"	"	0.131	2.8	43.1
13	"	"	"	0.966	"	"	0.102	0.47	1.01
23	"	0.0119	"	0.150	"	"	0.123	1.6	18.2
32	0.00057	0.0276	CA-a	0.230	0.125	5.8	0.319	1.8	0.67
41	"	0.0269	CA-c	"	0.50	6.0	0.307	1.7	0.63
42	0.00257	"	"	0.150	"	5.8	0.218	0.66	0.0028
43	0.00076	0.0247	"	0.225	0.25	---	0.344	0.94	0.18
45	0.00095	0.0223	"	0.226	"	5.9	0.548	0.80	0.062
46	0.0002	0.0096	glass	0.230	0.065	1.19	0.437	3.4	7.32

*Hamaker Constant 3×10^{-20} J.

Table V-D-1 Summary of Data Used to Test HRM

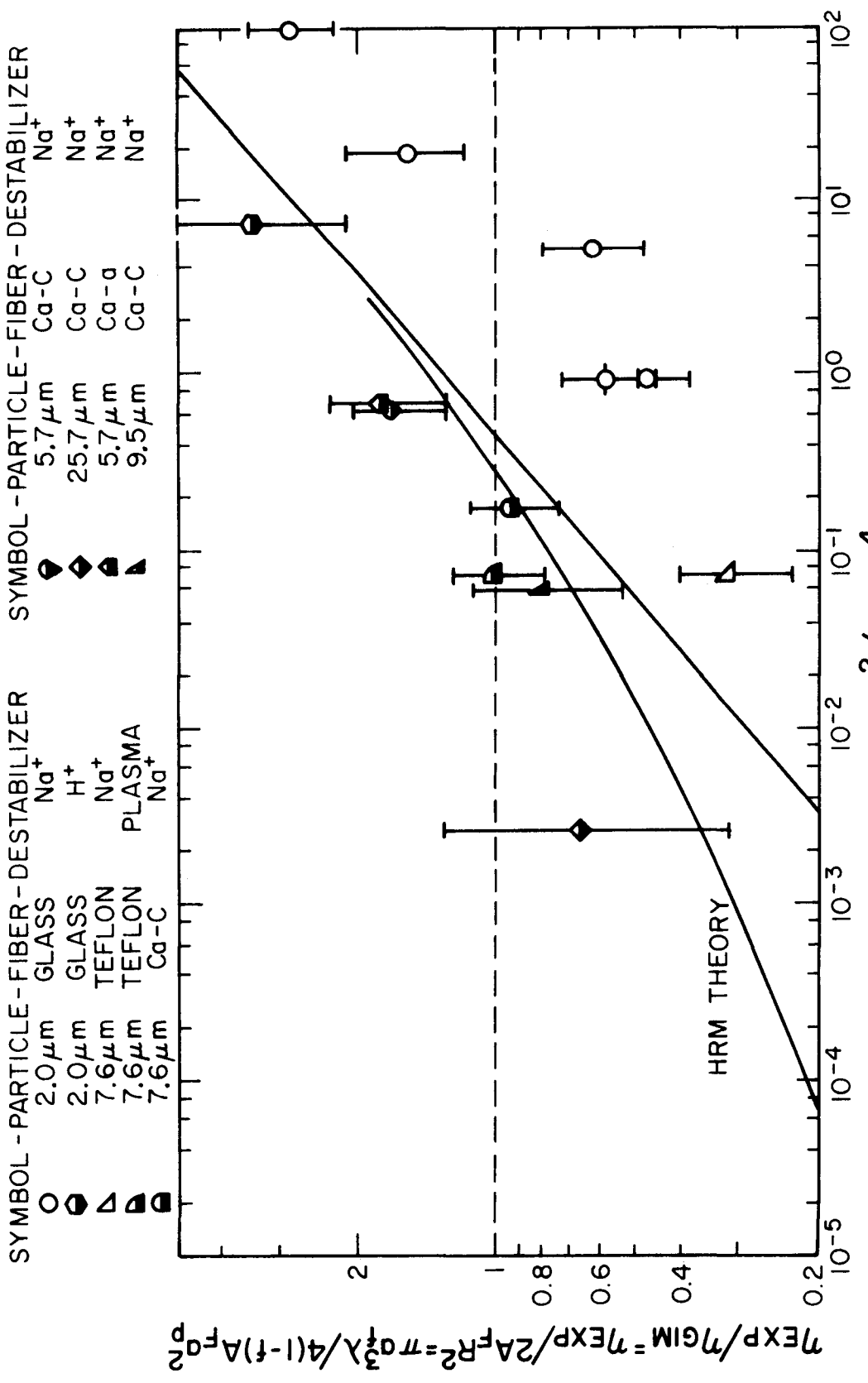

Figure V-D-1 Comparison of Experimental Data with HRM Using Hamaker Constant Q = 3×10^{-20} J Determined by VODL Theory Stability Criterion - Open Symbols Indicate Adsorbed Layer Interference

The same data are shown in Figure V-D-2 replotted with the dimensionless correlation suggested by Friedlander (1967a,b) for particles in the diffusion and interception range. The Friedlander correlation has been used successfully in aerosol filtration where the Stokes drag assumption is acceptable. The upper end of the curve is the region where interception dominates while in the lower portion diffusion controls. The same set of symbols are used for the data. The arrows appearing on the 2.0 μm PVTL data represent where the data would appear if the collision efficiency were three times greater. The data agree well in the diffusion-interception region if the factor of 3 increase is used. However, for the larger particles where diffusion is not so important, the data are lower than the semi-empirical correlation.

To test the concept of hydrodynamic retardation, a known flux of solution was drawn through the surface of an Ultrafilter[1] fiber. The induced flow should reduce the hyrodynamic resistance experienced by the particle as it approaches the surface, thus raising the observed efficiency. The measured Ultrafilter permeability for a given applied pressure is shown in Figure V-D-3. These data were taken using three different fibers with both distilled deionized water and 1 M NaCl solutions under ambient conditions (about 22°C). No decrease in the flux was measured even with NaCl added, indicating that the NaCl was highly permeable to the membrane. The effect of applying a slight suction to a fiber during a filtration run can be

---

[1]Molecular weight cutoff 30,000, CA-c.

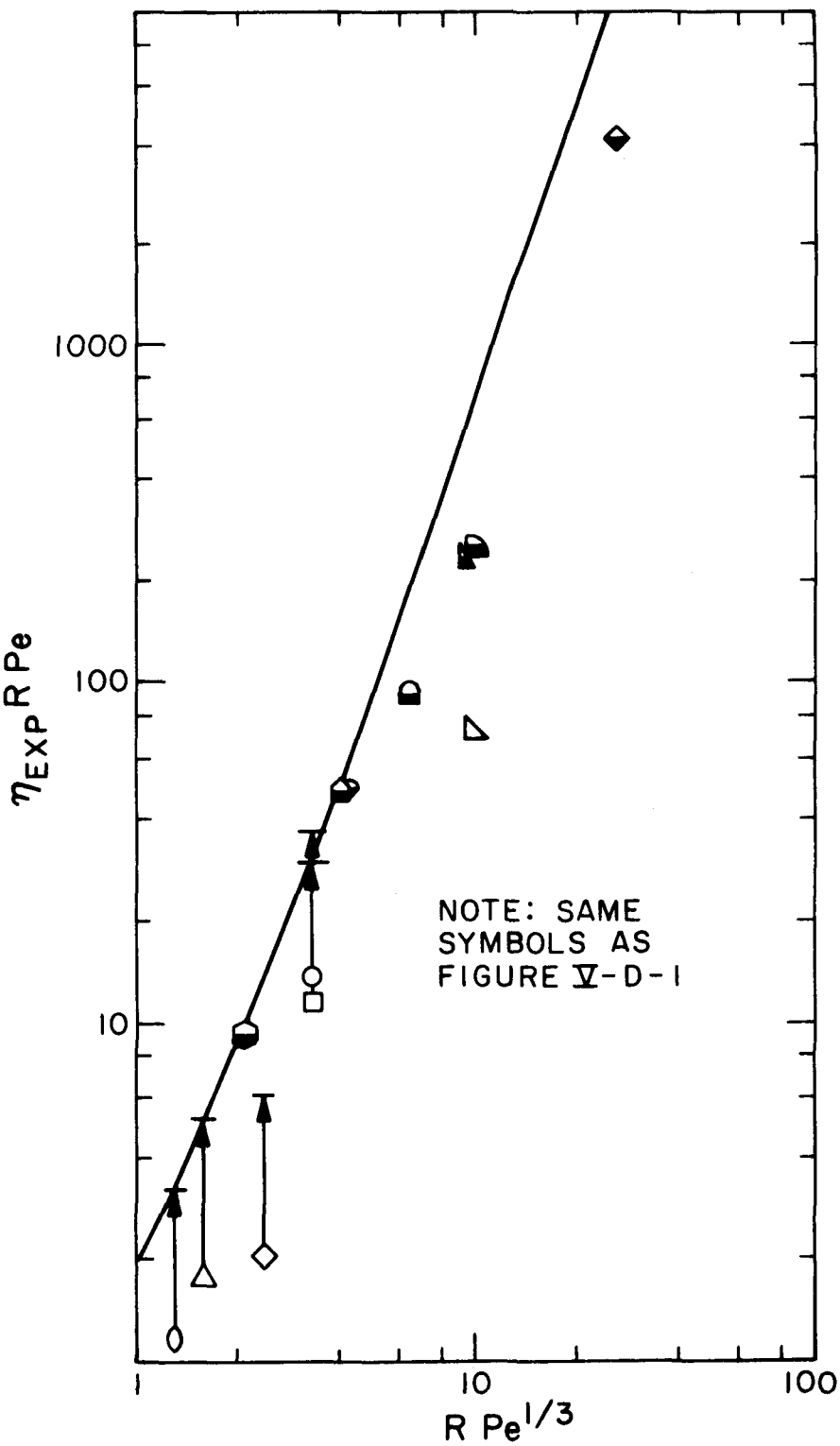

Figure V-D-2 Experimental Data versus Semi-Empirical Correlation Suggested by Friedlander (1967a,b). Arrows indicate where 2.0 μm latex data would lie for no adsorbed layer interference.

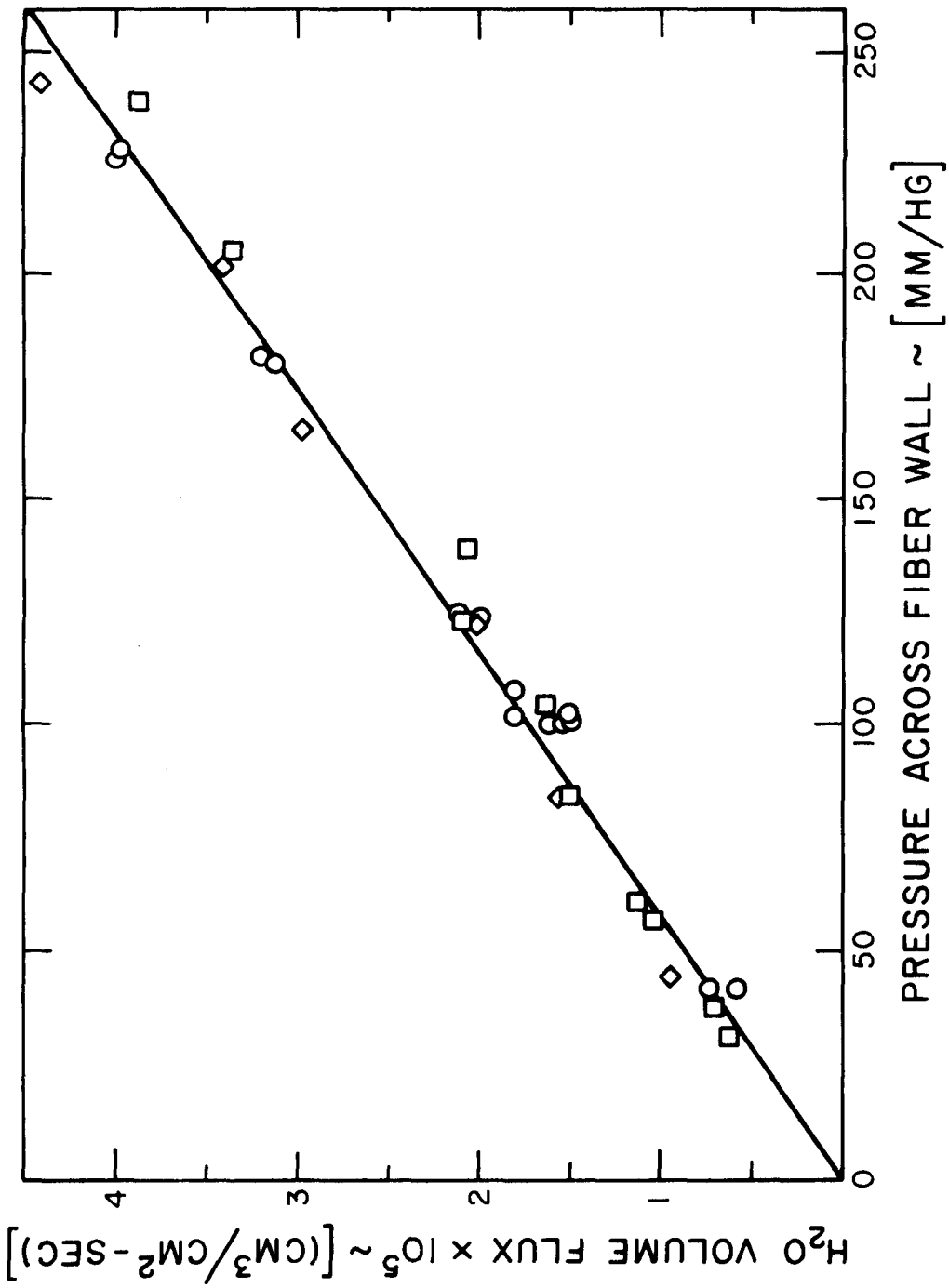

Figure V-D-3 CA-c "Ultrafilter" Membrane Permeability to H_2O

O, □, ◇, Δ Distilled Deionized H_2O: Δ 1 M NaCl

seen in Figure V-D-4. In this case 9.5 μm SDVBL particles were used. An arithmetic plot of the particle deposit per unit length and concentration of particles versus time is shown. The additional deposit caused by the flow of solution through the wall has been calculated from the applied pressure, permeability data and particle concentration. It lies well below the observed deposit.

D-2. Discussion

The data in Figure V-D-1 fall into two groups, both of which follow the trend of the HRM theory. The group of points falling below the curve (open points) were obtained with solid fibers and simple salt addition. The low efficiencies probably resulted from additional energy barriers associated with adsorbed counterions and water of hydration (see Section IV-B-2). When the barriers were removed by plasma adsorption or reduction of surface charge, the solid fiber data fell in the same band as the hollow fiber data (filled in points). The hollow fibers are probably better collectors even with "indifferent" electrolyte addition because they have "pores". Less of the adsorbed layer has to be displaced before the adhesive force becomes strong enough to bind the particle firmly.

The data in Figure V-D-2 make it clear that diffusion contributed to the experimental collection efficiency of the 2.0 μm latex particles. The good agreement with the HRM model for adhesion numbers much greater than unity was probably fortuitous and was not caused by the dispersion forces.

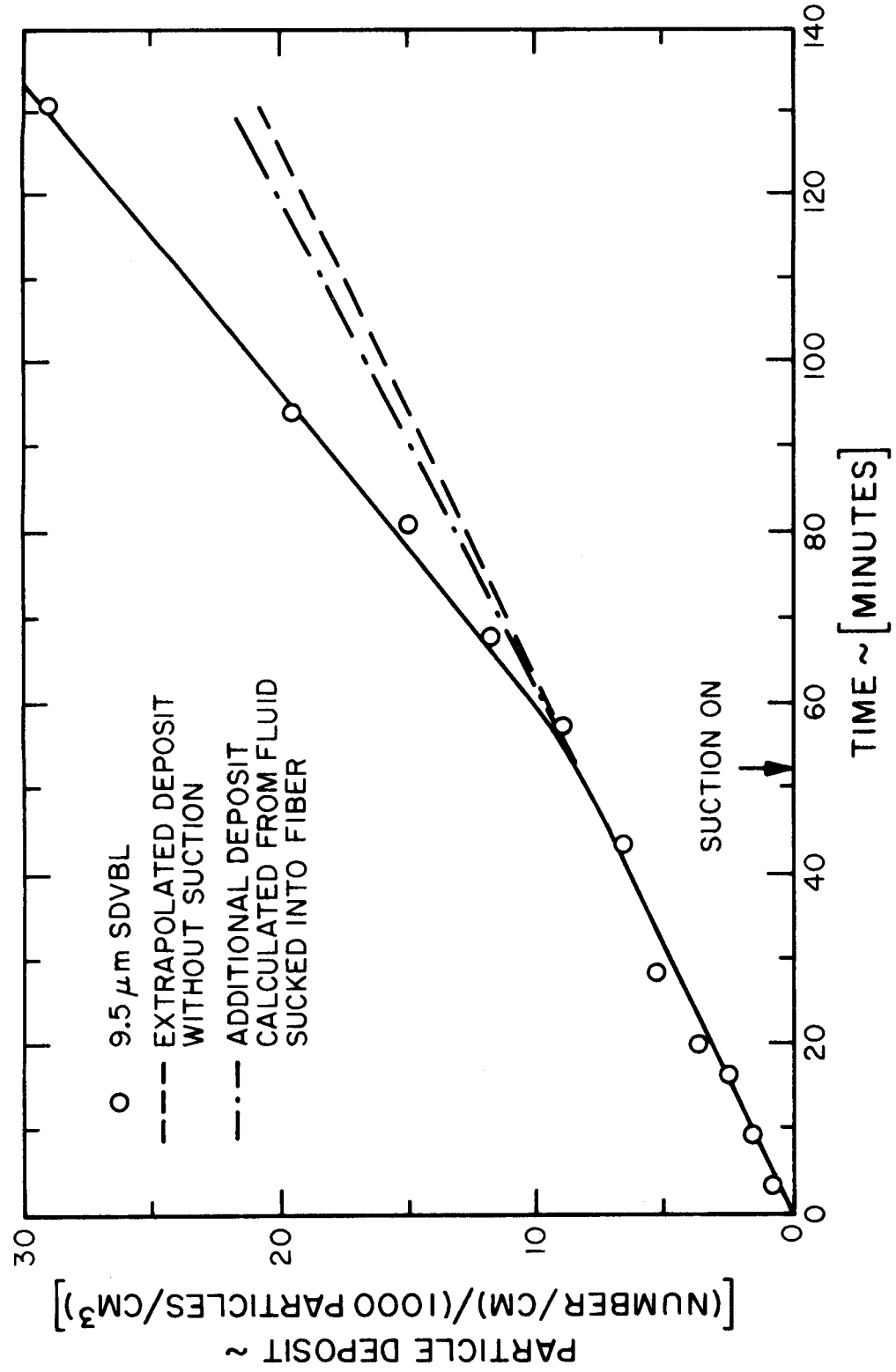

Figure V-D-4 Effect of Slight Suction on Particle Deposition on a CA-c Hollow Fiber

Fluid withdrawal at the fiber surface provided the final test of the HRM theory. For low adhesion numbers fluid withdrawal should lead to sizable increases in the collection efficiency, from the HRM value to about the GIM value. The increase in Figure V-D-4 was from 0.77 to 1.3. This cannot be accounted for by the amount of fluid sucked into the fiber, and resulted from reduction of hydrodynamic retardation.

Fitzpatrick and Spielman (1973) found that the packed bed data they obtained for low adhesion numbers fell below the theoretical curve. Visual observations of the largest particles 25.7 μm indicate that there is a strong dependence upon the velocity because of hydrodynamic shear forces on the particles. Increases in the flow rate resulted in removal of particles which had already been captured. Furthermore, very few particles were caught on the lateral sides of the fibers where the shearing forces are largest. This dependence was not studied in detail, but the work of Visser (1970) may be of use in predicting the importance of shearing forces.

E. Conclusions

Adhesion of RBC on both hydrophilic (glass and plasma-coated teflon) and hydrophobic (teflon) surfaces cannot be fully described by double layer theory (VODL). Additional energy barriers and possibly specific chemical reactions influence bioparticle deposition. Moreover, plasma proteins in whole blood coat surfaces within a short time after exposure, changing the nature of the original surface. The RBC seem to be able to recognize the surface coating. They

exhibit stability with respect to the protein-coated surfaces. They were also stable under conditions of high ionic strength.

In contrast, the collection efficiency of inert particles (2.0 μm PVTL) by solid fiber collectors (glass) depended strongly upon the electrolyte concentration, in qualitative agreement with VODL theory. However, no evidence for predicted secondary minimum deposition was found for the latices, while the literature suggests that secondary minimum collection occurs for bioparticles (RBC, E. coli). The 7.6 μm SDVBL carried charges of the same sign as the RBC, but were captured rather than stabilized by the protein-coated surface.

In agreement with RBC experiments, it is necessary to postulate additional energy barriers for inert particles as well as bioparticles. The nature of the barriers on the inert surfaces appears to be related to hydration and counterion adsorption on exposed surface charges. Increased collection efficiencies observed with porous-wall hollow fibers, plasma-coated solid fibers, and low charge density solid fibers (low pH) suggest that the adsorbed layers result in steric interference as the particle and fiber surface attempt to contact one another. Furthermore the small but finite deposition rate of RBC and latex particles, even in the presence of theoretically large double layer repulsion, indicates that there is surface heterogeneity, possibly imperfections, which lead to favorable deposition sites.

The complexity of the surface chemistry of biocolloids makes difficult a unified treatment of their stability with respect to

filter surfaces. Collection efficiencies generally will be higher for destabilization with polyelectrolyte additives than simple electrolytes, which rely solely upon electrostatic forces for effectiveness. Double layer concepts can still predict particle interactions at a distance and are useful in describing and understanding hydrophobic as well as hydrophilic particle interactions.

The current VODL theory must be modified to account for adsorbed layers, secondary minima, and deposition in the presence of energy barriers. Incorporation of additional energy barriers by Stern-type corrections to VODL theory might explain the role of adsorbed layers, but data needed for quantitative comparison are lacking. Surface imperfections have been suggested as the probable cause for deposition in the presence of energy barriers. No satisfactory explanation for the role of secondary minimum capture has been set forth.

The uncertainty in calculating the Hamaker constant does not permit accurate prediction of the optimum electrolyte concentration required to destabilize the particle-filter media system. This can best be accomplished by bench scale tests in which particle suspensions of varying electrolyte concentration are passed through the filter media.

From a combination of bench scale tests and measurements of particle and filter media zeta potentials, an effective value of the Hamaker constant can be calculated from the VODL stability criterion. This value can be used in the HRM model to predict the maximum removal efficiency by the interception mechanism. When Hamaker constants

can be evaluated more precisely, direct application of the value in the VODL stability criterion and the HRM may be possible.

Zeta potential measurements can further be used to evaluate the importance of potential-determining ions. For bioparticles, the hydrogen ion can be expected to be a potential-determining ion and alteration of the pH may be beneficial in raising the collection efficiency to the theoretical maximum.

Hollow fiber experiments confirm the solid fiber result that electrostatic interactions play a significant role in the collection of micron-size particles. The permeable wall can be utilized to control interfacial conditions at the hollow fiber surface. Each collision could be made to result in particle capture by providing a high ionic concentration in a thin surface boundary layer coupled with a slight amount of solvent withdrawal through the fiber wall.

The single fiber experiments correlate well with the hydrodynamic retardation theory. The range of values calculated for the Hamaker constant by the stability criterion is consistent with the HRM. The evidence for non-negligible hydrodynamic interaction with particles in the interception size range is convincing.

When non-spherical particles are involved, the proper radius to use in the HRM correlation is not clearly defined. In such cases, the GIM theory may be applied instead. The envelope of the particle motion in a two-dimensional laminar shear field can be predicted for a similarly shaped particle from hydrodynamic theory. The dimension of the envelope normal to the direction of flow can then be used in

the GIM calcualtion.

The experiments indicate that it may be possible to develop materials which reduce the fluid resistance and increase the initial collection efficiency. Lowered resistance may be achieved by "drainage" of the fluid into the fiber interior by osmotic or mechanical pressure gradients.

The existence of tiny pores (< 100 Å) in the collector surface may also increase the collection efficiency by minimizing adsorbed layer interference. Extremely porous fibrous materials might permit some fluid to flow right through the fiber and bring about the same effect as drainage. A fiber of this type would combine the best qualities of ultrafilters (high removal efficiencies) and conventional depth filters (low pressure losses and large particulate load capacities). The need for pore size uniformity decreases as the pores become larger and should improve the economics of fiber manufacture.

Chapter VI

Practical Applications of Hollow Fibers

A. Statement of Problem

Fibrous media are used extensively in the industrial filtration of liquids. Fibers may be woven into cloths, compressed into papers or used as mats. Typically fibrous media are highly porous and have low pressure losses. In cloths, the fibers operate primarily in the sieving mode while in papers and mats depth filtration occurs as well and may be the dominant removal mechanism. It is in the area of depth filtration that the results of this study are particularly applicable.

The filtration of particles from suspension can be considered a two step process. First, the particle must be transported to the vicinity of the collector surface where capture can occur. Second, the particle must become attached to the collector.

Filtration of liquid suspensions differs from that of gases in two important respects. In the transport step, the molecular density and viscosity of liquids results in non-negligible fluid mechanical interactions between particles and collecting surfaces. In the attachment step, surface chemical effects, not found in gases, are often important.

The hydrodynamic interaction involved in transporting the particle to the collecting surface had largely been neglected until the work of Spielman (1968). His results, those of Fitzpatrick and Spielman (1973) and the current study demonstrate that the hydro-

dynamic forces are significant, reducing collection efficiencies up to an order of magnitude below those predicted by the geometric interception model currently used for small and mean size particles ($\sim$ 1 μm - 30 μm).

The importance of surface chemical effects has been recognized for a considerably longer period. In aqueous suspensions where the high dielectric constant of water supports highly charged surfaces and large numbers of mobile ions, the effects are particularly pronounced. Specific chemical adsorption, surface reactions and hydration may additionally affect particle capture.

Since most surfaces become negatively charged in the neutral pH range (6-8), it is necessary to overcome the electrical double layer repulsion. Addition of chemical coagulants to the bulk solution is the method used most often. Simple electrolytes, highly charged hydrolyzable floc-forming metal ions, polymers and polyelectrolytes have been used to destabilize the suspensions. However, with increasingly stringent effluent requirements, reductions in the amount of chemicals added would be valuable.

To further complicate the problem of filter design the removal efficiency of different size particles differs and has a minimum value around 1 μm in aqueous suspensions. Since filter specifications usually require removal of a certain weight fraction of solids or removal of a minimum fraction of a given size, and since particles are generally non-uniform, information about the size distribution must be obtained. This must be used to weight the contributions of the different removal

mechanisms. Fortunately, many naturally occurring size distributions can be adequately described by a log-normal distribution. Mathematical techniques for manipulating log-normal distributions are treated in monographs treating the measurement and classification of particles (Orr and Dallavalle, 1959; Smith and Jordan, 1964).

There are additional problems associated with the calculation of the pressure drop, filter efficiency, and rate of clogging as functions of time. These areas require further study before accurate models can be developed. The design recommendations presented here are limited to the initial filtration efficiency of hollow fibers when interception is the dominant removal mechanism.

B. Design Recommendations

Fibrous media have several advantages over other filter materials. These include: a wide selection of materials and properties, relatively low fluid resistance, very fine fiber dimensions, and convenient gradation if desired.

The advantage of using fine fibers can be seen from the approximate dependence of the HRM efficiency on fiber size (Equation II-A-13 and Figure II-A-1). The dependence varies from about the inverse 1.3 power at high adhesion numbers to inverse 1.9 power at low adhesion numbers. As the fiber dimension approaches the particle dimension or becomes smaller, the hydrodynamic effects become less pronounced and the geometric interception model predicts an inverse 2.0 power dependence upon fiber diameter. Experimentally one finds roughly an inverse 1.0 to 1.5 power dependence upon fiber diameter. Therefore,

the filter coefficient has a 2.0 to 2.5 power dependence (Herzig, 1970; Spielman, 1968; Fitzpatrick and Spielman, 1973).

The pressure loss across a bed of fibers may be calculated from various flow models. A discussion of these models was given by Spielman and Goren (1968a). For a given porosity and overall removal, the pressure loss decreases as the inverse 0.0 to 1.0 power of the fiber diameter. Therefore, finer fibers lead to lower head losses which have a direct effect upon operating costs.

Decreasing the mat porosity improves the theoretical filter efficiency slightly (Spielman and Goren, 1968a) and results in smaller overall dimensions for the mat. However, the particulate load carrying capacity of the filter is sacrificed and the risk of blinding the filter with particles the size of the openings in the fiber mat is increased. Should blinding occur, the pressure drop would rapidly increase and surface rather than depth filtration would result. The concept of grading filter media has been applied successfully in modern multimedia sand filters to prevent blinding and extend filter runs. The principle should apply equally well to fibrous media. For this reason grading the filter with less closely packed or larger fibers near the inlet and more closely packed or finer fibers near the outlet merits consideration.

Hollow fibers share the inherent advantages mentioned above. Moreover, their potential use as a simple highly efficient filter and chemical feed system has been demonstrated during this study. The criterion for successful application of hollow fibers can be

established from the ratio of the mass transfer coefficients of particle to fiber and chemical to solution defined by the equation

$$\frac{k_{p,av}}{k_{\ell,av}} \propto \frac{A_F^{2/3} d_p^{\ 2} U^{2/3}}{d_f^{4/3} D_\ell^{2/3}} , \qquad \text{(III-B-12)}$$

for particles in the interception size range ($\sim$ 1 μm - 30 μm). Whenever the ratio is greater than unity, chemical addition through permeable fibers will be more efficient than addition to the bulk solution, roughly in proportion to the magnitude of the ratio.

One notes that the parameters over which the designer exercises control are the mainstream velocity (U), the diffusion coefficient of the chemical added (D_ℓ), and the fiber diameter (d_f). There is only a weak dependence on the parameter characterizing the flow model, A_F. Therefore, the orientation of the fiber axes, as long as they are perpendicular to the flow, does not exert a significant influence. Higher flowrates, higher solute diffusion coefficients and smaller fiber diameters contribute to more efficient operation. Table VI-B-1 gives values of the ratio under different conditions.

The calculations in Table VI-B-1 demonstrate that for most conditions simple electrolytes are not suited for use with hollow fibers. The electrolyte diffuses from the surface too rapidly, with the result that the mass transfer ratio becomes larger than unity. In that event, the effluent concentration of electrolyte will become as great or greater than that needed to destabilize the suspended particles. Furthermore, with simple electrolyte addition, the available high ionic strength sites would be occupied after a monolayer

Solute	$D_s \sim [cm^2/sec]$	$d_p \sim [cm]$	$U \sim [cm/sec]$	$d_f \sim [cm]$	N_{Re}	A_F	k_p/k_s
simple electrolyte	1×10^{-5}	0.0002	0.1	0.0500	0.5	0.186	0.00177
"	"	"	"	0.0100	0.1	0.116	0.0176
"	"	"	"	0.0010	0.01	0.076	0.438
"	"	"	1.0	0.0500	5.0	1.28	0.00431
"	"	"	"	0.0100	1.0	0.25	0.0157
"	"	"	"	0.0010	0.1	0.116	1.76
"	"	0.0005	0.1	0.0500	0.5	0.186	0.0110
"	"	"	"	0.0100	0.1	0.116	0.110
"	"	"	"	0.0010	0.01	0.076	2.74
"	"	"	1.0	0.0500	5.0	1.28	0.027
"	"	"	"	0.0100	1.0	0.25	0.397
"	"	"	"	0.0010	0.1	0.116	11.1
poly-electrolyte	1×10^{-6}	0.0002	0.1	0.0500	0.5	0.186	0.0082
"	"	"	"	0.0100	0.1	0.116	0.0820
"	"	"	"	0.0010	0.01	0.076	2.04
"	"	"	1.0	0.0500	5.0	1.28	0.020
"	"	"	"	0.0100	1.0	0.25	0.294
"	"	"	"	0.0010	0.1	0.116	8.20
"	"	0.0005	0.1	0.0500	0.5	0.186	0.0051
"	"	"	"	0.0100	0.1	0.116	0.0513
"	"	"	"	0.0010	0.01	0.076	12.8
"	"	"	1.0	0.0500	5.0	1.28	0.125
"	"	"	"	0.0100	0.1	0.25	1.85
"	"	"	"	0.0010	0.01	0.116	50.0

Table VI-B-1 Criterion for Hollow Fiber Use Evaluated for a Variety of Operating Conditions

of particles has been collected; therefore the fiber efficiency would diminish rapidly.

The high diffusion losses mentioned above should be remedied by using higher molecular weight solutes such as polyelectrolytes. The larger diffusion coefficient supports a thinner concentration boundary layer with lower losses to the bulk flow. Even after an initial monolayer of particles has been collected, it is believed that the polyelectrolyte can continue to diffuse, coat the collected particles, and thereby renew the capacity of the filter.

In certain cases, even when the mass transfer ratio is less than unity, the use of hollow fibers may be indicated, particularly if they are being used for surface rather than depth filtration. The total electrolyte flux from the fibers (J_ℓ) divided by the flowrate through the filter gives the average concentration in the effluent. The criterion then is that the average effluent concentration must be less than the concentration required to destabilize the particle-collector system. The calculation uses Friedlander's (1957) mass transfer analysis for the conditions of interest, i.e., low Reynolds numbers and moderate to large Peclét numbers.

The hydrodynamic resistance can be reduced by withdrawing water through the fiber wall or by using polyelectrolytes that stick out from the surface. The withdrawal of water can be accomplished either by mechanical (hydrostatic pressure) or chemical (osmotic pressure) means depending upon the permeability of the fiber employed.

The withdrawal rate should be small compared to the total flow-rate. No attempt was made to determine an analytical relationship

between collector efficiency and withdrawal rate. As a guideline, it is suggested that the normal velocity at the fiber wall should be a fraction of the fluid velocity at one particle radius from the wall. The particle radius used in the calculation should coincide with that of the minimum size particle whose removal is desired.

C. Alternative Uses of Hollow Fibers

Hollow fibers have several potential uses in filtration other than those identified above. They allow control of the surface chemistry. Theoretically they can be used to prevent as well as to promote deposition. In blood filters, heparin could be allowed to diffuse from the fiber to reduce the formation of emboli and thrombi.

If selective hollow fiber membranes can be developed, separation of dilute emulsions by fibrous media would be highly attractive. In oil-water separation, for example, suspended droplets which are too dilute to be coagulated and too small to settle rapidly are coalesced by porous media. However, the medium becomes clogged and larger globules are released. These are settled out downstream of the filter. With selective hollow fibers an immiscible solvent could be passed on the interior of the fiber and the coalesced droplets drawn into the fiber with the solvent. This would reduce pressure losses, obviate the need for an after-filter settling tank, and provide a filter with constant filtering efficiency.

As the size of the filtering element becomes smaller, the interception efficiency improves. If the filtering element was also made highly porous some of the flow might pass through the element, increas-

ing the filter efficiency. The success of one brand of diatomaceous earth has been attributed to this property[1]. In the past, the limiting factor has been the strength of such materials. However, it appears that the technology to produce strong porous fibers is now available. A filter mat composed of such fibers would really act as two filters in one. Each element serving as a micro-straining device as well as contributing to the depth filtration of the unit.

---

[1] "Celatom" filter aids - a product of Eagle-Picher Industries, Inc., Cincinnati, Ohio.

Chapter VII

Summary

A. Summary of Experiments

An experimental apparatus was constructed to permit visual observation of the deposition of micron-size particles on a single fiber from aqueous suspensions. Chemical and hydrodynamic conditions were controlled to conform with the assumptions of theoretical models for particle transport and attachment.

The following set of experiments was performed:

1) Deposition of a bioparticle (human erythrocytes-RBC) and a "similar" inert particle (7.6 μm styrene divinylbenzene latices-SDVBL) on several different fiber surfaces (teflon, glass) was compared.
2) The applicability of the Verwey-Overbeek, Derjaguin-Landau (VODL) theory of the electrical double layer to micron-size particles was tested by observing the deposition rate (2.0 μm polyvinyltoluene latices - PVTL on glass fibers) as a function of the counterion concentration of an unsymmetric electrolyte.
3) Tests of a recently proposed theory (hydrodynamic retardation model - HRM) which incorporates hydrodynamic and dispersion forces to predict particle capture by the interception mechanism were conducted.
4) Using the permeable membrane walls of hollow fibers, the effects of electrolyte addition and fluid withdrawal on

particle deposition were examined.

B. Summary of Results and Conclusions

Although RBC and SDVBL carry a net charge of similar sign, the RBC displayed stability toward plasma-coated teflon surfaces while the SDVBL were completely destabilized by the same surface. On the other hand, the RBC were destabilized by a cationic polyelectrolyte coating. In that case the RBC reached the same overall collection efficiency as that predicted by the geometric interception model (GIM) for 7.5 μm spheres with a 100% collision efficiency.

The effective size to be used in calculating the GIM efficiency can be estimated from the RBC experiments. The effective "diameter" of the particle is given by the envelope of the particle motion normal to the direction of flow as calculated from the hydrodynamics of particle motion in a shear field. The ability of the RBC to "recognize" the plasma-coated surface indicates that the evaluation of the collision efficiency of bioparticles will generally require study of each class of surface. Current VODL theory cannot predict the collision efficiency of bioparticles, but still describes the approach of charged particles toward charged surfaces.

Experiments with 2.0 μm PVTL particles depositing on glass fibers demonstrated that some particle collection occurs even in the presence of theoretically (VODL) large energy barriers. Although the deposition rate did increase rapidly over a narrow range of counterion concentration, it did not reach the predicted maximum value with simple electrolyte addition. The data were examined in terms of

sphere-plate interaction potentials and yielded an effective value of the Hamaker constant in the range from about 3×10^{-20} to 8×10^{-20} joules.

The experimental evidence suggests that either VODL theory must be modified or new theories proposed in order to explain particle attachment. In particular a new mechanism to explain particle deposition in the presence of large repulsive energy barriers needs to be developed. Stern-type corrections incorporated into the VODL theory would probably be able to explain a large class of hydrophilic surface interactions. Currently, the paucity of adsorption energy data prevents successful application of the corrections. Furthermore, there appears to be a statistical nature to particle capture which may be caused by discreteness of charge, surface roughness or surface heterogeneity. This cannot be explained by VODL theory even with Stern-type corrections. Quantitative predictions may not be possible without a statistical data base for a particular type of filtering material and particle suspension. VODL theory does, however, predict the onset of rapidly increasing deposition rate in at least a semi-quantitative manner. This provides a basis for selecting physical-chemical methods to increase collision efficiency.

The HRM theory for collection of particles was tested by varying particle diameters, fiber diameters, flow velocities and collecting surfaces. The ratio of the experimental collection efficiency to GIM efficiency was plotted against the adhesion number, $N_{Ad,f}$, suggested by Spielman (1968) and Spielman and Goren (1970). The lower value of the Hamaker constant (3×10^{-20} joules) calculated from the VODL stability criterion was used in computing the adhesion

number. The data were also compared with numerical calculations for single cylindrical collectors given by Fitzpatrick and Spielman (1973). An independent test of the influence of hydrodynamic retardation was made by withdrawing fluid at a known rate through a hollow fiber and observing the change in the deposition rate of the particles.

The increased rate of deposition found in the fluid withdrawal experiment could not be explained by the rate of fluid withdrawal. The additional increase in the deposition rate was attributed to a decrease in the hydrodynamic resistance.

Good agreement between the HRM and experiments was found. The agreement could be improved by choosing a slightly larger value of the Hamaker constant than that used (3×10^{-20} joules) to calculate the adhesion number, but the theoretical curve fell within the range of experimental error of most data points. The collection efficiency of latices from suspensions destabilized by a simple salt were consistently about a factor of three lower, but followed the theoretical trend. The porous nature of the hollow fiber surface, the projection of plasma proteins from the coated teflon surface and the absence of strongly adsorbed layers in the low pH, PVTL-glass experiment resulted in a maximum collision efficiency. This suggested that steric interference between adsorbed layers on the particle and fiber surface hindered particle attachment.

The HRM theory presents a correct description of particle capture, but adsorbed layers may interfere with particle attachment. Interference may be reduced by reducing adsorption energies or reducing the area of adsorbed layer interference.

By varying the electrolyte concentration inside the hollow fiber, the surface concentration and osmotic flow through the fiber wall could be controlled. Particle capture due to osmotic flow occurred, but the particles were released by subsequent flushing of the fiber interior with distilled deionized water unless the counterion concentration near the surface was sufficiently high. Increasing the electrolyte concentration outside the fiber reduced the amount of osmotic flow. Particles were made to deposit at the maximum interception rate by using hollow fibers.

Hollow fiber filters may be used to control the filtration efficiency by modifying the surface chemistry of the fiber. Experimental observations were satisfactorily interpreted in terms of concentration boundary layer theory. Using a boundary layer solution, an approximate criterion was developed which predicts when hollow fibers may be usefully employed to reduce the amount of chemical addition required to destabilize particles.

C. Suggestions for Further Research

Several questions were raised by the inadequacy of current VODL theory to predict observed deposition patterns. In particular further research is needed to devise a quantitative model for particle collection in the presence of electrostatic barriers. More data for energies of adsorption on different surfaces must be gathered before Stern-type corrections to VODL theory can be applied to particle adhesion.

The effects of shearing forces need to be studied further.

Visual evidence indicated that shearing forces became important for particles larger than ~ 10 μm for the range of operating conditions currently used in water filters. The role of surface chemistry on the adhesion of particles in the gravitational settling size range should be studied simultaneously.

The potential advantages of hollow fiber filtration should be explored. Experiments should be conducted to find compatible polyelectrolyte-hollow fiber combinations. Longer runs should be made to study whether polyelectrolytes diffusing from the fiber can be made to adsorb efficiently on previously deposited particles, thereby forming new collecting surfaces. Packed bed experiments are also needed to check the effects of electrolyte diffusion throughout the depth of the bed. Accurate prediction of the optimum amount of electrolyte addition can be made from numerical solutions of the convective diffusion equations with the appropriate porous wall boundary condition. Such studies might predict that concentration polarization would be beneficial in minimizing electrolyte losses.

Conceptually, hollow fibers may be particularly valuable in the separation of liquid-liquid suspensions of low droplet concentrations. A hollow fiber filter could maintain high constant filtration efficiencies if the membrane can be made selectively permeable to the droplet phase. The hollow fibers may also be useful in blood filtration. Studies should be conducted to determine the effects of heparin diffusion from the fiber surface.

APPENDICES

Appendix A

Discussion of Experimental Error

The largest experimental error was incurred in counting the number of particles deposited on the fiber. The statistics of the particle deposition rate are described by the Poisson distribution. The standard deviation, σ, of such a distribution is given by

$$\sigma = \sqrt{E} \ , \qquad \text{(A-1)}$$

where E is the expected value of the particle deposit.

The actual number of particles, N, counted probably does not coincide with the expected value of the distribution. Therefore, the standard deviation calculated by substituting N for E serves only as an estimate of the statistical error. A better method is to apply confidence limits to the data. The symmetrical 95% confidence limits, L, for a Poisson distribution are given by Wilson (1952) as

$$L = N + 1.92 \pm 1.96 \sqrt{N+1.0} \ . \qquad \text{(A-2)}$$

These were applied to the 2.0 μm PVTL data and the data used to check the HRM model.

Another source of error might have crept in through experimental bias (personal error). The counting procedure affords an opportunity for bias to enter because it is a visual rather than a mechanical measurement. A photographic record of the deposits might have improved the situation, but the number of photographs required for a through-

focus series of shots at each data point was prohibitive, and the time resolution would have been poor. Instead, every opportunity was taken to prevent foreknowledge of the theoretical deposition rate. This included preparing particle suspensions of unknown concentration immediately before each run, counting deposits at irregular intervals, and making calculations only after a series of runs had been completed. This caused occasional inconvenience (very high or very low deposition rates), but was deemed necessary in order to minimize the possibility of bias.

Further errors could have entered in the values used for fluid properties, flowrates, fiber dimensions etc., but these were comparatively small even on a cumulative basis. The error bars shown in Figures V-B-1, V-B-6, V-C-2 and V-D-1, are the combined estimate of personal, systematic and statistical errors.

Appendix B

Calculation of Collection Efficiency of a Fiber for Particles Diffusing Through an Energy Barrier

The parameter β appearing in Equation II-A-15 is given by Spielman and Friedlander (1973) as

$$\beta = \frac{1}{3}\Gamma\left(\frac{1}{3}\right)\left(\frac{3}{2}\right)^{1/3}\frac{1}{A_F^{1/3}}\left(\frac{D_p}{U a_f}\right)^{1/3}\left(\frac{k' a_f}{D_p}\right) \quad , \qquad \text{(B-1)}$$

where Γ is the Gamma function, A_F is given by Equation II-A-8, and D_p is the diffusion coefficient of the particle. The parameter k' accounts for the height of the energy barrier to deposition and the random thermal energy of the diffusing particle and is given by

$$k' = \frac{D_p}{\int_o^\infty \left(e^{V_T/kT} - 1\right) dh} \quad . \qquad \text{(B-2)}$$

Equation II-B-6,

$$V_T = -\frac{Qa_p}{6h} + 4\pi\epsilon\epsilon_o\left(\frac{\psi_{01}^2+\psi_{02}^2}{4}\right)\left[\frac{2(\psi_{01}\psi_{02})}{(\psi_{01}^2+\psi_{02}^2)}\ln\left(\frac{1+\exp(-\kappa h)}{1-\exp(-\kappa h)}\right) + \ln\left(1-\exp(-\kappa h)\right)\right] \quad ,$$

which assumes unretarded dispersion forces and low to moderate diffuse layer potentials (ψ_o < 50-60 mv) was used to describe the potential energy of the diffusing particles.

Equation B-2 was evaluated approximately. The integral appearing in the denominator was assumed to be given by the triangular

region defined by the maximum of the potential energy barrier, and the two points where the potential energy curve passes through zero. The height of the potential energy barrier and the roots of the potential energy curve where determined by successive iteration on a desk calculator.[1] For extensive calculations requiring changes in the values of many different variables, use of a digital computer is recommended.

---

[1] Compucorp Model 122 with 128-step programmable memory.

Appendix C

Experimental Sequence

Description of step	Reference
1. Prepare solution	Sect. III-B-4
2. Check pH, osmolarity[1]	" IV-B-2
3. Mount fiber in fixture[1,3]	" IV-B-1
4. Clean fiber[1]	" IV-C-2
5. Prepare stock of RBC[1]	" IV-C-1
6. Prepare Coulter counter	" IV-C-3
7. Prepare constant head tank and rotameter	" IV-C-4
8. Clean fiber[2,3]	" IV-C-2
9. Mount in fixture[2]	" IV-C-1
10. Prepare tunnel	" IV-C-4
11. Mount tunnel and connect to rotameter	" IV-C-4
12. Coulter count blank	" IV-C-3
13. Prepare particle suspension	" IV-C-1
14. Complete flow circuit connections	Fig. IV-B-4
15. Take initial sample	Sect. IV-B-2
16. Begin flow, start timer	" IV-C-6
17. Measure particle deposit, concentration, pH, temperature, conductivity	" IV-C-5, C-3, B-2
18. Start electrolyte flow[3]	" IV-C-6, B-1

[1] These steps included with RBC or Teflon fiber experiments.

[2] These steps included with glass fiber experiments.

[3] These steps included with hollow fiber experiments.

Appendix D

Size Distribution Correction

The particle size distributions were determined from optical or Coulter Counter measurements. The cumulative frequency distributions versus size were plotted on logarithmic-probability paper. The geometric mean diameter, M_g, and the geometric standard deviation, σ_g, could be obtained from the linear plots as the 50% size and the ratio of the 85.13% to 50% size respectively.

These parameters are related to the GIM efficiency of the distribution by the equation

$$\eta_{GIM\ dist.} = 2A_F \frac{M_g^2}{d_f^2} \cdot \exp\left[2 \ln^2(\sigma_g)\right] . \qquad (D\text{-}1)$$

The form of the equation was given by Hatch and Choate (1929), but was not derived explicitly for this case. The following outline of the derivation is supplied for those unfamiliar with the mathematics of logarithmic-normal distributions.

The GIM efficiency for any size particle, x, is given by

$$\eta_{GIM}^{(x)} = 2A_F \frac{x^2}{d_f^2} . \qquad (D\text{-}2)$$

The efficiency resulting from a distribution of sizes is given by

$$\eta_{GIM\ dist} = \int \eta(y)\ p(y)\ dy \qquad (D\text{-}3)$$

over the entire range of y, where p(y) is the probability density function. For a log-normal distribution, the density function is

given by

$$p(y) = \frac{1}{\sqrt{2\pi}\ \ln \sigma_g} \cdot \exp\left[- \frac{(y - \ln M_g)^2}{2\ \ln^2 \sigma_g} \right] . \qquad \text{(D-4)}$$

Substituting Equations D-2 and D-4 into Equation D-3, and making the change of variable,

$$x = e^y,$$

the following integral is obtained:

$$\eta_{\text{GIM dist}} = \int_{-\infty}^{\infty} 2A_F \frac{\exp(2y)}{d_f^2} \cdot \frac{1}{\sqrt{2\pi}\ln \sigma_g} \cdot \exp\left[- \frac{(y - \ln M_g)^2}{2\ln^2(\sigma_g)} \right] dy, \qquad \text{(D-5)}$$

for particle sizes, x, ranging from 0 to ∞. The integral can be evaluated with the aid of a table of definite integrals to give Equation D-1.

Appendix E

Calculation of Hamaker Constants from Refractive Index Data

Hamaker constants were estimated from refractive index data using the equations given by Gregory (1969):

$$Q_{12} = \frac{27}{64} h\nu_v \left(\frac{\epsilon_0 - 1}{\epsilon_0 + 2} \right)^2 \qquad \text{(E-1)}$$

and

$$\epsilon = n^2 \qquad \text{(E-2)}$$

Here n is the index of refraction, ϵ is the dielectric constant, h is Planck's constant, ν_v is the characteristic dispersion frequency, and ϵ_0 is the square of the limiting refractive index in the visible wavelength region. The Hamaker constant for two different materials 1 and 2 in water 3 was taken to be

$$Q = Q_{12} + Q_{33} - Q_{13} - Q_{23} \quad . \qquad \text{(E-3)}$$

The values of the refractive index and characteristic wavelength are given in Table E-1. The values used for cellulose-acetate and polyvinyltoluene latex are crude estimates based upon a knowledge of the structure of the molecules. The Hamaker constants calculated by this method range from 0.3×10^{-20} to 0.7×10^{-20} joules.

Substance	Refractive Index	Characteristic Frequency
Water	1.323	3.35×10^{15} sec^{-1}
Glass	1.57	3.78×10^{15} "
PVTL	1.581	2.62×10^{15} "
DVBSL	1.563	2.62×10^{15} "
CA-a, c	1.46	3.4×10^{15} "

Table E-1 Values of Refractive Index and Characteristic Frequency used in Hamaker Constant Calculation

Appendix F

Discussion of Boundary Conditions for Permeable Walls

The permeability of the hollow fiber wall permits both solvent and solute flux under applied pressure and concentration gradients. The mechanisms by which solvent and solute pass through the membrane depend upon the type of membrane used. Solvent and solute flow through the cellulose acetate membranes used in these experiments probably proceeded as a combination of diffusion and viscous flow.

The flux of solvent (subscript "w") and solute (subscript "s") are proportional to the driving forces. The chemical potentials, μ_w and μ_s, were the motive forces. Fluxes are given by Thompson (1967) as

$$J_w = L_{ww}\,\Delta\mu_w + L_{ws}\,\Delta\mu_s$$

and

$$J_s = L_{sw}\,\Delta\mu_w + L_{ss}\,\Delta\mu_s \quad , \qquad \text{(F-1)}$$

where the L's are the phenomenological coefficients and the Onsager reciprocal relation requires $L_{ws} = L_{sw}$. The linear laws should be good approximations when the gradients are small.

For small concentration differences the chemical potentials are given by Thompson (1967) as

$$\Delta\mu_w = RT\,\Delta\ln a_w + \bar{v}_w\,\Delta p = \bar{v}_w(\Delta p - \Delta\pi)$$

and

$$\Delta\mu_s = RT\,\Delta\ln a_s + \bar{v}_s\,\Delta p = \frac{n_w \bar{v}_w}{n_s}\,\Delta\pi + \bar{v}_s\,\Delta p \qquad \text{(F-2)}$$

where the $\bar{v}$'s are the partial molar volumes, Δp is the applied pressure difference, $\Delta\pi$ is the osmotic pressure difference, $\left(= \frac{RT}{\bar{v}_w} \Delta \ln a_w \right)$, and n's are mole fractions.

The activities of the solvent and solute on the particle suspension side of the membrane can be seen to depend upon the solute distribution, which in turn depends upon the solution of the hydrodynamic equations and boundary conditions. The boundary conditions (Equation III-B-2) involve the flux of solute. Therefore the equations are coupled.

To develop a reasonably simple criterion which could be applied to describe efficient operation of hollow fibers, the following reasoning was applied to the relative importance of the fluxes. For efficient operation, the solvent flux must be small compared to the flow past an individual fiber, otherwise the fiber would act as a sieve and a large fraction of the suspension would be processed through the fiber wall. Therefore, the assumption that the impermeable wall solution for the velocity field given by Lamb (1932) (Equation III-B-1) is justified in developing the criterion for efficient operation.

The solution of the convective diffusion equation with its boundary conditions provides an estimate of the surface concentration. This can in turn be used to calculate the flux of solution through the membrane wall if the membrane permeability to solvent is known. Thus a check on the assumption of negligible solvent flux can be made.

No measurements of solvent permeability were made with the cellulose acetate membranes. Literature values indicate that simple electrolyte addition using cellulose acetate membranes developed for

reverse osmosis would not satisfy the criterion. However, reverse osmosis membranes are designed for maximum solvent (water) passage and do not represent ideal membranes for hollow fiber filtration.

Several other effects which may be important in the operation of hollow fiber filters have been neglected. These include charge effects, coupled flows for higher order systems, and the applicability of a uniformly permeable membrane boundary condition. These effects are treated in texts dealing with membrane transport and the thermodynamics of irreversible processes (Prigogine, 1961; Lakshminarayanaiah, 1969).

Appendix G

Calculation of an Effective Hamaker Constant

The stability criterion proposed by Verwey and Overbeek (1948) takes as the condition for the onset of rapid coagulation, the point at which the maximum in the potential energy curve passes through zero. The potential energy of the sphere-plate double layer interaction is given by Equation II-B-6,

$$V_T = -\frac{Qa_p}{6h} + 4\pi\epsilon\epsilon_0\left(\frac{\psi_{01}^2+\psi_{02}^2}{4}\right)\left[\frac{2(\psi_{01}\psi_{02})}{(\psi_{01}^2+\psi_{02}^2)}\ln\left(\frac{1+\exp(-\kappa h)}{1-\exp(-\kappa h)}\right)+\ln(1-\exp(-\kappa h))\right],$$

for unretarded dispersion forces and low to moderate diffuse layer potentials ($\psi_0 < 50$-60 mv). The equation was solved directly for V_T for the experimentally determined values of particle radius a_p, surface potentials ψ_{01} and ψ_{02}, double layer thickness κ^{-1}, and varying values of gap width, h, and Hamaker constant Q. A desk calculator was used to generate the curves shown in Figures II-B-1 and II-B-2.[1] An estimate of the effective Hamaker constant could be read from the graphs directly.

---

[1] Compucorp Model 122 with 128-step programmable memory.

NOTATION

Each symbol used in the text was defined when first used. Only symbols appearing throughout the text are listed here for convenient reference.

Symbol		Definition
English Upper Case		
A_F	-	parameter characterizing flow model
$\mathring{A}$	-	Angstroms (10^{-10} meters)
CA-a	-	cellulose acetate-a, 200 MW cutoff
CA-c	-	cellulose acetate-c, 30,000 MW cutoff
D	-	diffusion coefficient (with subscripts)
DDH_2O	-	distilled deionized water
FEP	-	fluoroethylene propylene
GIM	-	geometric interception model (also used as subscript)
HRM	-	hydrodynamic retardation model (also used as subscript)
J	-	flux; also denotes joules
M	-	moles per liter
MW	-	molecular weight
$N_{Ad,f}$	-	Adhesion number for fiber collector
N_{Nu}	-	Nusselt number (based on diameter)
N_{Pe}	-	Peclet number (based on diameter)
N_{Re}	-	Reynolds number (based on diameter)
PVTL	-	polyvinyltoluene latex
Q	-	Hamaker constant
R	-	interception parameter

SDVBL - styrene divinylbenzene latex

T - absolute temperature, degrees Kelvin

U - approach velocity of fluid

V - potential energy of interaction

VODL - Verwey-Overbeek, Derjaguin-Landau theory of diffuse electrical double layer

English Lower Case

a - radius (with subscripts)

d - diameter (with subscripts)

e - electronic charge (1.6×10^{-19} coulombs)

f - porosity

g - gravitational acceleration

h - sphere-plate gap width

k - mass transfer coefficient or Boltzmann's constant (1.38×10^{-23} joules/degree Kelvin)

n - concentration (with subscripts)

p - pressure

r - radial coordinate

$\vec{v}$ - vector velocity

v - velocity component (with subscripts)

z - charge number of ion

Greek Upper Case

Ψ - stream function

Greek Lower Case

α - collision efficiency

β - parameter characterizing convective diffusion through an energy barrier

ϵ - dielectric constant

ϵ_o - permittivity of free space (8.85×10^{-12} farads/meter)

ζ - zeta potential

η - collection efficiency; with subscripts signifies transport efficiency

θ - angle measured counterclockwise

κ - reciprocal of "double layer thickness" also called reciprocal "Debye length"

λ - "filter coefficient" also called "impediment modulus"

μ - absolute viscosity

μm - microns (10^{-6} meters)

ν - kinematic viscosity

ρ - density (with subscripts)

φ - membrane permeability

ψ - electric potential (with subscripts)

Subscripts

A - attractive

D - diffusion

EXP - experimental

G - "gravity" also termed "sedimentation"

R - repulsive

T - total

f	-	fiber
ℓ	-	species "ℓ"
m	-	membrane
p	-	particle
r	-	radial direction
s	-	settling velocity, sphere, or solute as appropriate
t	-	transport
w	-	solvent
δ	-	location of Stern layer or membrane thickness as appropriate
θ	-	tangential direction
o	-	value at a surface
∞	-	value far from a surface

REFERENCES

1. Abramson, H. A., L. S. Moyer, and M. H. Gorin. Electrophoresis of Proteins. New York: Hafner Publishing Co. Inc. (1964).

2. Adamson, A. W. Physical Chemistry of Surfaces 2d ed. New York: Interscience Publishers (1967).

3. Agrawal, G. D. "Electrokinetic Phenomena in Water Filtration." Unpublished Doctoral Dissertation, University of California, Berkeley (1966).

4. Allen, L. H. and E. Matijević. "Stability of Colloidal Silica - I. Effect of Simple Electrolytes." J. Colloid Interface Sci., 31, 287 (1969).

5. Allen, L. H. and E. Matijević. "Stability of Colloidal Silica - II. Ion Exchange." J. Colloid Interface Sci., 33, 420 (1970).

6. Ambrose, E. J. "Cell Contacts." Recent Progress in Surface Science, 1, 338 (1964).

7. Ashmore, P. G., et al. "Effect of Dacron Wool Filtration on Microembolic Phenomena in Extracorporeal Circulation." J. Thoracic and Cardiovascular Surg., 63, 240 (1972).

8. Black, A. P. and A. L. Smith. "Determination of the Mobility of Colloidal Particles by Microelectrophoresis." J. AWWA, 54, 926 (1962).

9. Boddy, P. J., W. H. Brattain, and P. N. Sawyer. "Some Electrochemical Properties of Solid-Liquid Interfaces and the Electrode Behavior of Erythrocytes." In Biophysical Mechanisms in Vascular Homeostasis and Intravascular Thrombosis, edited by P. N. Sawyer. New York: Appleton, Century, Crofts (1965).

10. Brooks, D. E., et al. "Some Physicochemical Factors Relevant to Cellular Interactions." J. Cell. Physio., 69, 155 (1967).

11. Camp, T. R. "Theory of Water Filtration." J. Sanit. Eng. Div., Am. Soc. Civ. Engrs., 90:SA4, 1 (1964).

12. Chemical Engineering, Author Anonymous. "Why Hollow-Fiber Reverse Osmosis Won the Top CE Prize for DuPont." Chemical Engineering, 78, 54 (Nov. 29, 1971).

13. Cohen, M. E., M. A. Grable, and B. M. Riggleman. "Hollow-Fiber Reverse Osmosis Membranes." In Reverse Osmosis Membrane Research, edited by Lonsdale, H. K. and H. E. Podall. New York: Plenum Press (1972).

14. Cole, C. A. and E. J. Genetelli. "Decarbonation and Deaeration of Water by Use of Selective Hollow Fibers." Env. Sci. Tech., 4:6, 514 (1970).

15. Cookson, J. T., Jr. and W. J. North. "Adsorption of Viruses on Activated Carbon: Equilibria and Kinetics of the Attachment of Escherichia coli Bacteriophage T_4 on Activated Carbon." Env. Sci. Tech., 1:1, 46 (1967a).

16. Cookson, J. T., Jr. "Adsorption of Escherichia coli Bacteriophage T_4 on Activated Carbon as a Diffusion Limited Process." Env. Sci. Tech., 1:2, 157 (1967b).

17. Cookson, J. T., Jr. "Mechanism of Virus Adsorption on Activated Carbon." J. AWWA, 61:1, 52 (1969).

18. Cookson, J. T., Jr. "Removal of Submicron Particles in Packed Beds." Env. Sci. Tech., 4:2, 128 (1970).

19. Coulter Electronics Industrial Division. "Instruction Manual: Coulter Counter Industrial Model B." Hileagh, Florida.

20. Davis, J. Dow Chemical Co. Personal communication (1972).

21. Derjaguin, B. V. "Effect of Lyophile Surfaces on the Properties of Boundary Liquid Films." Disc. Faraday Soc., No. 42, 109 (1966).

22. Djerassi, I., et al. "Continuous Flow Filtration - Leukophoresis." Transfusion, 12:2, 75 (1972).

23. Edmark, K. W., J. W. Davis, and H. C. Milligan. "Streaming Potential - An Analysis of the Test Technique and Its Application to the Study of Thrombosis on Implant Materials." Thrombosis Et Diathesis Haemophagica, 24, 286 (1970).

24. Egleblad, K., et al. "Blood Filtration During Cardiopulmonary Bypass." Thoracic and Cardiovascular Surg., 63, 385 (1972).

25. Eisenman, G. "The Electrochemistry of Cation-Sensitive Glass Electrodes." In The Glass Electrode. New York: Interscience Publishers (1965).

26. Federation of American Societies for Experimental Biology, "Conference on Mechanical Surface and Gas Layer Effects on Moving Blood." Bethesda, Maryland: Fed. Am. Soc. Exp. Bio., Proc., 30:5 (1971).

27. Fitts, C. T., et al. "Closed-Circuit Extracorporeal Filtration of Thoracic Duct Lymph." Surgery, 70, 786 (1971).

28. Fitzpatrick, J. A. and L. A. Spielman. "Filtration of Aqueous Latex Suspensions Through Beds of Glass Spheres." To be published in J. Colloid Interface Sci. (1973).

29. Foss, O. P., O. T. Messelt, and L. Efskind. "Isolation of Cancer Cells from Blood and Thoracic Duct Lymph by Filtration." Surgery, 53, 241 (1963).

30. Friedlander,S. K. "Mass and Heat Transfer to Single Spheres and Cylinders at Low Reynolds Numbers." A. I. Ch. E. Journal, 3:1, 43 (1957).

31. Friedlander, S. K. "Aerosol Filtration by Fibrous Filters." In Biochemical and Biological Engineering Science Vol. I, edited by N. Blakebrough. New York: Academic Press (1967a).

32. Friedlander, S. K. "Particle Diffusion in Low-Speed Flows." J. Colloid Interface Sci., 23, 157 (1967b).

33. Galletti, P. M., and G. A. Brecher. Heart-Lung Bypass: Principles and Techniques of Extracorporeal Circulation. New York: Grune and Stratton (1962).

34. Gileadi, E., et al. "Antithrombogenic Characteristics of Cathodically Polarized Copper Prostheses." J. Biomed. Mat. Res., 6, 489 (1972).

35. Goldsmith, H. L. and S. G. Mason. "Axial Migration of Particles in Poiseuille Flow." Nature, London, 190, 1095 (1961).

36. Goldsmith, E. I. and B. H. Kean. "Schistosomiasis: Experimental Surgical Removal of Adult Worms." Gastroenterology, 50, 805 (1966).

37. Goldsmith, E. I., et al. "Surgical Recovery of Schistosomes from the Portal Blood." J. AMA, 199, 235 (1967).

38. Goldsmith, E. I. and B. H. Kean. "Surgical Treatment of Schistosomiasis by Extracorporeal Hemofiltration in Baboons and in Man: S. Mansoni and S. Haematobium." Annals of the New York Acad. Sci., 162, 453 (1969).

39. Gregory, J. "The Calculation of Hamaker Constants." Advan. Colloid Interface Sci., 2, 396 (1969).

40. Happel, J. and H. Brenner. Low Reynolds Number Hydrodynamics. Englewood Cliffs, New Jersey: Prentice Hall (1965).

41. Hatch, T. and S. P. Choate. "Statistical Description of the Size Properties of Non-Uniform Particulate Substances." J. Franklin Institute, 207, 369 (1929).

42. Heertjes, P. M. and C. F. Lerk. "The Functioning of Deep-Bed Filters: Part II: The Filtration of Flocculated Suspensions." Trans. Inst. Chem. Engrs., 45, T138 (1967).

43. Herzig, J. P., D. M. Leclerc, and P. Le Goff. "Flow of Suspensions through Porous Media-Application to Deep Filtration." In Flow Through Porous Media, Washington D.C.: American Chemical Society Publications (1970).

44. Hill, J. D., et al. "Experience Using a New Dacron Wool Filter During Extracorporeal Circulation." Arch. Surg., 101, 649 (1970).

45. Hogg, R., T. W. Healy, and D. W. Fuerstenau. "Mutual Coagulation of Colloidal Dispersions." Trans. Faraday Soc., 62:522, 1638 (1966).

46. Hull, M. and J. A. Kitchener. "Interactions of Spherical Colloidal Particles with Planar Surfaces." Trans. Faraday Soc., 65, 3093 (1969).

47. Hunter, R. J. and H. J. L. Wright. "The Dependence of Electrokinetic Potential on Concentrations of Electrolyte." J. Colloid Interface Sci., 37:3, 564 (1971).

48. Ison, C. R. and K. J. Ives. "Removal Mechanisms in Deep Bed Filtration." Chem. Eng. Sci., 24, 717 (1969).

49. Ives, K. J. and I. Sholji. "Research on Variables Affecting Filtration." J. Sanit. Eng. Div., Am. Soc. Civ. Engrs., 90:SA4, 1 (1965).

50. James, R. O. and T. W. Healy. "Adsorption of Hydrolyzable Metal Ions at the Oxide-Water Interface." J. Colloid and Interface Sci., 40, 42 (1972).

51. Johnson. G. A., et al. "Role of Water Structure in the Interpretation of Colloid Stability." Disc. Faraday Society, No. 42, 120 (1966).

52. Kasper, D. R. "Theoretical and Experimental Investigations of the Flocculation of Charged Particles in Aqueous Solutions by Polyelectrolytes of Opposite Charge." Unpublished Doctoral Dissertation, California Institute of Technology (1971).

53. Kruyt, H. R. Colloid Science Vol. I. New York: Elsevier Publishing Co. (1952).

54. Lakshminarayanaiah, N. Transport Phenomena in Membranes. New York: Academic Press (1969).

55. Lamb, Sir Horace. Hydrodynamics 6th ed. New York: Dover Publications (1932).

56. Mackrle, V. and S. Mackrle. "Adhesion in Filters." J. Sanit. Eng. Div., Am. Soc. Civ. Eng., 87:SA5, 17 (1961).

57. Majeski, J. A. "Lymphocyte Depletion By Generalized or Selective Filtration." Unpublished Doctoral Dissertation, Medical University of South Carolina (1972).

58. McNamara, J. J., et al. "Effective Filtration of Banked Blood." Surgery, 71, 594 (1972).

59. Marshall, J. K. and J. A. Kitchener. "The Deposition of Colloidal Particles on Smooth Solids." J. Colloid Interface Sci., 22, 342 (1966).

60. Mintz, D. M. "Modern Theory of Filtration." Int. Water Supply Assn., Congr., London (1966).

61. Natanson, G. L. "Deposition of Aerosol Particles on the Streamlined Cylinder Under the Influence of Electrostatic Attraction." Translated by J. Vuceta. Dokl. Akad. Nauk. SSSR, 112, 100 (1957a).

62. Natanson, G. L. "The Condensation of Aerosol Particles by Electrostatic Attraction on a Cylinder Around Which They are Streaming." Dokl. Akad. Nauk. SSSR, 112, 696 (1957b).

63. Neihof, R. "Microelectrophoresis Apparatus Employing Palladium Electrodes." J. Colloid Interface Sci., 30:1, 125 (1969).

64. O'Melia, C. R. and W. Stumm. "Theory of Water Filtration." J. AWWA, 59, 1393 (1967).

65. Orr, C., Jr. and J. M. Dallavalle. Fine Particle Measurement. New York: Macmillan Co. (1959).

66. Osborne, J. J. "Experience with an Air-Driven Pump Oxygenator with Reference to Blood Coagulation." Trans. Am. Soc. Art. Int. Org., 1, 81 (1955).

67. Ottewill, R. H. and J. N. Shaw. "Stability of Monodisperse Polystyrene Latex Dispersions of Various Sizes." Disc. Faraday Soc., 42, 154 (1966).

68. Ottewill, R. H. and J. N. Shaw. "Characterization of Latex Particles Produced by Emulsion Polymerisation." Br. Polymer J., 2, 116 (1970).

69. Pethica, B. A. "The Physical Chemistry of Cell Adhesion." Exp Cell. Res., Suppl. 8, 123 (1961).

70. Prigogine, I. Thermodynamics of Irreversible Processes 2d ed. New York: Interscience Publishers (1961).

71. Rubin, A. J. and G. P. Hanna. "Coagulation of Escherichia coli by Aluminum Nitrate." Env. Sci. Tech., 2:5, 358 (1968).

72. Rubin, A. J., P. L. Hayden, and G. P. Hanna. "Coagulation of Escherichia coli by Neutral Salts." Water Res., 3, 843 (1969).

73. Rutgers, A. J. and M. De Smet. "Researches on Electro-Endosmosis." Trans. Faraday Soc., 41, 758 (1945).

74. Saffman, P. G. "The Lift on a Small Sphere in a Slow Shear Field." J. Fluid Mech., 22, 385 (1965).

75. Sakthivadivel, R. and S. Irmay. "A Review of Filtration Theories." Interim Report of the Hydraulic Engineering Laboratory, College of Engineering, University of California, Berkeley, HEL 15-4 (1966).

76. Salyer, J. O., G. L. Ball III, and G. L. Beemsterboer. "The Monsanto Polyacrylonitrile Hollow Fiber Artificial Kidney." In Membrane Processes in Industry and Biomedicine, edited by M. Bier. New York: Plenum Press (1971).

77. Sawyer, P. N., ed. Biophysical Mechanisms in Vascular Homeostasis and Intravascular Thrombosis. New York: Appleton, Century, Crofts (1965).

78. Sawyer, P. N., W. H. Brattain, and P. J. Boddy. "Electrochemical Precipitation of Human Red Blood Cells and Its Possible Relation to Intravascular Thrombosis." Proc. Nat. Acad. Sci., 51, 428 (1964).

79. Sawyer, P. N. and S. Srinivasan. "Electrochemistry of Thrombosis - An Aid in the Selection of Prosthetic Materials." J. Biomed. Mat. Res., 4, 43 (1970).

80. Schaller, E. J. and A. E. Humphrey. "Electroviscous Effects in Suspensions of Monodisperse Spherical Particles." J. Colloid Interface Sci., 22, 573 (1966).

81. Schenkel, J. H. and J. A. Kitchener. "Test of Derjaguin-Verwey-Overbeek Theory." Trans. Faraday. Soc., 56, 151 (1960).

82. Schlicting, H. Boundary Layer Theory 6th ed. Translated by J. Kestin. New York: McGraw-Hill Book Co. (1968).

83. Schraub, F. A., et al. "Use of Hydrogen Bubbles for Quantitative Determination of Time-Dependent Velocity Fields in Low-Speed Water Flows." Trans. ASME, J. Basic. Engr, 87:D2, 429 (1965).

84. Smith, J. E. and M. L. Jordan. "Mathematical and Graphical Interpretation of the Log Normal Law for Particle Size Distribution Analysis." J. Colloid Interface Sci., 19, 549 (1964).

85. Spielman, L. A. "Separation of Finely Dispersed Liquid-Liquid Suspensions by Flow Through Fibrous Media." Unpublished Doctoral Dissertation, University of California, Berkeley (1968).

86. Spielman, L. A. "Viscous Interactions in Brownian Coagulation." J. Colloid Interface Sci., 33, 562 (1970).

87. Spielman, L. A. and P. M. Cukor. "Deposition of Non-Brownian Particles Under Colloidal Forces." To be published in J. Colloid Interface Sci. (1973).

88. Spielman, L. A. and J. A. Fitzpatrick. "Theory for Particle Collection under London and Gravity Forces for Application to Water Filtration." To be published in J. Colloid Interface Sci. (1973).

89. Spielman, L. A. and S. K. Friedlander. "Deposition of Colloidal Particles Under Convective Diffusion." To be published.

90. Spielman, L. A. and S. L. Goren. "Model for Predicting Pressure Drop and Filtration Efficiency in Fibrous Media." Env. Sci. Tech., 2, 279 (1968a).

91. Spielman, L. A. and S. L. Goren. "Improving Resolution in Coulter Counting by Hydrodynamic Focusing." J. Colloid Interface Sci., 26, 175 (1968b).

92. Spielman, L. A. and S. L. Goren. "Particle Capture by London Forces From Low-Speed Flows." Env. Sci. Tech., 4, 135 (1970).

93. Spielman, L. A. and S. L. Goren. "Theory of Coalescence by Flow Through Porous Media." Ind. Eng. Chem. Fund., 11:1, 66 (1972a).

94. Spielman, L. A. and S. L. Goren. "Experiments in Coalescence by Flow Through Fibrous Mats." Ind. Eng. Chem. Fund., 11:1, 73 (1972b).

95. Stumm, W. and C. P. Huang. "Specific Chemical Interaction Affecting the Stability of Dispersed Systems." Croatica Chemica Acta, 42, 223 (1970).

96. Stumm, W. and J. J. Morgan. Aquatic Chemistry. New York: Interscience, Publishers (1970).

97. Swift, D. L. and S. K. Friedlander. "The Coagulation of Hydrosols by Brownian Motion and Laminar Shear Flow." J. Colloid Sci., 19, 621 (1964).

98. Tenney, M. W. and W. Stumm. "Chemical Flocculation of Microorganisms in Biological Waste Treatment." J. Wat. Poll. Cont. Fed., 37, 1370 (1965).

99. Thompson, A. F., Jr. "The Ultrafiltration of Salt-Polyelectrolyte Solutions." Unpublished Doctoral Dissertation, California Institute of Technology (1967).

100. Vanderhoff, J. W. Formerly of Dow Chemical Co. Personal communication (1972).

101. van Olphen, H. An Introduction to Clay Colloid Chemistry. New York: Interscience Publishers (1963).

102. Verwey, E. J. and J. Th. G. Overbeek. Theory of the Stability of Lyophobic Colloids. Amsterdam: Elsevier Publishing Co., (1948).

103. Visser, J. "Measurement of the Force of Adhesion Between Submicron Carbon-Black Particles and a Cellulose Film in Aqueous Solution." J. Colloid Interface Sci., 34, 26 (1970).

104. Vroman, L., A. L. Adams, and M. Klings. "Interaction Among Human Blood Proteins at Interfaces." In "Conference on Mechanical and Gas Layer Effects on Moving Blood." Federation of Am. Soc. for Exp. Biol., Proc., 30:5, 1494 (1971).

105. Watillon, A. and A. M. Joseph-Petit. "Interactions Between Spherical Particles of Monodisperse Polystyrene Latices." Disc. Faraday Soc., 42, 143 (1966).

106. Wiersma, P. H., A. L. Loeb, and J. Th. G. Overbeek. "Calculation of the Electrophoretic Mobility of a Spherical Colloid Particle." J. Colloid Interface Sci., 22, 78 (1966).

107. Wiley, R. M. "Limited Coalescence of Oil Droplets in Coarse Oil-in-Water Emulsions." J. Colloid Sci., 9, 427 (1954).

108. Wilson, E. B., Jr. An Introduction to Scientific Research. New York: McGraw-Hill Book Co., Inc. (1952).

109. Yao, K. M. "Influence of Suspended Particles Size on the Transport Aspect of Water Filtration." Unpublished Doctoral Dissertation, University of North Carolina (1968).

110. Yao, K. M., M. T. Habibian, and C. R. O'Melia. "Water and Wastewater Filtration: Concepts and Applications." Env. Sci. Tech., 5, 1105 (1971).